MATTHEWS, ABRAHAM MUJADID

KINETICS OF METABOLIC ACTIVATION AND DEACTIVATION OF CHEMICAL CARCINOGENS: WITH BETA-NAPHTHYLAMINE AND BETA-NITRONAPHTHALENE AS MODEL COMPOUNDS

The University of Oklahoma PH.D. 1979

PLEASE NOTE:

In all cases this material has been filmed in the best possible way from the available copy. Problems encountered with this document have been identified here with a check mark ✓.

1. Glossy photographs _____
2. Colored illustrations _____
3. Photographs with dark background _____
4. Illustrations are poor copy _____
5. Print shows through as there is text on both sides of page _____
6. Indistinct, broken or small print on several pages _____ throughout _____
7. Tightly bound copy with print lost in spine _____
8. Computer printout pages with indistinct print ✓
9. Page(s) _____ lacking when material received, and not available from school or author _____
10. Page(s) _____ seem to be missing in numbering only as text follows _____
11. Poor carbon copy _____
12. Not original copy, several pages with blurred type _____
13. Appendix pages are poor copy _____
14. Original copy with light type _____
15. Curling and wrinkled pages _____
16. Other _____

University Microfilms International

300 N. ZEEB RD., ANN ARBOR, MI 48106 (313) 761-4700

THE UNIVERSITY OF OKLAHOMA

GRADUATE COLLEGE

KINETICS OF METABOLIC ACTIVATION AND DEACTIVATION OF CHEMICAL CARCINOGENS: WITH β-NAPHTHYLAMINE AND β-NITRONAPHTHALENE AS MODEL COMPOUNDS

A DISSERTATION

SUBMITTED TO THE GRADUATE FACULTY

in partial fulfillment of the requirements for the degree of

DOCTOR OF PHILOSOPHY

By

ABRAHAM M. MATTHEWS

Norman, Oklahoma

1979

KINETICS OF METABOLIC ACTIVATION AND DEACTIVATION OF CHEMICAL CARCINOGENS: WITH β-NAPHTHYLAMINE AND β-NITRONAPHTHALENE AS MODEL COMPOUNDS

APPROVED BY

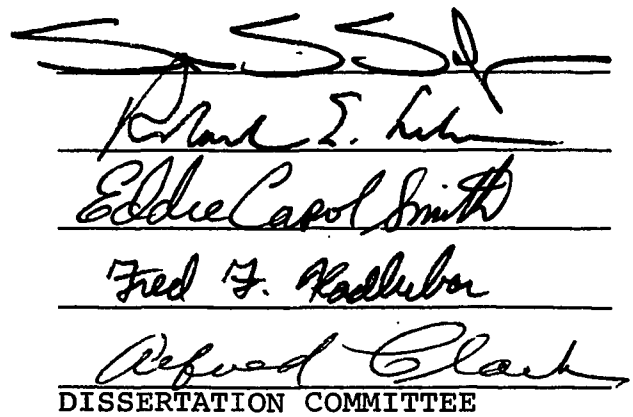

DISSERTATION COMMITTEE

ACKNOWLEDGMENTS

The author gratefully acknowledges the encouragement, enthusiasm and faith, and most of all the friendship of his supervising professor, Dr. Sam S. Sofer.

Special thanks are due to Dr. F. Kadlubar of the National Center for Toxicological Research, Jefferson, Arkansas, a member of the author's dissertation committee, for his material contributions as well as his suggestions in this multi-disciplined project. Thanks are also due to the rest of the members of the dissertation committee, Dr. Arthur Aldag, Dr. Eddie Smith, and Dr. Roland Lehr for their constructive criticism and help in planning of the project.

The author is also grateful for the personal financial assistance afforded to him through teaching assistantship by the Department of Chemical Engineering and Materials Science, The University of Oklahoma, Norman, Oklahoma.

Particular recognition is owed to Sam Penrod, Carlos Suarez and all the rest of the carcinogen-kinetics research team for their invaluable cooperation and assistance in the course of this work.

Last but not least, special appreciation is due Margaret Williford for swift helping-hand, and especially for her gracious services in typing this manuscript.

TABLE OF CONTENTS

LIST OF TABLES

LIST OF ILLUSTRATIONS

Figure | Page

ABSTRACT

The growing concern for a cleaner environment and human health has created today a myriad of stiff regulations with regard to the production and use of chemicals. These regulations have presently called for a serious attention of the chemical industry and the chemical engineer. Of particular importance are those chemicals which are suspected to cause cancer in humans. A short-term test for carcinogenicity of chemicals, involving metabolic activation by the liver microsomal enzyme system, is being widely used at present. This work investigates the kinetic problems associated with the metabolic activation of some chemicals catalyzed by liver microsomal enzymes.

Using pig liver microsomes as a model enzyme system with β-naphthylamine (β-NA) and β-nitronaphthalene (β-NN) as model carcinogen substrates, the work herein is comprised of three major phases of kinetic study. The first phase of study investigates the kinetics of the metabolic activation catalytic reaction and the various parameters which affect the outcome of carcinogen screening tests from a kinetic standpoint. It is shown that the catalytic activation of β-naphthylamine to N-hydroxy β-naphthylamine

(N-HO-βNA) in liver microsomes is specific to the mixed-function microsomal flavoprotein amine oxidase (MFMFO) activity. The metabolic activation of β-nitronaphthalene to N-HO-βNA in liver microsomes in-vitro is shown for the first time in this work experimentally. The catalytic formation and accumulation of N-HO-βNA, the reactive carcinogenic intermediate form, in the liver microsomal assay system is significantly affected by variables such as temperature, pH, reaction time, concentration levels of substrate and microsomes and by diffusion limitation. The second phase of this work shows that carcinogen metabolic activation reaction is accompanied by a deactivation reaction by a consecutive kinetic mechanism involving a second enzyme, UDP-glucuronyltransferase in this case. Concentration-time profiles of the substrate, the intermediate and the glucuronide conjugate product of the sequential reaction mechanism were measured experimentally for β-NA. Periodical addition of the substrate by small amounts to the assay medium in a batch stirred microreactor at optimum conversion time-intervals, seems to be the best kinetic strategy to study the metabolic activation/deactivation of chemical carcinogens in vitro for specific cases. The reaction rate constant for the glucuronidation step reaction appears to be a hundred times greater than the metabolic N-oxidation step. A theoretical two-step dynamic kinetic model was proposed for the metabolic activation/deactivation

mechanism and solved on the computer. The fit of the model to the experimental data was quite satisfactory.

The third and final phase of this work considers the use of immobilized microsomes to improve the kinetic problems associated with native (liquid) microsomes. Pig liver microsomes were successfully immobilized on CPG porous glass beads by covalent binding, using a technique developed by this work. A high metabolic activation/deactivation activities as well as a significant improvement in the stability of the respective enzymes were achieved. Improvement in the stability of the reaction kinetics, especially that of the metabolic activation stage, makes glass-beads mounted microsomes attractive for application in carcinogen screening reaction design. To achieve higher conversion rates and for a better control of the assay products, continuous-flow reactor configurations with recirculation are recommended.

CHAPTER I

INTRODUCTION

Environmental awareness and the problem of environmental control had never reached such a bewildering magnitude as it has today. Environmental protection means many things; from preserving the Alaskan wilderness to saving endangered species, to reducing our exposure to toxic substances in the air, in water, in food, in the workplace, and at home. The problem of toxic substance control, especially with respect to chemicals that cause cancer in humans, has become first and foremost. It is estimated that 80-90% of all human cancers are environmentally caused [1,2,3]. In recent years, we have witnessed a number of tragedies caused by toxic substances in the environment: asbestos, kepone, polyvinyl chloride, and mercury come readily to mind. Although environmental toxins cause a variety of human ailments, including birth defects, miscarriages, heart disease, strokes, emphysemia, and neurological deficiencies, it is the fear of cancer, "cancerophobia", that touched off a wave for committment for a safer environment.

In order to cope with this eminent crisis of cancerophobia, the U.S. Congress has enacted eight laws specifically

designed to regulate toxins in the environment. The newest and perhaps the most far-reaching of the eight is the Toxic Substances Control Act (TSCA), passed in late 1976. TSCA gives the federal government control over chemicals through the Environmental Protection Agency (EPA). EPA was given a first-strike authority with respect to clearing an agent before it enters the marketplace, in addition to power to control existing chemicals if they are shown to be hazardous. Thus, the possibility of carcinogenic risk that might be posed by a wide variety of industrial, agricultural and pharmaceutical chemicals has drawn the attention of investigators in various areas during the last few years. Devicing of short-cut test methods to screen the thousands of chemicals in the environment for possible carcinogenic risk assessment has been the major emphasis of research. Short-term tests using liver homogenates for enzymatic metabolic activation of test chemicals are in common use today for carcinogen screening.

While there exists much controversy between regulatory government agencies and industry with regard to the efficacy of these simplified test procedures with bacteria, very little qualitative information is available concerning the kinetics of the metabolic activation system. The complexity of the reaction mix from the kinetic standpoint, existence of competing activation and deactivation reactions, non-enzymatic side

reactions, diffusion limitation, and enzyme stability under in-vitro experimental conditions, has hindered advancement in this area. Lack of proper kinetic design of the metabolic activation reaction system in-vitro could significantly reduce the efficiency of these tests and make the prediction of hazard from a given test compound or mixture quite unreliable. Frantz and Malling [4], Weisburger [5], and De Serres [6], among others have pointed out the critical importance of this problem. Major kinetic problems of concern in microsomal metabolic activation of test chemicals can be summarized as follows:

1) Optimum concentration levels of substrate (test compound), cosubstrates and microsomal protein are important. The catalytic character of the microsomal enzymes coupled with possible substrate and/or product inhibition could significantly affect the quantitative formation of the required intermediate.

2) The formation of the activated intermediate by microsomal enzyme activation is generally accompanied by deactivation reactions [7]. Chemical metabolizing enzyme systems which are localized principally in the liver, are usually divided into two groups: phase I and phase II [8]. The phase I enzymes (mainly oxidative enzymes) catalyze the conversion of parent compounds to oxidized reactive intermediate forms, while the phase II ones (e.g.,

UDP-Glucuronyl transferase) mediate the transformation of the activated intermediates into a deactivated conjugate. Excellent recent reviews on the relationship between these enzymes and cancer or toxicity are given by Sims and Grover [9], Heidelberger]10], Nebert, et al. [11], Nebert and Felton [12], and Thorgeirsson, et al. [13].

Due to such a delicate equilbrium between activation and deactivation, the examination of the concentration profile of the intermediate as a function of time is essential.

3) The effect of such reaction parameters as temperature and pH on microsomal enzyme activity and stability under in-vitro assay conditions is critically important for a productive reaction design. For instance, approximately the first half hour of the metabolic activation reaction in short-cut carcinogen screening test systems is run at 45°C [14] when the temperature optimum for microsomal oxidative reaction is about 40° as can be seen from the result of this work. About 60% or less of Flavoprotein monooxygenase activity and a half-life of about 50 minutes is expected around 45°. The pH optimum of microsomal Flavoprotein oxidase is around 8.0. The reaction pH of metabolic activation reactions in short-term testing systems referred to

above is not reported, but is probably neutral.

4) An important problem is that of diffusion of reactants into reaction sites of enzyme proteins. Diffusion and mass transfer limitations would play a significant role in the kinetics of carcinogens in microsomal membrane-bound enzymes.

5) The major problem in using native or liquid microsomal enzyme system in carcinogen testing is that of stability. This system is stored and kept for further use under -20°C [15,16] and for a maximum of 3-4 months. Repeated thawing and freezing during this period for withdrawing portions for various experimental runs also adversely affects the activity of the system. Moreover, due to a rapid loss of activity during a given reaction assay, the microsomal enzyme system is not recovered but discarded. These problems of stability and reusability can be solved by successfully immobilizing the enzyme system on a porous solid support without a significant loss in activity. Potential application of CPG Porous glass beads-mounted microsomes is preliminarily investigated in this work.

The objective of this work is to investigate the significance of the problems outlined above in order to improve the credibility and success of carcinogen screening by metabolic

activation short-term tests. A well known arylamine carcinogen β-naphthylamine, is taken as a model compound for this study. The kinetic study technique used for the arylamine is further extended with success to explain the metabolic activation kinetics of aryl-nitro-compound analogs, with β-nitronaphthalene as an example. Pig hepatic microsomes are used for metabolic activation. Kinetic investigations are primarily carried out in a stirred constant-temperature batch microreactor. Taking account of the major factors which affect the metabolic activation phenomenon, a kinetic model is postulated and a satisfactory fit of the model to experimental data is obtained. Based on porous glass beads-immobilized microsomes, two continuous flow reactor configurations are suggested for advantageous application in short-term tests. It is hoped that the kinetic optimization study conducted in this work would give an indication of the various factors affecting the sensitivity of prediction of carcinogenicity by metabolic activation tests and the ways to minimize these factors for an efficient design.

CHAPTER II

BACKGROUND

Environment vs. Industry

The impact of the regulatory process is being painfully felt by the chemical industry. It is estimated that compliance with TSCA will cost the chemical industry $2 billion a year [17]. Even though "Environment does not equal industry," to use the statement of frustration by John F. Schmutz, a chemical executive of E.J. DuPont [18], the bare inescapable fact stays firm—that all already untested chemicals have to go through carcinogenicity testing and as a consequence face possible banning, irrespective of their relative usefulness in chemical technology. Some estimates hold that 1000 chemicals enter the marketplace each year [19]. Of the estimated 4.3 million chemicals in existence, some 63,000 are said to be in common use in the U.S. [20].

One major area of concern is the pesticide, insecticide and herbicide industry. About 50,000 pesticides are due to be screened for carcinogenicity.

"What does a chemical engineer have to do with this?", one might ask. Obviously, a chemical engineer by the nature

of his profession is involved in the design and development of better chemical processes and equipment as well as opening new technological and engineering break-throughs to improve our society. But one would hate to be in a position of a chemical engineer who after putting-in years of professional work of solving technological and engineering problems and turned-out the first batch of his product, only to discover that the product cannot be marketed. It cannot be marketed not because the manufactured chemical is economically unfeasible or the market demand is low; but just can't be put into the market—by law! Because, the chemical product is found to be carcinogenic by bioassay tests. Here is then that the engineer starts worrying about what has come to be the first and foremost problem today—the environmental consequences of his product, whether new or already in production. In this regard, James Wei, head of the Department of Chemical Engineering at MIT, had the following to say [2],

> "The chemical industry needs people who can understand the impact of their work, who can 'see the whole picture' and 'hear the whole music'... Environmental issues will be important threats and opportunities for chemical engineers in the next century. The world needs chemical engineers who are environmental specialists to work in the chemical process industries, in universities and in government. The world will also need chemical engineers who understand the impact of their work and who can relate to the public. Just because Charley plays the cello well does not necessarily mean that he knows the whole music without serious study. Many of our own chemical engineers are just as uninformed about the

> positive or negative impact of their work. Consumers ringing the cash register are economically sovereign in our land. Voters going to the polls are politically sovereign in our land. We must serve them well to survive."

Thus, the need for understanding the scientific basis of these regulatory carcinogenicity tests and their design is crossing today the traditional boundary from biochemists and toxicologists to engineers, and particularly chemical engineers. Improvement of the design of these tests, to increase their screening efficiency and at the same time minimize the probability of undue risks for the chemical manufacturer accruing from false positive data from such tests, should undoubtedly attract chemical engineers' attention.

This work is one of the first engineering attempts in this direction.

Carcinogen Testing Via Metabolic Activation

First, of all, what are carcinogenicity tests? Effective regulation of toxic substances requires identification of carcinogens before there is significant human exposure, or better, before they enter the marketplace. The conventional method to achieve this is with bioassays in animals. Practical considerations dictate that such testing be performed in small

animals with short life spans. Typically, these are rodents. In practice, at least 500 animals are required, including controls. The total time required is at least 3.5 years or more and the cost ranges from $150,000-$500,000 per substance [21], with about 1000 new chemicals being introduced each year, as indicated earlier, besides thousands of other substances already in use, carcinogen screening by long-term animal bioassay tests is too slow, cumbersome and prohibitively expensive venture. Therefore, there has been a great deal of research effort made to develop short-term or short-cut, relatively inexpensive, and quick in-vitro carcinogen screening tests. There are now at least 80 different tests in various stages of development [22]. One of the first short-term tests, and the most successful one is what is called the Ames test, [23-25], developed by Bruce Ames of the University of California at Berkeley. This test is being widely applied today for carcinogen screening not only by environmental control agencies, but also by chemical companies such as DuPont, American Cyanamid, Procter & Gamble, Dow Chemical, to name just a few.

The improved Ames test [26,27], referred to as Salmonella-mammalian microsome mutagenicity test is based upon the metabolic activation phenomena of carcinogens. It has been known for a long time that induction of cancer by chemicals results from covalent binding of the latter to one or more of cellular macromolecules, DNA [28,29], RNA or proteins of the cells in target tissues. Among the important classes of chemical

carcinogens that become covalently bound to tissue macromolecules are polycyclic aromatic hydrocarbons (PAH), aromatic amines, nitrosamines and Safrole. Nevertheless, none of the individual compounds in these classes become covalently bound to cellular macromolecules when incubated in a test tube [30]. Later, from the classical work of the Millers [31-33], who investigated the mechanism of biotransformation of aromatic amines using mammalian liver microsomal enzyme system, it became apparent that chemical agents must be enzymatically metabolized or converted in-vivo into a chemically reactive form before they are able to bind. In other words, for the overwhelming majority of chemical carcinogens, metabolic activation must first occur in the microsomal enzyme system in order to yield a reactive intermediate (proximate carcinogen) which subsequently participates in its electrophilic form in cancer initiation. These enzymatically activated proximate or ultimate carcinogenic forms (species) were later on shown by Ames and co-workers to be mutagenic in Salmonella bacteria [34]. Based on the finding that there exists correlation between carcinogenicity and mutagenicity, the Ames test detects carcinogens as mutagens in a reaction system composed of a test compound, mammalian liver homogenates or microsomes and various strains of Salmonella bacteria.

Characterization of the Liver Microsomal Enzyme System

Among other diverse physiological functions, the liver operates as a major chemical-processing plant in the body. It is responsible for a great majority of chemical transformations of drugs and other foreign chemicals and environmental pollutants to which the body is exposed. These reactions are accomplished catalytically by several remarkable enzymes naturally existing in the cell. The enzymes are embedded in the membranes of the endoplasmic reticulum of the cytoplasm of the cells. If these liver cells are homogenized and centrifuged successively at higher speeds (higher gravity), broken bits of membranes of the endoplasmic reticulum are obtained in the form of tiny vesicles or sacs called microsomes. These microsomes are the potential source of the liver enzymes for model studies of various reactions of drugs and environmental chemicals. Even though some enzymatic biotransformations of endogeneous as well as exogeneous substrates occur in cytosols and even in mitochondria, by far the greatest number of biotransformations take place in microsomal fraction. The main enzymatic reactions that occur in microsomes are: oxidation, reduction, hydrolysis and conjugation. An excellent review of the role of microsomal enzymes in the metabolism of various drugs and other foreign compounds is given by Kappas and Alvares [35]. While reduction and hydrolysis reactions are less common,

oxidation processes account for most of the enzymatic transformations, simply because there are so many ways of oxidizing exogeneous compounds.

Oxidation biotransformations of chemicals is mediated in the microsomal fraction by oxidases and cytochromes that function in the electron-transport reactions requiring molecular oxygen and reduced pyridine nucleotides. The oxidases of microsomal membrane can be classified into three major groups [36]; those which catalyze the transfer of:

1) Both atoms of oxygen molecule to substrate, and known as dioxygenases;
2) One atom of oxygen to substrate, and the other reduced to water—called mixed function oxidases or monooxygenases; and
3) O_2 to H_2O_2 or H_2O [37] and oxidize substrates to one, two or four equivalents and generally referred to as electron-transferring oxidases.

Principal emphasis has been directed to the understanding of the kinetics of cytochrome P-450 dependent mixed function oxidation (monooxygenation) reactions. A broad spectrum of mixed-function oxidations encompassing from the oxidation of polycyclic aromatic hydrocarbons to the oxidation of pesticides and insectides, steroids and fatty acids, drugs and pharmaceuticals, and metabolic activation of fluorocarbons to hepatotoxins all make this system important. Special

attention has been given in recent years to a particular oxidative enzyme, a component of the mixed function monooxygenases system called Flavoprotein monooxygenase (dimethylaniline monooxygenase EC 1.14.13.8), isolated and purified by Ziegler and Petit from hog liver microsomes [38,39]. This flavoprotein mixed function oxidase is of special interest because 1) its activity is much greater in the liver than in other tissues, and 2) this enzyme is present in unusually high concentrations in hog and human liver [40]. The flavoprotein oxidase catalyzes the N-oxidation of a variety of tert-, and sec-alkyl or arylamines, some primary arylamines, and 1,1-disubstituted hydrazines. The reactions require an external electron donating system, and equimolar amounts of reduced nicotinamide adenine dinucleotide phosphate (NADPH) and oxygen. The general scheme can be represented as follows:

$$X - \underset{\displaystyle R_2}{\overset{\displaystyle |}{N}} - R_1 + NADPH + H^+ + 0_2 \rightarrow X - \overset{\displaystyle O}{\overset{\displaystyle \uparrow}{\underset{\displaystyle R_2}{\overset{\displaystyle |}{N}}}} - R_1 + NADP^+ + H_20$$

$$X - \underset{\displaystyle H}{\overset{\displaystyle |}{N}} - R_1 + NADPH + H^+ + 0_2 \rightarrow X - \overset{\displaystyle O}{\overset{\displaystyle \uparrow}{\underset{\displaystyle H}{\overset{\displaystyle |}{N}}}} - R_1 + NADP^+ + H_20$$

"X" is a lipophylic alkyl or aryl group free from polar groups on the alpha carbon. A functional group more polar than a hydroxyl group within a two atom radius of the nitrogen prevents oxidation. R_1 and R_2 could be methyl or ethyl groups

or just hydrogen atoms, as in the case of 2-naphthylamine. Tertiary amines are converted to N-oxides, while secondary amines are N-hydroxylated. It has been shown recently that the oxidase also catalyzes the S-oxidation of a variety of sulfur-containing compounds [41]. Ziegler showed that from among primary arylamines, the flavoprotein oxidase catalyzes the N-hydroxylation of only β-naphthylamine [41]. Moreover, the author has also postulated that the N-hydroxylation of this compound even in whole microsomes may be specific to this particular monooxygenase. Thus, in relation to short-term carcinogen screening tests using whole microsomal fraction for metabolic activation, it is decided to investigate the kinetic problems discussed in Chapter I using β-naphthylamine-oxidase activity in microsomes. Pig liver microsomal fraction is used in the study, since its oxidase content is higher as noted above.

Metabolic Activation of β-naphthylamine

The metabolism of the carcinogen β-naphthylamine has been widely investigated, both *in vivo* and *in vitro*. Boyland and Manson [42] treated animals with this amine and isolated a variety of metabolites from the urine of the test animals. Boyland, Dukes and Grover [43]; Booth and Boyland [44]; Arcos and Arays [45] showed that the metabolic N-oxidation of β-naphthylamine, like the N-oxidation of N-acetylaminofluorene [46] leads to the formation of more carcinogenic intermediates.

The N-oxidation intermediate, β-naphthylhydroxylamine, was next shown by Bonser et al. [47], and Bryan, et al. [48], to produce statistically more tumors than the parent compound when implanted surgically in the bladders of mice. Subsequently, Radomski and Brill [49], after similar experiments with dogs reported the N-hydroxy derivative induced bladder tumors. Later on, it was shown that this same carcinogenic intermediate exists as a urinary metabolite in dogs [50], and in humans [51].

But very little of the metabolic mechanism of β-naphthylamine N-hydroxylation was known until this point. It was assumed that N-oxidations of various arylamine compounds were all catalyzed by a single microsomal mixed function oxidase. However, subsequent studies of Lange [52] and Uehleke [53-55] with hepatic microsomes from phenobarbital-treated animals, and with rabbit lung microsomes gave a satisfactory evidence that the microsomal cytochrome P-450 terminal electron-transport system participated in the N-oxidation of primary arylamines but not secondary and tertiary arylamines. As mentioned earlier, the N-oxidation is NADPH and oxygen dependent. At about the same time, Ziegler and Mitchell [56] had isolated a mixed-function flavoprotein oxidase from pig liver microsomes and reported that the flavoprotein oxidase is specific to catalyzing rapid N-oxidation of a variety of lipid-soluble secondary and tertiary amines, but not of primary alkylamines or arylamines other than β-

naphthylamine. This was surprisingly consistent with the findings of Uehleke as noted above. Moreover, cytochrome P-450 is activated by pheno-barbital and inhibited by CO. The mixed function oxidase exhibits none of these properties [57,58].

The catalytic N-oxidation of β-naphthylamine by the mixed function oxidase as an exception to other primary arylamines can be explained by the fact that the nitrogen atom in β-naphthylamine has some nucleophilic character [59]. In contrast to other primary arylamines, β-naphthylamine exists in equilibrium with its imine tautomer form in aqueous solutions. This imine form with its lone pair of electrons on the nitrogen atom with no possibility of delocalization into the aromatic ring is conjectured to be the active or nucleophilic form of the amine for N-oxidation by flavoprotein monooxygenase. Figure 1 shows a simplified possible mechanism of N-oxidation as illustrated by Ziegler. But even though the flavoprotein monooxygenase catalyzes the rapid oxidation of β-naphthylamine to its N-hydroxy derivative, a successful accumulation of this oxidation product with the pure enzyme assay, has been difficult. Ziegler [60] reported that the isolated and purified mixed function oxidase catalyzed the N-oxidation of β-naphthylamine to β-naphthylhydroxylamine, but this product of the reaction was rapidly oxidized non-enzymatically to the nitroso-derivative. But, the study of the N-oxidation of the compound in discussion, using whole pig

FIGURE 1. Possible mechanism of formation of β-naphthylamine intermediates catalyzed by flavoprotein monooxygenase (mixed-function amine oxidase) [59]. The imine tautomer of β-NA, due to its nucleophilic character, reacts with the peroxy flavin prosthetic group of oxidase to give the enzyme-bound hydroxylamine. Cleavage of this intermediate via routes (a) and (b) could lead to the indicated final products, with route b predominating.

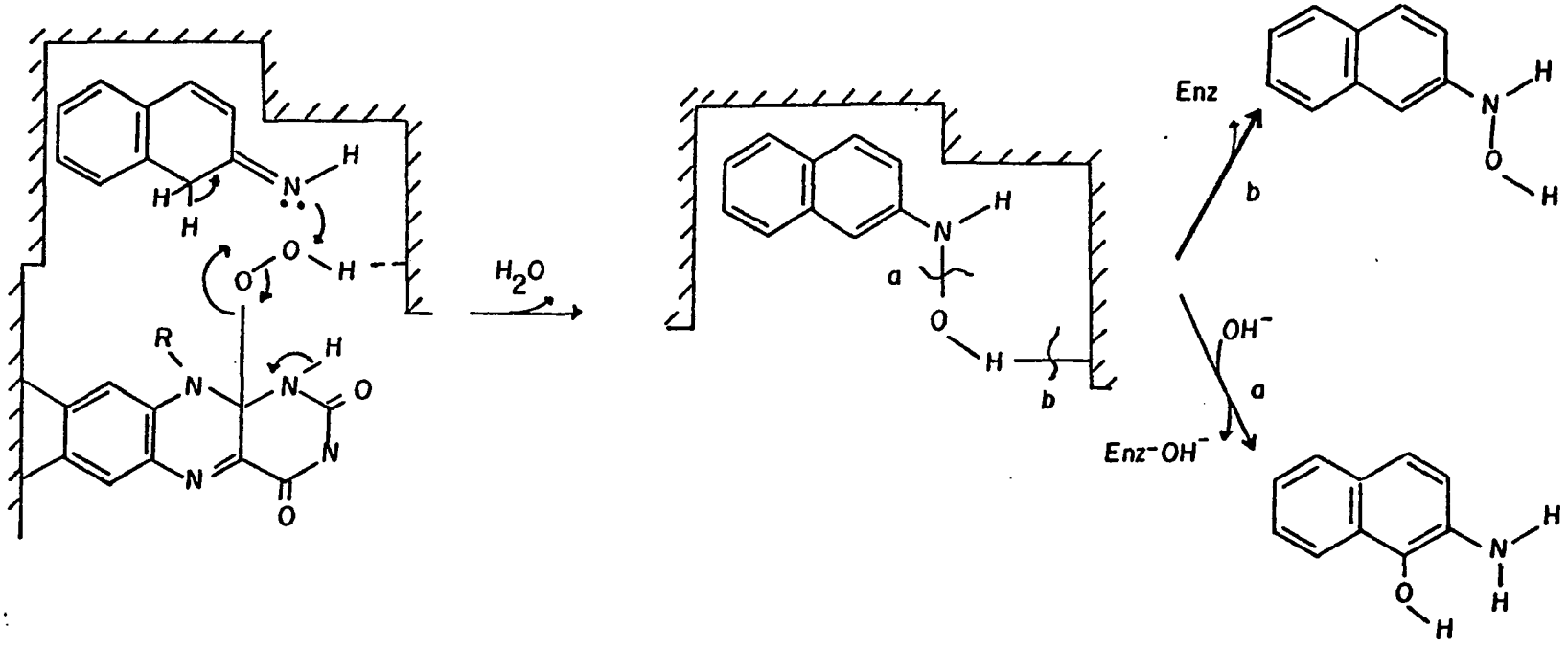

FIGURE 1

liver microsomes, showed [59] that the N-oxidized carcinogenic intermediate product (β-naphthylhydroxylamine) accumulates in the reaction mixture for prolonged times. Matthews and Sofer, et al. [61] also have shown the same behavior in their study of optimization of the formation of the N-hydroxy intermediate in a stirred-tank microassay reactor. It is concluded that even though the cytochrome P-450 terminal electron transport system is not required for N-hydroxylation of β-naphthylamine, its component NADPH-cytochrome C reductase, and microsomal phospholipids are necessary factors for the stability and accumulation of the N-hydroxy-β-naphthylamine in the reaction medium during the course of the reaction. The effect of these microsomal components on β-naphthylamine metabolic N-oxidation has been well elucidated by the recent study of Poulsen, et al. [59]. Therefore, doubtlessly it is essential that any in-vitro study of the chemical transformation of carcinogens as a model of metabolic activation in-vivo, use whole microsomal system. The authors have not, however, demonstrated the effect of essential reaction parameters such as temperature, pH, concentration of cofactors, and enzyme stability on the kinetics of microsomal β-NA N-oxidation. Moreover, whole microsomal fraction contains various enzyme systems (oxidative, conjugative, hydrolysis, etc.) as noted earlier in this chapter. Since the intermediate oxidized form of most arylamines, especially that of β-NA, is a very unstable reactive product, metabolic activation (oxidation) study should consider the effect of microsomal enzyme

systems other than oxidases. As has been pointed out in Chapter I, there exists the possibility of a sequential kinetic mechanism of oxidation followed by relatively significant conjugation with endogeneous substrates via transferases. Evidence of this has been shown by in-vivo studies with rodents (Kadlubar, et al. [62], and others [63]). But, the kinetics of this sequential mechanism has not been successfully shown by in-vitro studies with microsomes up to date. This second stage microsomal conjugation reaction which involves the N-oxidized intermediate product (N-HO-βNA) and a second microsomal enzyme UDP-Glucuronyltransferase will be briefly described in the following section.

Microsomal Conjugation of N-hydroxy-β-Naphthylamine

The N-hydroxylated β-naphthylamine intermediate can be further conjugated with an endogeneous substrate γ'-uridine 5'diphosphoglucuronic acid (UDPGA) enzymatically to form a conjugate N-hydroxy β-naphthylamine glucuronide (N-HO-βNAGluc) [62]. While the intermediate is an activated and highly potent carcinogenic form, the conjugate is inactive. This second stage reaction is mediated by a microsomal enzyme UDP-Glucuronyltransferase (UDP-GT). An excellent characterization of this enzyme is given by the recent work of Zakim and Vessey [65]. A series of studies have been done by the same authors on the conjugation of P-nitrophenol by UDP-GT and the various factors which enhance the activity of the enzyme [66-69]. Conjugation

of N-HO-βNA with UDP-glucuronic acid by microsomal UDP-Glucuronyltransferase has been adequately studied by Kadlubar, et al. [70]. These authors demonstrated that dog, rat and human hepatic microsomes rapidly conjugated N-HO-βNA (obtained by non-enzymic organic synthesis) with UDPGA to form the glucuronide conjugate. The reaction scheme is as follows:

$$\text{N-HO-}\beta\text{NA} + \text{UDPGA} \underset{\longleftarrow}{\xrightarrow{\text{microsomes (UDP-GT)}}} \text{N-HO-}\beta\text{NA-Gluc} + \text{UDP}^{+}$$

But, the possibility of the consecutive mechanism of β-NA N-oxidation to N-HO-βNA and further glucuronidation of this intermediate to N-HO-βNA Gluc by microsomes, which contain both oxidase and UDP-GT, has never been shown successfully by in-vitro experimencs. By a proper consecutive reaction kinetic design strategy, this work successfully shows this possibility in a single experimental step.

Immobilization of Microsomes

To improve their potential application as catalysts for carcinogen screening by metabolic activation in various reactor configurations, microsomes can be immobilized on appropriate solid supports. Immobilization, here, refers to the process of physical confinement or localization of enzyme molecules, a group of enzymes or a whole cell on an adequate porous support. Immobilization of enzymes can be achieved by

diverse means. However, one can classify all the methods employed into two classes: chemical methods and physical methods. Chemical methods, as the name suggests, involve covalent attachment of the enzyme to water-insoluble functionalized polymer. Physical methods vary from adsorption of enzymes to water-insoluble inorganic or organic supports, entrapment within gel matrices or semipermeable microcapsules, to their containment within semipermeable membrane-dependent devices. Excellent and comprehensive reviews on immobilized enzymes and their present role in laboratory research as well as in industrial technology are given by Zaborsky [71] and Wingard [72]. Here, we confine our discussion to only immobilization by chemical bonding. The secret of the game lies in finding a mechanically and chemically stable porous solid support with a large surface area on which one can successfully immobilize the enzyme(s) of interest without significant loss of original activity. A great deal of discussion has been devoted in recent literature [71-73] to solid matrices used as supports. An enormous number of solid supports of organic and inorganic nature, pure metals and metal alloys are in use or being researched. What would one achieve by immobilizing? The advantages are manyfold. The most significant advantages are: (1) considerable increase in stability over freely mobile enzymes; (2) operational flexibility and re-usability; and (3) greater probability to serve as model systems for natural, in-vivo cell-bound enzymes.

The first two factors are especially important. Dramatic increase in stability of the activity of enzymes toward heat [74-77], extremes of pH [78-81], and storage [82-84] due to immobilization is widely reported. The operational advantages are great. Reuseability, possibility of batch or continuous operational reactor configurations, rapid termination of reactions if necessary, controlled product formation and possible greater efficiency in consecutive multistep reactions are some of the positive facets of immobilized enzymes.

All the advantages outlined above accruing from successful immobilization by covalent attachment are highly desired for operational capability of microsomes as catalysts for metabolic activation purposes. For the first time, Sofer, et al. [85], immobilized microsomes on porous glass beads by covalent attachment and found that the microsomal oxidation activity was in fact, enhanced. The procedure involved consists of first, activating the matrix surface with a multifunctional, low molecular weight reagent to create a "spacer arm", followed by attachment of a functional group of an enzyme in the microsomal membrane. Even though the exact mechanism of the binding of microsomal membrane enzymes is yet unknown and being studied, immobilization of microsomes on porous glass bead matrices has increased the potential application of microsomes. In this work, a slightly different procedure of binding microsomes to porous glass bead supports is investigated. The application of glass-bead-mounted microsomes is extended from oxidation reactions to conjugation.

CHAPTER III

SUMMARY OF OBJECTIVES AND PLAN OF STUDY

The metabolic activation kinetic study plan using pig hepatic microsomes is divided into three sections:

A) Optimization of the kinetics of β-naphthylamine (β-NA) N-oxidation, and its kinetic model.

B) Study of the possibility of consecutive kinetic mechanism.

   1) Possibility of the consecutive kinetics of β-NA oxidation and conjugation in-vitro, and its kinetic model.

   2) Possibility of the consecutive kinetics of β-nitronaphthalene (β-NN) reduction and conjugation.

C) Application of glass-beads-immobilized microsomes for metabolic oxidation and conjugation: demonstration with β-naphthylamine.

A) Kinetics of β-NA catalytic N-oxidation by pig hepatic microsomes.

The oxidation reaction scheme can be given as follows:

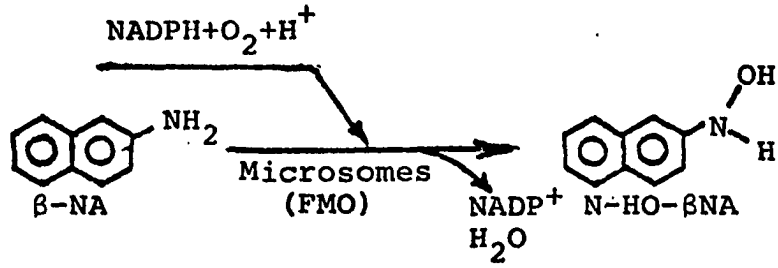

where: NADPH is the reduced nicotinamide adenine dinucleotide phosphate;

N-HO-βNA is the target product, N-hydroxy-β-naphthylamine;

FMO is the microsomal mixed function flavoprotein oxidase, herein referred to simply as flavoprotein monooxygenase (FMO)

This first approach of study is necessary to obtain kinetic parameters for optimum yield of N-HO-βNA. Here, the oxidation reaction kinetics is studied and analyzed without considering the possibility of a further conjugation mechanism.

B) 1) Kinetics of consecutive oxidation and conjugation of β-NA by microsomes.

The kinetic mechanism can be illustrated as follows:

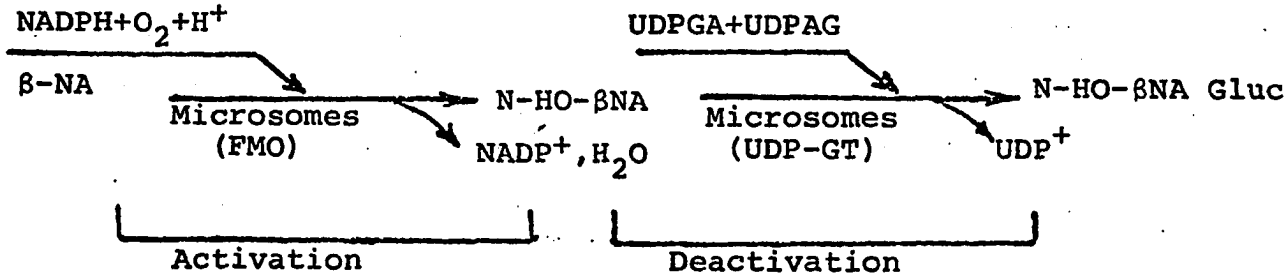

where: UDPAG is the UDP-N-acetyl glucosamine;

UDPGA is UDP-Glucuronic acid

and, N-HO-βNA-Gluc is the conjugation product, N-hydroxy β-naphthylamine glucuronide.

The possibility of such a sequential bienzymic kinetic model of activation and deactivation of the carcinogen β-naphthylamine will be experimentally investigated and a theoretical kinetic model will be examined.

2) If objective B(1) is accomplished, it may also be reasonable with the same token to postulate a similar sequential kinetic mechanism for an aryl-nitro analog, e.g. β-nitronaphthalene (β-NN) which has been shown to be carcinogenic in animals [86]. The first stage would presumably be a partial reduction of the nitro group by microsomal nitro-reductase in an oxygen-free atmosphere to yield N-HO-βNA, followed by a second stage of conjugation analoguous to the second stage in the case of β-NA.

Schematically, this can be postulated as:

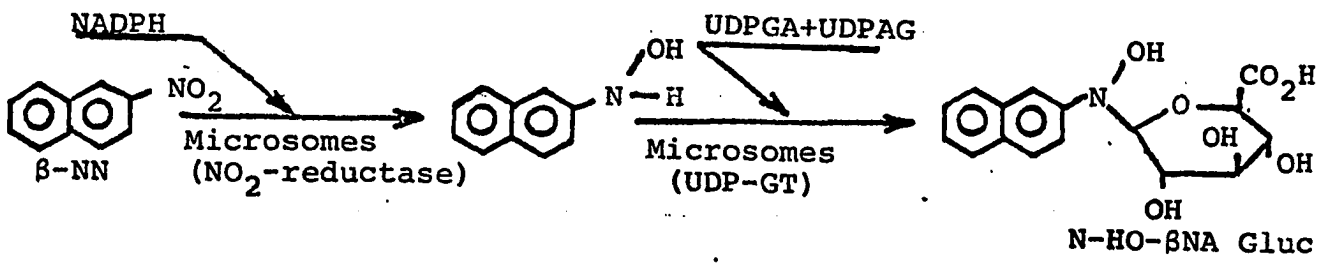

A successful in-vitro experimental validation of the two sequential kinetic mechanisms catalyzed by microsomal oxidative (or reductive) and conjugative enzymes, as given in B(1) and B(2) above, would be a concrete proof for the theory of metabolic activation and deactivation of the majority of chemical carcinogens.

An outline of the experimental investigation plan with β-NA as a model compound is given in the following sections:

Kinetics of Hog Liver Microsomes-Catalyzed N-Oxidation of β-NA

The following essential kinetic investigations have to be conducted in order to probe the effect of critical reaction parameters on the formation of N-HO-βNA intermediate at in-vitro assay conditions:

Time-history profile of the formation of the intermediate with the reaction coordinate. From this data it would be possible to obtain information about the quantitative formation and stability of the N-HO-βNA intermediate in the reaction as well as substrate conversion limitations under given conditions.

Initial rates of activity of microsomal flavoprotein monooxygenase with various substrate (β-NA) concentrations. This investigation is important for two main purposes. First, it will help clarify possible substrate inhibition zones, and

secondly, important kinetic constants such as maximal velocity (Vmax) and Michaelis-Menten constant ($K_{\beta-NA}$)-concentration of β-NA required to half-saturate the enzyme, would be obtained from these data.

Effect of microsomal proteins (enzyme) concentration. Since the objective of this work is to investigate what is happening kinetically in metabolic activation systems practically applied in carcinogen screening tests, the concentration level of microsomes to be used would be very high. This study will examine the kinetic alterations as the microsomal enzyme concentration is increased linearly. It has been discussed in the previous chapter that the accumulation of N-HO-βNA is dependent on the amount of microsomal fraction added. However, from the kinetic standpoint, it is conceivable that there could be an optimum limit to the amount of microsomes one could use above which there would be no advantage, if not disadvantage.

Effect of the concentrations of cosubstrates and/or cofactors. For microsomes-catalyzed oxidation the cosubstrates(cofactors) are O_2 and NADPH.

pH effect on N-oxidation. This investigation is important because during a regular in-vitro experimental run, pH changes are possible during the course of the reaction.

Temperature effect. As described earlier, microsomal oxidative enzymes are very sensitive to temperature changes.

Rapid FMO (Flavoprotein monooxygenase) denaturation or deactivation associated with irreversible structural changes in the enzyme is possible at elevated temperatures of 40-45°C. As has been indicated earlier, in carcinogen screening assays using metabolic activation, the microsomal fraction is briefly subjected to 45°C. Thus, the profile of N-HO-βNA formation actively as a function of temperature will indicate optimum operating conditions with respect to temperature.

Investigation of diffusion limitation. Diffusion limitation in a homogeneous reaction system can be overcome by stirring the reaction mass. It is necessary to determine from product yield vs. agitation speed data, the optimal stirring speed in the batch reactor which maximizes diffusion. All kinetic runs will be conducted using this optimal speed setting. Here, it would be particularly interesting to compare product formation profile from optimized stirred batch-reactor used in this work, with a similar profile obtainable from a conventional bioassay run using incubation in a shaker-bath.

Modelling of β-NA microsomal oxidation kinetics. After obtaining the kinetic data outlined above for β-NA microsomal N-oxidation, a rate equation will be sought which best correlates the experimental data.

β-NA N-Oxidation And Simultaneous Conjugation - Consecutive Reaction Catalyzed By Pig Hepatic Microsomes

1) Design of the consecutive reaction in a batch stirred-tank reactor - maximization of the intermediate (N-HO-βNA), maximization of the end product (N-HO-βNAGluc).
2) Development of separation and analytical technique for N-HO-βNA, and N-HO-βNAGluc.
3) Development of the kinetic model, and the fit of the model to experimental data.

Immobilization Of Microsomes

1) Establishment of immobilization technique.
2) Immobilization of microsomes.
3) Activity of glass-beads immobilized microsomes (GBIMM) for β-NA oxidation, and N-HO-βNA conjugation.
4) Choice of reactor configurations for potential application of GBIMM in carcinogen testing.

The methods used to achieve the desired objectives will be given in more detail in Methods section of the next chapter.

CHAPTER IV

MATERIALS AND METHODS

Materials

Cofactors, Organic Chemicals, Allied Enzymes and Supports

Table 1 summarizes the pertinent specifications.

Purified Flavoprotein Mixed Function Amine Oxidase and Microsomes

Pig hepatic microsomes and purified mixed function amine oxidase (Flavoprotein monooxygenase) were obtained from Dr. Dan Ziegler, of the Clayton Foundation, University of Texas, Austin. The primary sources of microsomes with high amine oxidase activity are adult hogs. The specific activity is, however, affected by such factors as age, sex and even hair color. Five-to-ten fold variations in monooxygenation activity among liver tissues of different adult hogs are not uncommon [87]. Microsomes with the highest and more stable activity are usually obtained from large

TABLE 1

Chemical Specifications

Acetone, reagent grade, Mallinckrodt

γ-aminopropyltriethoxy Silane(Aldrich analyzed) Chemical Co., Aldrich amyl-acetate, purified, Baker Chemical Co.

*Bovine serum albumin, 96-99% albumin, Sigma Chemical Co. Biuret Reagent, 540-2, Sigma Chemical Co.

*catalase, Bovine, purified powder, Sigma Chemical Co.

Chloroform, analytical reagent, Mallinckrodt

*N, N-Dimethylaniline, analytical reagent, Matheson Coleman and Bell

Ethylenediamine tetraacetic acid, disodium salt, Sigma grade, Sigma Chemical Co.

Ethyl alcohol, absolute, reagent quality, U.S. Ind. Chemicals Co.

Ethyl ether, anhydrous, Mallinckrodt

Glass bead supports, alkylamine Zir-clad CPG-1350 porous glass beads, Corning. Distributed by Pierce Chemical Co. Nominal surface area: 34 m^2; particle diameter: 177-840 microns; nominal pore diameter; 1350Å.

*D-glucose-6-phosphate, monosodium salt, Sigma Chemical Co.

*D-glucose-6-phosphate dehydrogenase, type XV, Sigma Chemical Co.

Hydrofluoric acid, analytical reagent, Mallinckrodt

Methyl alcohol, absolute, spectro-grade, Baker Chemical Co.

β-naphthylamine, recrystallized, Sigma Chemical Co.

*β-naphthylhydroxylamine, obtained from Dr. Kadlubar, NCTR, Jefferson, Arkansas.

β-nitronaphthaline, 98%, Aldrich Chemical Co.

p-nitrobenzoylchloride, reagent grade, Matheson Coleman and Bell

*Nicotinamide adenine dinucleotide phosphate, oxidized ($NADP^+$), sodium salt, from yeast extract, Sigma Chemical Co.

*Nicotineamide adenine dinucleotide phosphate, reduced, (NADPH), monosodium salt, from yeast extract, Sigma Chemical Co.

Potassium phosphate, mono-, and di-basic, anhydrous, Fisher Scientific Co.

*UDP-N-acetyl glucosamine (UDPAG), sodium salt, Grade 1, Sigma Chemical Co.

*UDP-glucuronic acid (UDPGA), sodium salt, sigma grade, 98-100%, Sigma Chemical Co.

Sephadex G-10-120 gel filtration chromatography matrix, particle size in swollen state 40-120μ in avg. molecular exclusion limit: 700; Sigma Chemical Co.

Sodium dithionite, purified powder, Matheson Coleman & Bell

Tri-sodium penta cyanoamino ferrate - analytical grade, Fisher Sci. Co.

Sulfamic acid, 99%, Mallinckrodt

Triethylamine, aldrich analyzed (99%), Aldrich Chemical Co.

*These chemicals were stored at -20°C for use.

(in excess of 200 kg live weight) moderately lean sows, excluding red-colored ones. Liver tissue processing procedure to extract microsomes and the technique for further isolation and purification of the amine oxidase from microsomes has been dealt with in detail elsewhere [88]. Here, a cursory review of the preparation of microsomes as modified recently by Ziegler [89] is given. Liver obtained from the selected host is immediately sliced into strips not more than 2 cm. thick, transferred to plastic bags containing cold (0° - 2°C) 0.25M Secrose, 50 mM potassium phosphate buffer (pH 7.5), and packed between layers of crushed ice to facilitate rapid chilling. All subsequent steps in tissue processing are carried out at or near 0°.

After reaching the laboratory, a small sample of the tissue is homogenized in 0.25M Sucrose and the oxidase activity of the homogenate is checked. The tissue is then cut into smaller pieces, rinsed with 0.25M Sucrose, and suspended in an equal volume of the sucrose solution. The pH of the medium should be kept around 7.7 with KOH. After 10-15 min., the medium is replaced with fresh 0.25M Sucrose and the pH is again adjusted. Processing of the tissue to obtain microsomes is then started by first removing the tissue from the medium and mincing it with an electric meat grinder, followed by suspension of the minced tissue in 0.25M Sucrose solution, pH adjusted to 7.5. This suspension is next passed through a continuous-flow homogenizer, after which successive

centrifugation is performed at successively higher gravity. First, the homogenate is centrifuged at 1200 rpm for 15 min. and the supernatant fluid is taken. The supernatant obtained is then re-centrifuged at 10,000 rpm for 10 min. to remove the mitochondria. The supernatant is collected, adjusted to pH 5.7 with 1M acetic acid, and centrifuged at 12,000 rpm for 10 min. to obtain acid-precipitated microsomal pellets which are immediately re-suspended in 0.25M Sucrose and adjusted to pH 7.8 by Phosphate buffer. The microsomes are next re-sedimented by centrifugation at 30,000 rpm for one hour, re-suspended in 0.25M Sucrose and re-sedimented to remove excess soluble protein. These washed microsomes are re-suspended in 0.05M Phosphate buffer and stored at -20°C. The purified oxidase and microsomes are shipped on dry ice from the Clayton Foundation Biochemistry Labs in Austin, Texas, to the Norman Campus via air freight. The enzyme batches upon arrival are stored at -20°C. A 5-10 ml samples are dialyzed for use against 0.01M K-phosphate buffer, pH 7.6, at 0°C to remove glycine buffers. 500 ml of fresh and chilled buffer are changed three times during a two-hour dialysis. This results in a final total protein concentration of 7-10 mg/ml, and 70-80 mg/ml for amine oxidase and microsomes, respectively, assayed by Sigma biuret method [103].

Methods

Experimental Equipment

Kinetic study microreactor. Assay microreactor used for all kinetic studies with microsomes and amine oxidase is illustrated in Figure 2. Its specific design features include: a constant-temperature water-jacket integrated with a Haake bath and temperature controller, a liquid-sealed injection port to insure a closed reaction system and an oxygen electrode to measure the substrate-dependent consumption of oxygen. The reaction mass volume is 1.94 mls. Such a microreactor design has two major advantages: 1) High turnover rates are obtained by only moderate stirring, due to fast and uniform concentration distribution of reagent molecules to the enzyme reaction sites; 2) Substrates, cofactors, and the enzyme system, which are usually expensive, are economically used. As shown by Sofer [89], the reaction rate as well as the electrode performance critically depend upon agitation. The reactor is equipped with a magnetic stirrer to improve agitation rate.

Oxygen polarograph. Microsomal oxidative enzyme reaction rates were measured polarographically by monitoring the substrate-dependent rate of decrease in oxygen concentration in the reaction medium of the closed system. A Yellow Springs

FIGURE 2. Assay microreactor. All kinetic studies with liquid as well as immobilized microsomes were conducted in this reactor. Fine temperature control, adequate magnetically-stirred mixing of the reaction mass, and accurate measurement of the rate of oxygen consumption in the closed system during reaction by the use of an oxygen probe are the distinct features of this reactor design. Low catalyst and substrate requirements, and short assay time needed to complete a given run are two advantages of the design. The reactor is emptied by vacuum aspiration.

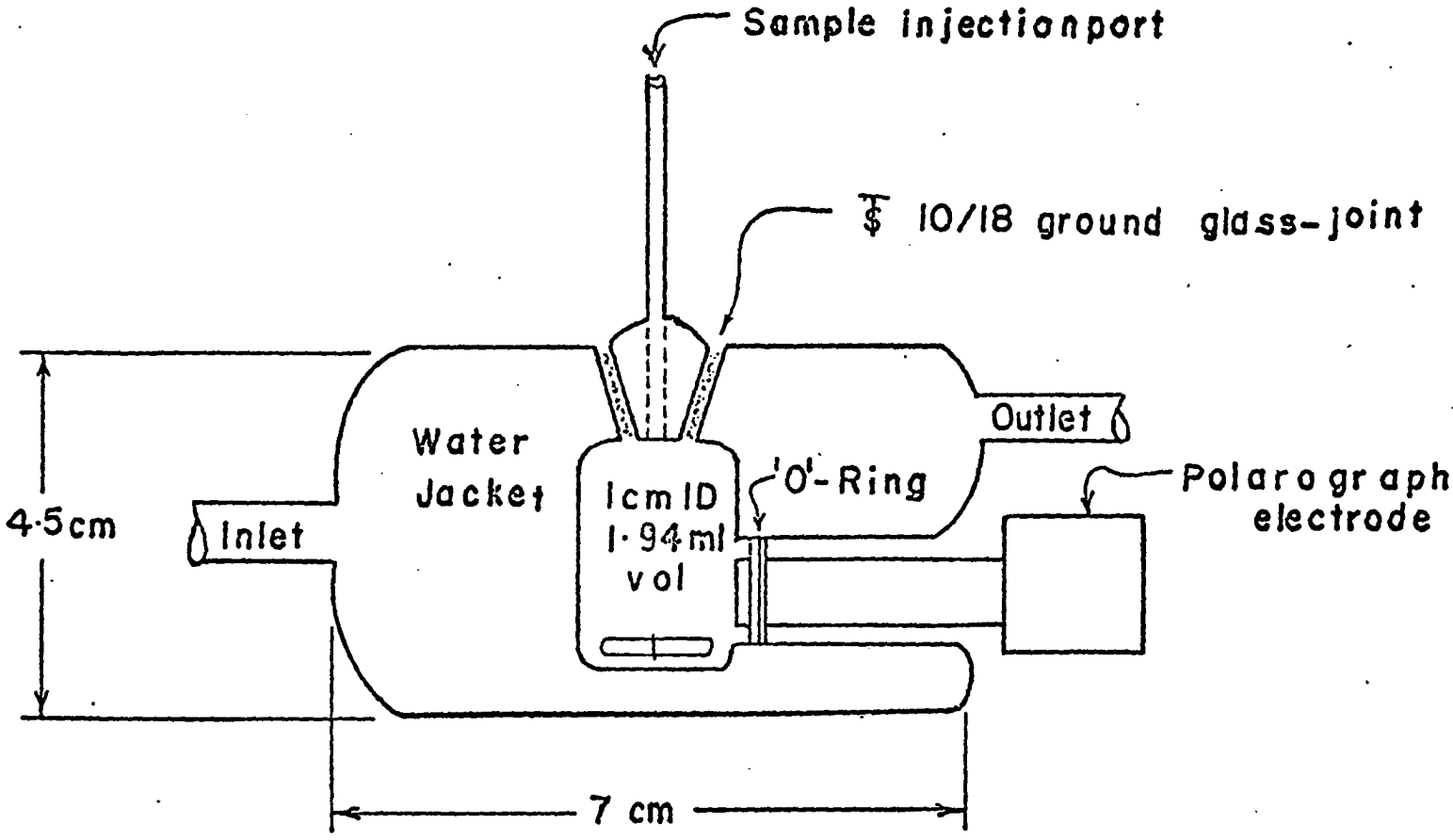
Sample injectionport
$ 10/18 ground glass-joint
Outlet
Water
Jacket
1cm ID
1·94ml
vol
'O'-Ring
Polarograph
electrode
4·5cm
Inlet
7 cm

FIGURE 2

instrument company Model No. 4004 Clark-type oxygen electrode was coupled to the stirred-batch microreactor and a Heath/ Schlumberger model EU-205-11 strip chart recorder via a potentiometric trimming circuit. The schematic diagram of the entire oxygen polarograph system is shown in Figure 3. Monitoring the concentration of oxygen as a substrate polarographically (as opposed to amine substrates and cofactors) has two major advantages and conveniences: 1) Initial rates are recorded instantaneously on the chart recorder in the form of slopes of oxygen decrease. Thus, accuracy of measuring initial enzymatic rates is highly enhanced by avoiding errors introduced due to non-precise quantitative analyses and imperfect termination of the reaction used by other techniques; 2) The time involved in carrying out any required microsomes-catalyzed oxidation assay is reduced to the minimum.

High pressure liquid chromatography apparatus (HPLC). Qualitative analyses of reaction products from microsome-catalyzed two-step sequential kinetic experiments were performed by HPLC. This is one of the most, (if not the most), powerful analytical and separation tools available today in terms of convenience, efficiency of resolution, and sensitivity. The HPLC apparatus used consists of a Rheodyne syringe loading sample injector model 7120, a mini-pump model 396/89 of Milton Roy Co., a μ-Bondapak matrix packed 1/4" OD x 1' column of WATERS Associates (Flow rate: min/max 46/460 ml/hr @ 60Hz, max. Pressure: 5000 Psig), a high sensitivity ALTEX

FIGURE 3. Oxygen polarograph. The polarographic input from the microassay reactor is monitored on the strip-chart recorder via the potentiometric trimming circuit. A microamp box is used for coarse adjustment of the electrode input to the recorder. Finer adjustments and zeroing may be done at the recorder.

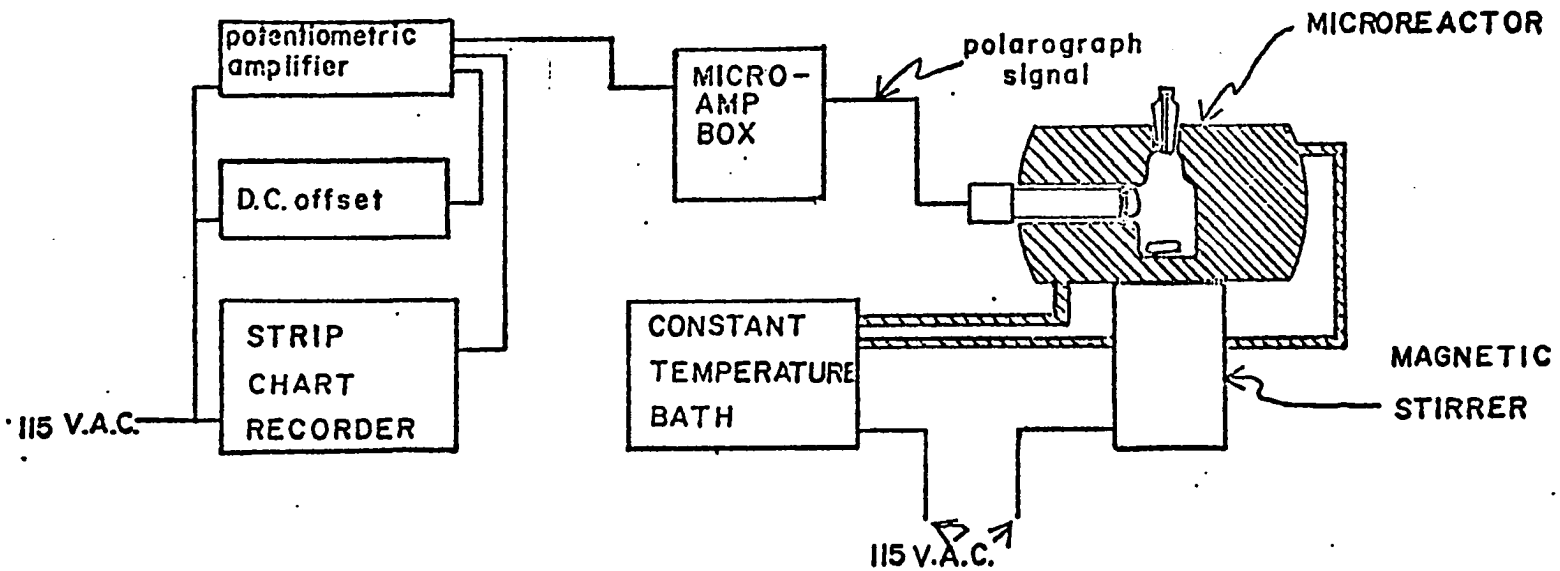
potentiometric amplifier
D.C. offset
STRIP CHART RECORDER
115 V.A.C.
MICRO-AMP BOX
polarograph signal
MICROREACTOR
CONSTANT TEMPERATURE BATH
MAGNETIC STIRRER
115 V.A.C.

FIGURE 3

UV-Monitor and Detector Model 150, and an Omniscribe strip-chart recorder of Houston Instruments.

Gel Permeation Chromatography

Besides HPLC, separation of reaction products, especially N-HO-βNAGluc final product, from the sequential mechanism were also routinely carried out by gel permeation chromatography. Even though this method does not possess as high a resolution as HPLC, it has considerable advantages if an efficient column gel-matrix with minimum retention is used. Adequate separation can be obtained by simple gravity flow through the column by means of a static pressure head of the elution fluid over the column or by applying a low pressure peristaltic pump to introduce the displacing elutant. Another advantage is that one can load at once and separate large volumes of samples in a considerably shorter time than the time required in case of HPLC, where only micro-quantities can be introduced at a time.

The gel-filtration column used was a 2.5 cm ID x 39 cm glass tube packed with Sephadex G-10-120 beads. The bed volume was about 131 cm^3. The eluent wavelength was monitored at 254 nm with a Biochemical UV-Monitor and Altex UV-detector integrated with an Omniscribe chart recorder. A model 1200 Pup Golden Retriever automatic fraction collector from ISCO was used to collect various peak fractions.

Spectrophotometers. Identification of the concentrations of substrate (β-NA); the product of oxidation (N-HO-βNA);

and the conjugation product from the two-step kinetics (N-HO-βNAGluc) for all assays were performed spectrophotometrically where the products exhibited sharp absorption peaks in the characteristic wavelengths corresponding to the respective compounds. Two spectrophotometers were used in this work. A Hitachi model H-191 Single beam spectrophotometer and Beckman DB-GT double-beam grating spectrophotometer. The latter one was especially convenient for automatic scanning of samples over a wide range of wavelengths, both UV(190-340nm), and visible (340-800nm).

Reaction rate assays. Initial activity of microsomes catalyzed N-oxidation of β-naphthylamine was measured polarographically by monitoring the substrate-dependent up-take of oxygen in the reaction medium in the batch magnetically-stirred constant temperature microreactor. The procedure of routine kinetic assay runs is as follows: the oxygen polarograph apparatus, and the water batch which circulates water at a desired temperature through the reactor jacket was turned on. The first essential task is to calibrate the oxygen electrode. This is easily achieved by the following method. The reactor was filled with double-distilled de-ionized water and the magnetic stirrer was turned on. After the desired constant-temperature was obtained in the reactor and after equipment warm-up, which usually takes 15-20 minutes, filtered air was then bubbled through the reactor at a constant slow rate and the oxygen concentration was monitored via the

oxygen electrode on the chart recorder. Air was bubbled until maximum oxygen saturation in the medium (~200 nmoles/ml) was obtained and until this value remained constant with any more further bubbling. After the oxygen concentration reading was calibrated on the chart scale of the recorder in the range of 0-200 nmoles, the air-stream was removed and the water was sucked-off from the reactor by vacuum aspiration. The reactor was next rinsed well with spectro-grade methanol and double-distilled water and was ready for the kinetic run.

Unless otherwise indicated, the reaction medium contained:

—0.1 M K-phosphate buffer, pH 7.4

—NADPH or NADPH-generating system consisting of 0.5 mM $NADP^+$, 1mM G6P and 1 U/ml G6PD

—0.25 mM $MgCl_2$

—0.36 mg/ml pig liver microsomes

After an initial 1-2 min. temperature equilibration, the reaction was started by adding specified amounts of β-naphthylamine. All standard kinetic runs were conducted at 38°C. Since catalytic poisoning of the enzyme amine oxidase by hydrogen peroxide that can be formed during the reaction is well-documented [91], catalase, an excellent decomposer of hydrogen peroxide formation [92], is routinely added to the assay medium. Initial reaction rates were calculated from linear velocities measured during the first 10-20 seconds.

Reaction rates as a function of cofactor/cosubstrate, namely NADPH or oxygen, concentrations were also measured polarographically by varying the concentrations of the respective cosubstrate while keeping all the rest of the reaction components constant. Oxygen concentrations in the assay medium were varied by briefly purging the medium with nitrogen. 0.5 mM constant β-NA concentration was used in the kinetic assays.

Effect of pH. Reaction rates as a function of pH were measured polarographically at 38°C by varying the pH of the reaction medium with the appropriate K-phosphate buffer. Any specified reaction pH was measured simultaneously by using an accurate pH Needle Electrode (MI-408 Needle Electrode) with an external reference electrode (MI-409 microreference electrode), both obtained from Microelectrodes, Inc. The electrodes were coupled to a Perkin-Elmer (Coleman 80) digital pH meter. pH fluctuations in the reaction mass from a specified value during 2-3 min. runs were insignificant.

Effect of temperature. The activity of microsomal oxidative enzymes for β-NA N-oxidation were measured at several constant temperatures ranging from 28°C-56.5°C at pH 7.5. The assay medium used was as given in the reaction rate measurement above. 0.5 mM constant β-NA concentrations were used in all the assays as a reasonably optimum level of substrate concentration which was determined from the previous kinetic runs. Further, reaction rates were investigated as a function

of β-naphthylamine concentration at four different constant temperatures in the range of 27-42°C.

Level of Microsomal Protein Concentrations. To examine the effect of the level of microsomal enzymes, initial reaction rates and N-HO-βNA product yields were measured by varying the concentration of microsomal protein in the reaction medium. The initial rates were measured polarographically, while product yields for specified reaction times were calculated from amylacetate reducing equivalents determined by the method of Tsen [92].

Reaction time-history. N-hydroxy β-naphthylamine formation as a function of assay time from both β-naphthylamine and β-nitronaphthalene was measured by withdrawing serial aliquots as the reaction proceeded. The reaction medium used for β-NA N-oxidation was as described before. However, for β-nitronaphthalene (β-NN) reduction, oxygen had to be completely purged from the reaction medium by nitrogen at the beginning of the experiment. The system was then stoppered tightly and a small constant stream of nitrogen was allowed to flow continuously through a microhole in the stopper for the complete duration of the assay to insure isolation of reaction mass from oxygen leak. No catalase was needed in the β-NN run, but 0.1 mg/ml (F.C.) bovine serum albumin was routinely used. 0.5 mM concentration of each substrate was used for the assays. Concentrations of β-naphthylhydroxylamine were calculated from amyl-acetate reducing equivalents determined by Tsen's Method. This method is briefly described below.

At specified times, as the reaction proceeded, aliquots (.05-.1 ml) of the reaction media were quickly withdrawn and transferred to test tubes containing 1 ml ice-cold water-saturated amyl-acetate and 0.1 ml 1M sodium acetate pH 4.6 in an ice-bath to quench the reaction. Then the samples and the control (withdrawn before the substrate was added) were mixed for 30 seconds on a test tube mixer. The amyl-acetate extract (0.5 ml), separated by centrifugation, was transferred to tubes containing 0.8 ml 0.0025 M bathophenanthroline in absolute ethanol and 0.2 ml of 1M sodium acetate pH 4.6. Then, 0.04 ml of .01 M $Fe(NO_3)_3$ in 0.01 M acetic acid was added and, exactly one minute later, .05 ml of .02 M H_3PO_4 added to stabilize the ferrous bathophenanthroline complex. The absorbance of the complex was measured at 535 nm against a reagent blank using Hitachi Digital spectrophotometer. The validity of these data was also checked by Trisodium pentacyanoamino-Ferrate (TPF) method as described by Poirier and Weisburger [98].

Substrate diffusion limitation. To investigate diffusion limitation of β-NA to the enzyme reaction sites on the microsomal membrane, magnetic stirrer agitation rates were varied from 0 to 800 rpm and reaction rates were measured for each agitation rate polarigraphically. Composition of the reaction mixture and the amount of microsomes used in each assay was as given previously in this chapter, and was identical for all agitation runs.

β-NA and β-NN Sequential Reaction Experiments

Theoretical Analysis

We know from reaction engineering analysis that in the case of 2-step sequential reactions in a homogeneous system, one can control the concentration distribution profiles of the intermediate and end product in a batch reactor as desired by controlling the concentration of the feed [93,94]. For instance, let's assume a first order reaction sequence $A \xrightarrow{k_1} B \xrightarrow{k_2} C$ taking place in an isothermal batch stirred-tank reactor, where $k_1 \leq k_2$. If all of A is fed at once, the concentration distribution profiles of reagent and products in the reactor with time may look like as illustrated in Figure 4a. On the other hand, if A were added in small amounts at a time, making sure that the amount added is practically consumed before the next addition, the profiles will assume a form of distribution indicated in Figure 4b which maximizes the end product. For bienzymic two-step consecutive reaction assays, $A \underset{E_1}{\overset{\leftarrow}{\rightarrow}} B \underset{E_2}{\overset{\leftarrow}{\rightarrow}} C$ where E_1 and E_2 are enzymes 1 and 2, Segel [95], points out that the following conditions should be met: a) none of the conditions required for the second stage reaction should be detrimental to the first step reaction, and vice-versa; b) the first stage reaction must be zero-order with respect to A over the assay time and irreversible; and c) the second-stage reaction must be first order with respect to B and irreversible. Let's look back to our reaction system

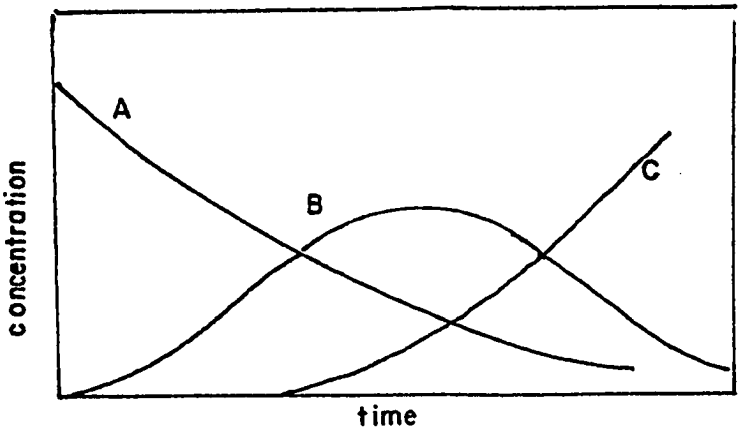

(a)

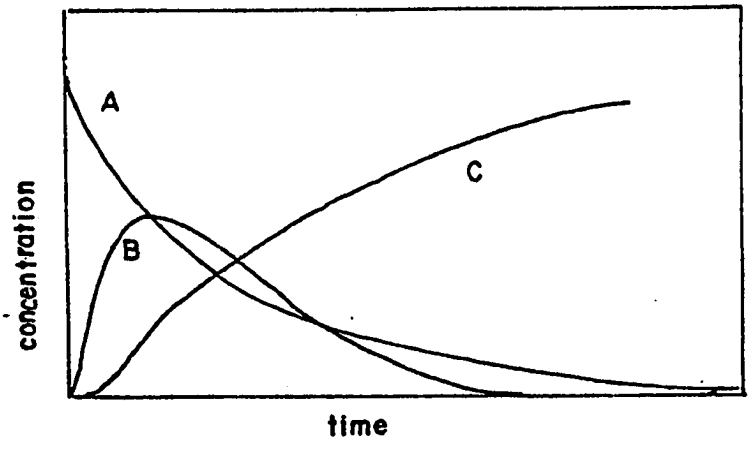

(b)

FIGURE 4

of concern here. Taking β-NA consecutive reaction scheme:

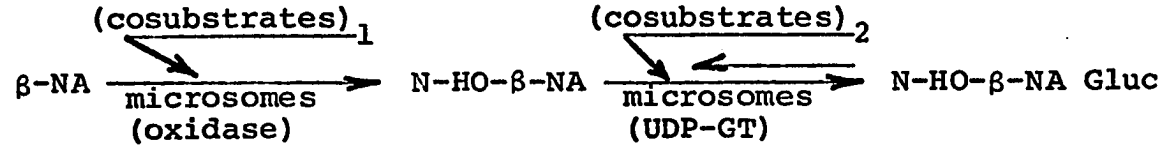

the assay conditions of pH and temperature are approximately the same for both stages of the reaction (pH 7.4-7.6, and T = 38°C). The zero-order requirement for the first stage reaction in (b), however, is not essential especially in cases where the concentration build-up of the intermediate is not desireable due to its inherent unstability. This is the case with N-HO-βNA intermediate as discussed earlier. Therefore, N-HO-βNA concentration build-up and the resulting loss of it through degradation pathways can be avoided while at the same time satisfying the irreversibility condition, if excess enzyme system (microsomes) is used in combination with the strategy of portional addition of the substrate in small quantities in order to push the equilibrium far to the right. The kinetics of the second stage reaction, i.e. N-hydroxy-β-naphthylamine (-N) glucuronide product formation catalyzed by microsomal UDP-glucuronyltransferase obeys first order law at assay conditions specified in this work, as will be shown in the next Chapter. But this second step reaction is reversible [96]. Vessey, et al. [97], have studied the second stage glucuronidation reaction with p-nitrophenol using purified UDP-GT and have reported that UDP-N-acetylglucosamine (UDP-AG) almost completely inhibited the reverse reaction,

while activating the enzyme for the forward reaction at the same time. Therefore, in this work UDP-AG was used with success in the 2-step kinetic assays as an inhibitor of the reverse reaction. Concluding from the analyses presented above, portional addition of substrates (β-NA and β-NN) was used as an optimal technique for in-vitro production of glucuronides via a 2-step sequential mechanism catalyzed by hog liver microsomes.

Experimental Procedure

β-naphthylamine and β-nitronaphthalene microsome-catalyzed 2-step sequential reaction kinetic experiments were conducted in 5 ml volume stirred-tank pyrex-glass reactor with a water-jacket constructed in the laboratory. This reactor is a scaled-up version of the microreactor which was used for all kinetic experiments described in the previous sections. The scale-up of the volume of the reaction mass was necessary in order to obtain larger samples for product separation and analysis as well as to increase the chances for quantitative formation of the glucuronides. The experiments were conducted at 38°C. For β-NA sequential reaction experiment, the reaction medium contained:

2.6 mls 0.1M K-phos. buffer, pH 7.5

0.5 mM $NADP^+$ + 0.2 mM NADPH

2.5 mM glucose-6-phosphate (G6P)

1 u/ml glucose-6-phosphate dehydrogenase (G6PD)

0.1 mM Ethylene-diamine tetraacetic acid (EDTA)

0.1 mM $MgCl_2$

0.5 mM UDP-N-acetylglucosamine (UDPAG)

3.25 mg/ml hog liver microsomes

2.5 mM UDP-glucuronic acid (UDPGA)

The reaction components were added to the reactor in the order of their appearance above from top to bottom, while the mixture was continuously agitated in the reactor. The oxygen concentration in the reaction medium was approximately 0.5 mM. The pH of the reaction mixture was kept at 7.5. After addition of microsomes, the reaction mass temperature was gradually brought up to the experimental reaction temperature (38°C) and 15 µl of .05 M β-NA was introduced to the reactor with a micro-syringe. Immediately after that, 2.5 mM (final concentration) UDPGA, as indicated above, was introduced. Thereafter, with continuous optimal agitation of the reaction mass, 15 µl of .05 β-NA in EtOH were added to the reactor every 4 minutes for 28 minutes making a total of 8 portional injections or an equivalent of 0.12 mls of .05 M β-NA. The reaction was run for 36 minutes, after which the reaction mass was transferred from the reactor into a large test tube and the reaction was quenched by dunking the test tube in boiling water for about 1-2 minutes gently shaking it by hand. The denatured precipitating proteins were removed by centrifugation. The clear reaction mass was then extracted with equivalent volume of diethyl ether in order to remove possible unreacted β-NA. It was next placed in a 40°C water

bath and flushed with nitrogen for 5 minutes to remove any dissolved ether.

Product Separation and Analysis

The clear acquous reaction mixture obtained after the sequence of procedures described above was then transferred to a pre-equilibrated Sephadex G-10-120 gel permeation chromatography column for separation. The elution fluid used was 90% 0.01M K-phosphate buffer, 10% Methanol and 0.01 M EDTA. The pH of the fluid was 7.8. As described earlier, the separation column was equipped with a UV-monitor, detector, chart-recorder and automatic fraction collector. Fractions corresponding to various peaks were collected separately, and each peak fraction was tested for absorption maximum of N-HO-βNA(N) glucuronide by scanning in a Beckman double-beam spectrophotometer. The absorption maximum of the glucuronide was pre-established from a reference standard glucuronide obtained directly from N-HO-βNA by modification of the method described by Kadlubar [70]. The peak fractions, identified as containing the N-hydroxy β-naphthylamine (N) glucuronide product, were combined together and concentrated by freeze-drying at about 60 mm vacuum. The dried sample, (~1.5 g along with K-phosphate salts) dissolved in 4 mls of double-distilled deionized water, was also analyzed by high pressure liquid chromatography (HPLC) against a standard glucuronide sample. The elutant used was H_2O/spectro-grade methanol (1:1 V/V).

β-nitronaphthalene 2-step sequential reaction experiments of N-glucuronidation and product analysis procedures were exactly analoguous to the procedures applied for β-naphthylamine, except that 0.1 ml of 10 mg/ml serum albumin was included in the assay mixture and that oxygen was continuously purged from the reaction medium during the whole assay period.

Immobilization of Microsomes on Porous Glass Beads

a) Bead-surface preparation and activation

The activation of the surface of porous glass beads and preparation for subsequent immobilization of microsomes was performed by a modification of the method reported by Ramachandran and Perlmuter [99]. This procedure of glass surface activation was used by the authors for immobilization of Glucose oxidase. The method adapted is as follows: 5 mls of distilled water was added to 2.5 g alkylamine glass beads in a beaker and then 5 mls of 48% hydrofluoric acid was added slowly, allowing the contents of the beaker to cool between additions. After the mixture was allowed to react for 1 hour, the supernatant was decanted off and 10 N NaOH was added just enough to cover the beads. The slurry was then heated to 80°C for 1 hour, washed with distilled water, and dried overnight in an oven at 80°C. After a fresh and clean bead-porous-surface was renovated by the above procedure,

the dry beads were immersed in a 2% solution of 3-amino-propyltriethoxy silane in acetone in order to introduce 3-aminopropyl chain to the glass surface. Besides playing the role of an extension "arm" to reduce the stearic hindrance to catalyst activity, the alkylamine chain acts as an amine intermediate for chemical linkage of an arylamine for further attachment of the enzyme via diazotation and coupling. After decanting excess liquid, the beads were placed in an oven at 40°C for 24 hours. Next, the alkylamine glass was refluxed for 24 hours in 50 mls of chloroform containing 0.5 ml triethylamine and 1g of P-nitrobenzoyl chloride. Subsequently, after washing with chloroform and ethanol, the beads were dried in an oven at 60°C for 12 hours. Obtained arylnitro glass was reduced by refluxing in 10ml 5% (W/V) sodium dithionite for 1 hour at 125°C. The arylamine glass beads were then washed with water and benzene and dried overnight at 60°C.

b) Diazotation of the arylamine glass and attachment of microsomes

The arylamine glass beads obtained above were slurried in 50 mls of 2N HCl and placed in an ice-bath in a dessicator connected to a vacuum aspirator. When cool (0-4°C), 0.125 g of sodium nitrite was added and the reaction was allowed to proceed under vacuum for 20 minutes. The beads were thoroughly washed next with ice-cold 1% (W/V) sulfamic acid and rinsed

finally twice with 0.1M K-phosphate buffer, pH 7.5. 4 mls freshly dialyzed P.L. Microsomes (70 mg/ml total protein content) were then added to the diazotated arylamine glass beads in a glass beaker. The slurry was gently shaken by hand and then allowed to stand in a refrigerator (0-48) overnight. The next morning, the supernatant was decanted into a separate beaker, and the beads were washed three times with 5 ml volumes of double-distilled water and rinsed twice with 0.1 M K-phosphate buffer (pH 7.5) until no mcirosomal activity was observed in the supernatant. All the supernatants were combined and the amount of left over protein was determined. About 0-2 g of the beads (wet weight basis) was then tested for microsomal N-oxidation activity in the microassay reactor by using dimethylaniline and β-naphthylamine as substrates. After positive results, i.e., relatively high oxidative activities, were identified, the stability of activity was checked every day for four days. The potential of immobilized microsomes-glass beads conjugate was assessed through UDP-glucuronyltransferase activity by synthesizing the N-hydroxy β-naphthylamine glucuronide from N-hydroxy β-naphthylamine using the beads. The active glass beads prepared were stored for further use in the refrigerator.

CHAPTER V

RESULTS AND DISCUSSION

The results of this work can be divided into three main categories. The first broad section deals with the results of the kinetic study of β-naphthylamine N-hydroxylation catalyzed by pig liver microsomes. In this section, results of investigation of reaction rates as functions of the substrate (β-NA), and cosubstrates/cofactors (O_2 and NADPH) concentrations are given. Then, a kinetic model equation that best fits the experimental data is given. Next, the effects of all essential reaction parameters on the rate of β-naphthylhydroxylamine formation are presented and discussed. The second part of the results of this work pertain to the successful in-vitro demonstration of the kinetics of the two-step sequential reactions of N-hydroxylation and subsequent N-glucuronidation of β-naphthylamine and β-nitronaphthalene catalyzed by microsomal enzymes. Based on the experimental conditions and procedures used in this work, this kinetic process was then approximated by a dynamic kinetic model of two-step irreversible first order series reaction. Computer simulation of the concentration-time profiles from the differential rate equations with actual initial conditions

and measured rate constants is given. These data are then compared with similar concentrations vs. time curves obtained experimentally for the substrate (β-NA), the intermediate (N-HO-βNA), and the glucuronide conjugate.

The third part of this work extends the carcinogen kinetics to porous glass-beads immobilized microsomes. Possible covalent attachment mechanism of microsomal amine oxidase to the glass surface is indicated. Then, the potential of immobilized microsomes for metabolic activation of carcinogens was preliminarily assessed with β-naphthylamine. And finally, significant practical advantages accruing from immobilization of microsomes for metabolic activation studies or for carcinogen testing in the long run are discussed and recommendations are formulated to that effect.

PART I

A. β-naphthylamine N-oxidation Kinetics Catalyzed by P.L. Microsomes

Diffusion Limitation

The first item of concern for the kinetic study was the determination of optimal agitation speed of the reaction mixture at which diffusion limitation of the reactants to the microsomal enzyme reaction sites is minimized. Figure 5 shows reaction rate as a function of stirring speed. As can be seen from this curve, maximum oxidation reaction rate is observed at about 400 rpm (the speed setting of 3 on the magnetic stirrer). The reaction rate begins to drop rapidly

FIGURE 5. Rate of reaction as a function of agitation speed. The reaction medium was agitated by a magnetic stirrer (MICRO V, Cole-Palmer, Model #4805). The maximum reaction velocity corresponding to minimum diffusion limitation was observed between 300-400 rpm (between 3-4 speed settings). The reaction medium contained: 0.1M K-phosphate buffer, pH 7.4; NADPH-generating system, consisting of 0.5mM $NADP^+$, 1mM G6P and 1.0 U/ml G6PD; 0.25mM $MgCl_2$; 29.0 U/ml catalase; 0.2mM oxygen; 0.36 Mg/ml pig liver microsomes; and 0.5 mM β-NA. The experimental run was made at 38°C. The sharp decline in the rate of the reaction above 500 rpm's can be partially explained by possible "clumping up" together of the microsomal vesicles as the result of which access of reagents to the catalytic reaction sites is being blocked off. For another explanation, see text.

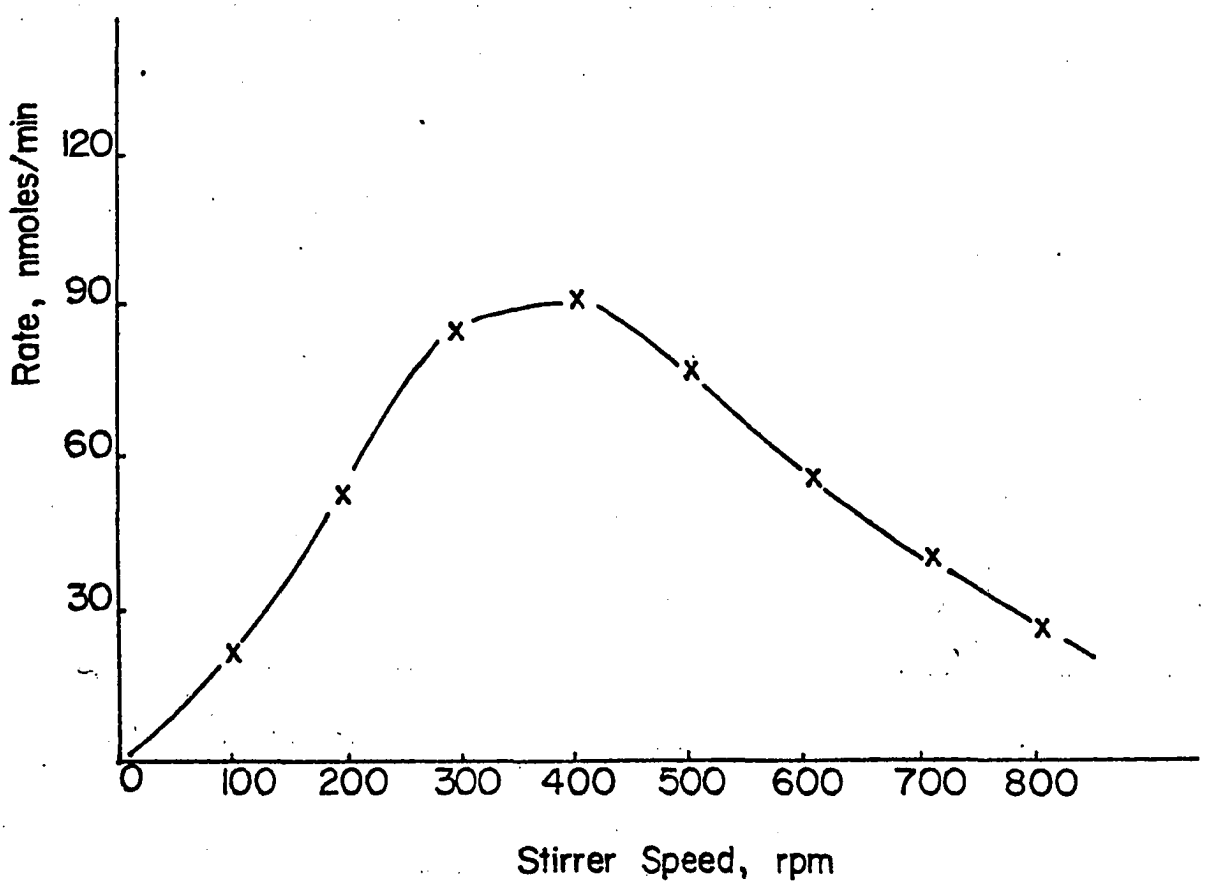
Rate, nmoles/min
120
90
60
30
0
100
200
300
400
500
600
700
800
Stirrer Speed, rpm

FIGURE 5

at higher rpm's, possibly due to the degradation of microsomal membrane proteins. In this work, all kinetic assay runs were conducted at 350 rpm stirring speed in order to avoid any possible harm to microsomal activity and to operate close enough to the maximum diffusion enhancement at the same time.

In order to examine whether the stirred batch microreactor design, with the agitation rate as determined above, had any kinetic advantages over the conventional biochemical incubation assay technique; identical runs were made in the microreactor and in the incubator (Dubnoff Metabolic Shaking Incubator). The results are given in Figure 6. The shaking speed used for the incubator was as commonly reported in the literature [100] (4.5 setting). The concentrations of N-hydroxy β-naphthylamine product were calculated from amylacetate reducing equivalents determined by the Method of Tsen as described in the Methods Section. From the comparison of these two sets of data one could clearly see the strikingly significant advantage of the stirred isothermal microreactor. In fact, for any given time during the first 4-5 minutes of the reaction, the isothermal optimally stirred microreactor gives more than twice the yield of product than that of the incubator.

Reaction Time-History

Figure 7 shows the time history of the formation of N-hydroxy β-naphthylamine in the reaction medium as the reaction progresses. This time profile was measured for

FIGURE 6. Microassay stirred-batch reactor (MASR) vs. shake-bath incubator data. The assay mixture and the reaction conditions are as indicated under the legends to Figure 5 and in the Methods. The fact that MASR yields more than twice the amount of product in comparison with the conventional incubation technique (especially, during the first 4-5 minutes of assay), emphasizes the advantage of this system for application in carcinogen kinetics study.

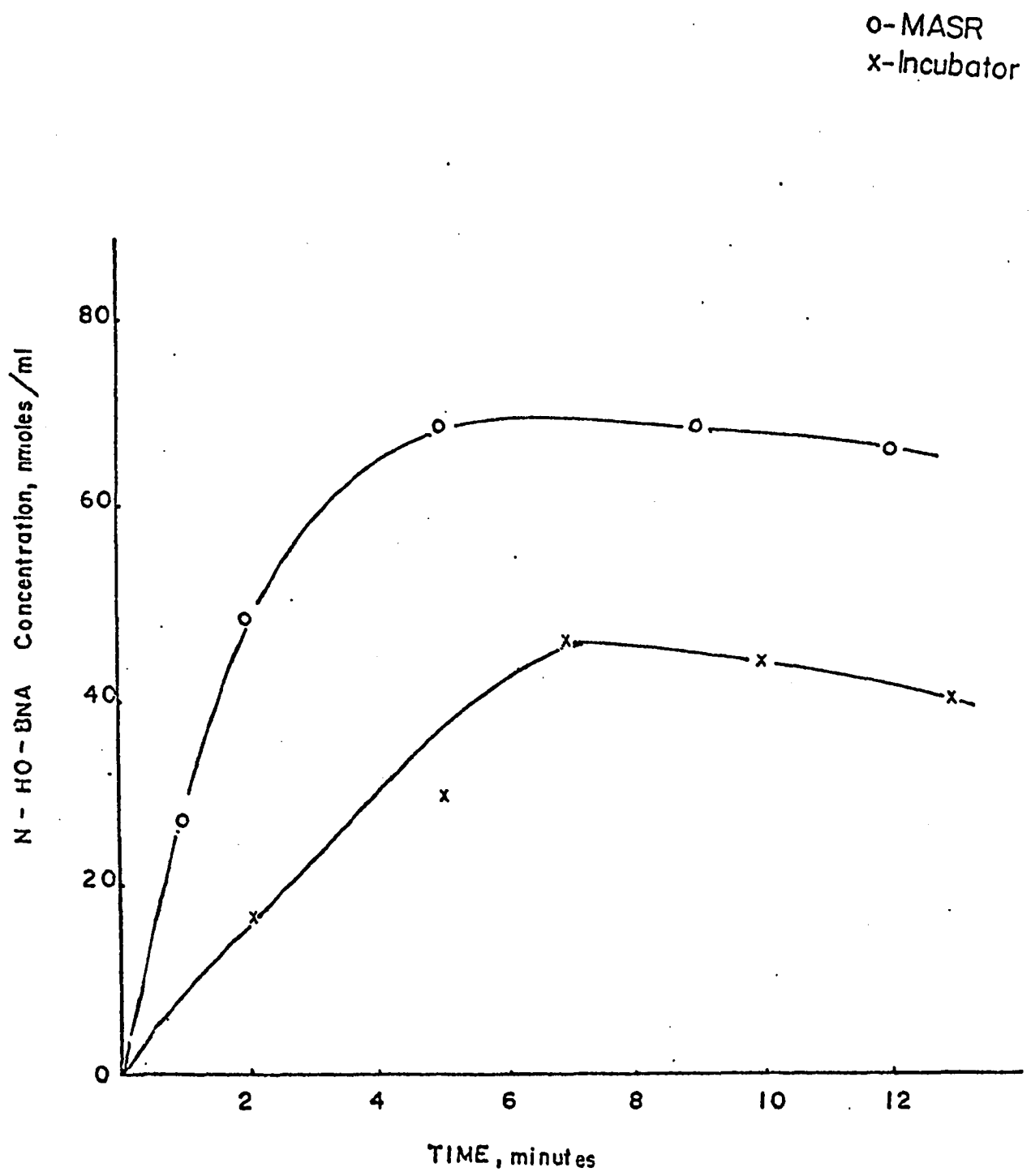
o-MASR
x-Incubator
N - HO - BNA Concentration, nmoles/ml
80
60
40
20
0
2
4
6
8
10
12
TIME, minutes

FIGURE 6

various microsomal protein concentrations ranging from 0.21 mg/ml to 1.75 mg/ml. The reaction mixture was as indicated in Methods. The most important conclusion that can be drawn from these data is that the time optimum for maximum product formation, [N-HO-βNA] max, lies between 4-6 minutes for all practical concentrations of microsomes. At prolonged assay times the N-hydroxy product follows a decreasing trend. This evidence has also been apparent from Figure 6. The decrease could be explained to occur due to a couple of factors. First, it could be due to the inherently unstable nature of the N-HO-βNA which would in time undergo a non-enzymic oxidative degradation. Secondly, as the N-hydroxy accumulates, the deactivation reaction is likely to occur in the presence of a small amount of the endogenous microsomal UDPGA via UDP-Glucuronyltransferase by a sequential mechanism. Evidence on this possible mechanism would be the subject of Part II. As was given in the Methods Section of this work, the time optimum for N-HO-βNA formation obtained from the experimental results of Figure 7 was applied in the two-step sequential reaction experiments to control the concentration of this intermediate. At low microsomal concentration however, the concentration-time profile is approximately linear.

It would be quite interesting to compare the results of Figure 7 with similar profiles of N-hydroxy product formation vs. assay time for pure microsomal flavoprotein amine oxidase catalyzed reaction. Product formation vs. reaction coordinate curves investigated using pure amine

FIGURE 7. Reaction time-history for β-NA N-oxidation: microsomes assay. N-hydroxy β-naphthylamine formation (yield) as a function of assay time was measured at 38°C for four different concentrations of microsomal protein as indicated in the figure. The composition of the reaction medium was as described in Methods. It appears that for all microsomal concentrations of practical interest, the maximum for N-hydroxy β-naphthylamine concentration is observed between 4-6 minutes, and that the concentration of the latter starts to decrease continuously thereafter, possibly, via the deactivation pathway or side-reactions.

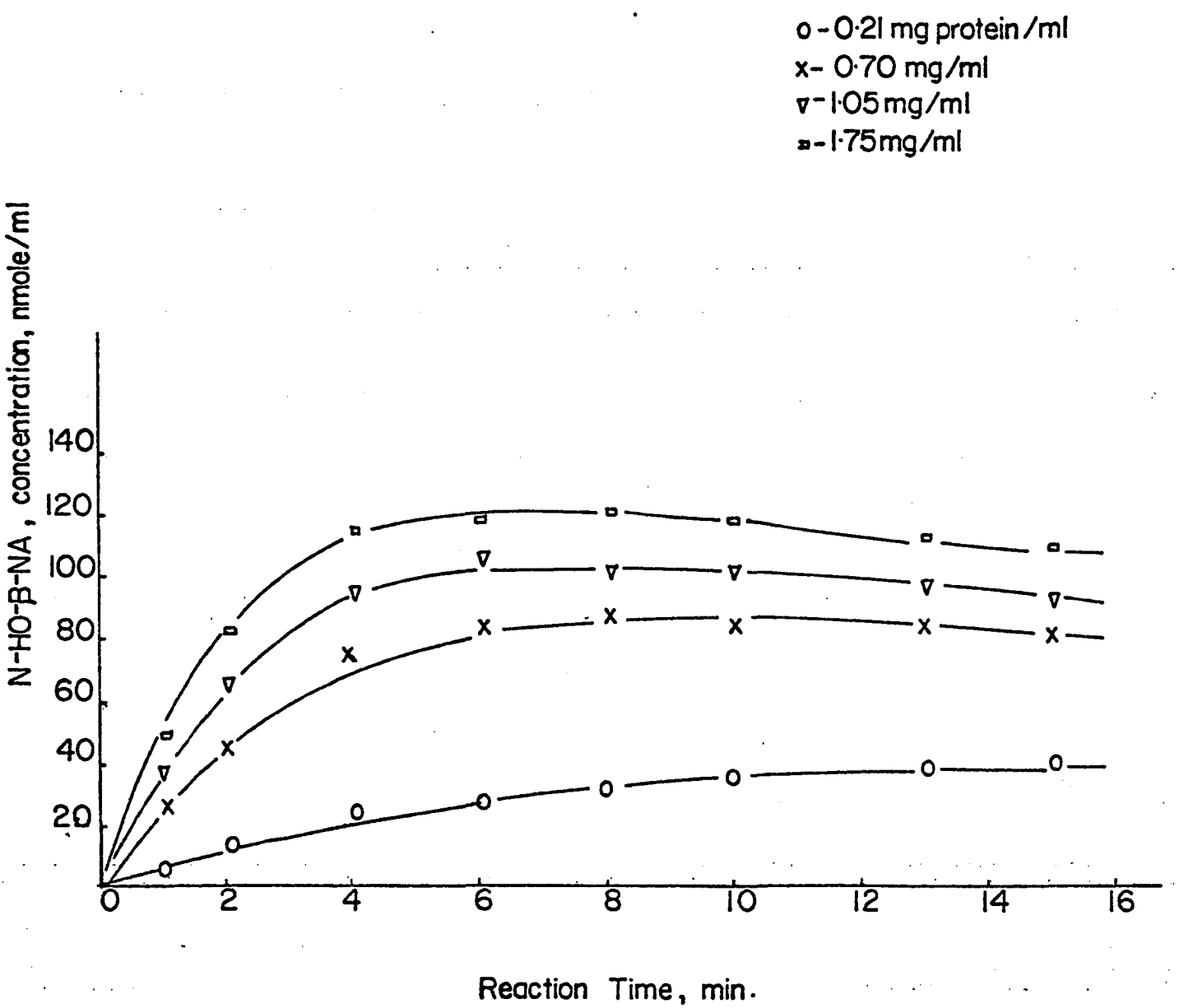
o - 0·21 mg protein/ml
x - 0·70 mg/ml
▽ - 1·05 mg/ml
▫ - 1·75 mg/ml
N-HO-β-NA, concentration, nmole/ml
140
120
100
80
60
40
20
0
2
4
6
8
10
12
14
16
Reaction Time, min.

FIGURE 7

oxidase enzyme are shown in Figure 8 for four different concentrations of the enzyme. Striking similarity pattern between these two results with respect to the catalytic N-oxidation of β-naphthylamine to N-hydroxy-β-naphthylamine stresses the fact that, indeed even in whole microsomes, the oxidation of the primary arylamine is amine oxidase-specific. However, two important points need to be stressed here. First, as can be seen from close examination of Figures 7 and 8, the linearity of product formation in the case of pure oxidase is about 1 minute for practically all the concentrations of oxidase shown, while in the case of microsomes, the linear portion is generally about twice larger than that of pure oxidase. Secondly, product accumulation with reaction time for microsomes-catalyzed N-oxidation is much higher than that of pure amine oxidase-catalyzed reaction. This enhanced stability of product formation and accumulation in microsomes can be explained by the following possibilities: 1) microsomal lipids stabilize the N-hydroxy product by inhibiting to a significant degree the non-enzymic auto-oxidation pathway of the product to the Nitroso form. 2) Microsomal NADPH-cytochrome c reductase is known to stabilize N-hydroxy 2-naphthylamine formation and accumulation by catalyzing the backward reaction of 2-nitroso naphthalene (imminently formed in the reaction mixture to some degree) to the N-hydroxy product. These possibilities have been vividly demonstrated by Ziegler [59]. The above comparison of data for pure oxidase and whole microsomes is based upon 4-10 wt.% oxidase

FIGURE 8. Reaction time-history for β-NA N-oxidation: MFMF amine oxidase assay. N-hydroxy β-naphthylamine formation as a function of reaction time was measured at 38°C for varying concentrations of amine oxidase as indicated in the figure. The composition of the reaction medium was as described in Methods. The time-optimum for maximum N-HO-βNA formation lies between 4 and 5 min., after which, the N-hydroxy product continues to follow a decreasing pattern.

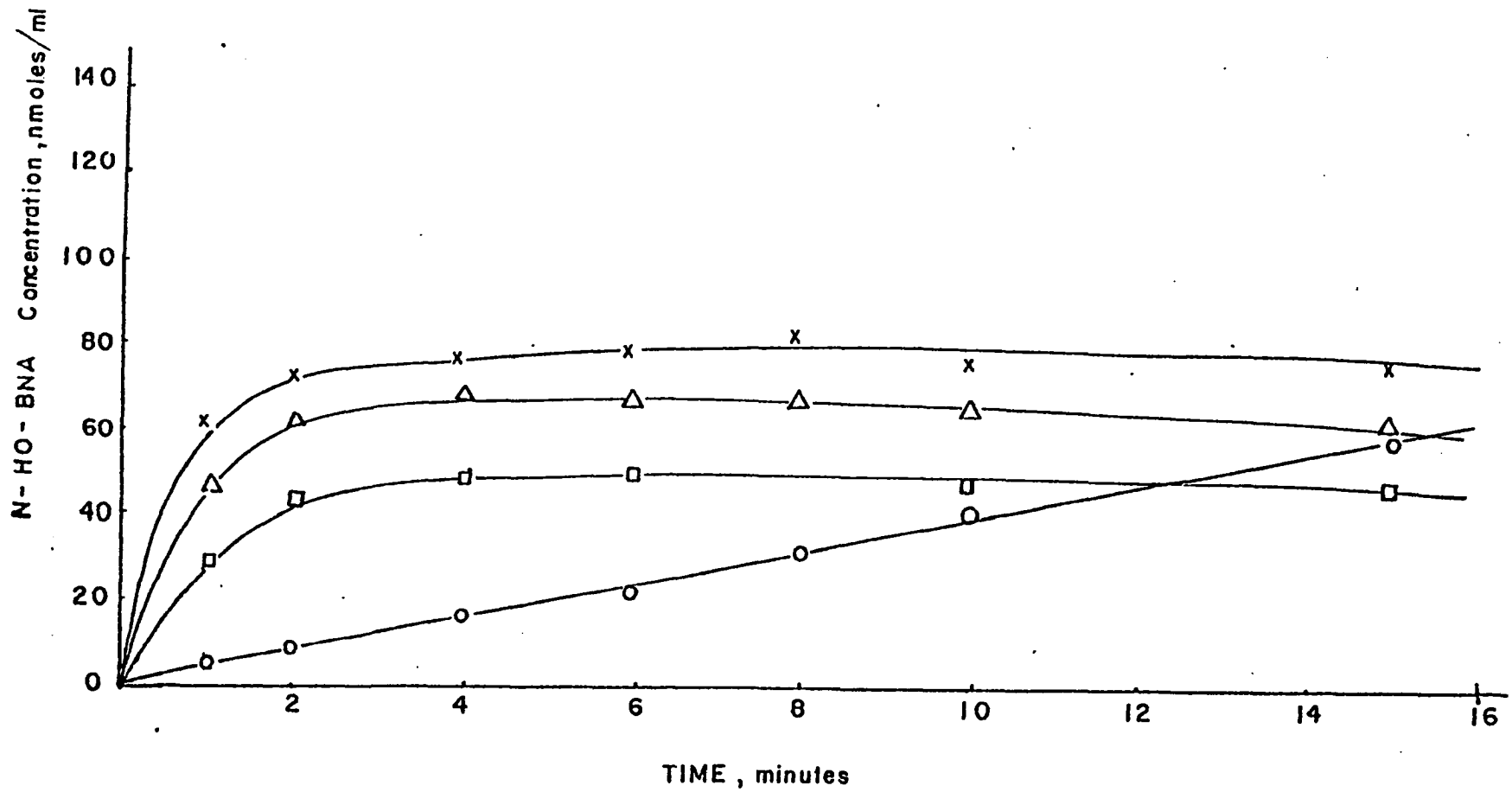
o – 1.4 X 10⁻² mg/ml
□ – 2.8X 10⁻² mg/ml
Δ – 4.2X 10⁻² mg/ml
X – 6.5X 10⁻² mg/ml
N-HO-BNA Concentration, nmoles/ml
0
20
40
60
80
100
120
140
2
4
6
8
10
12
14
16
TIME, minutes

FIGURE 8

concentration in P.L. microsomes total protein content [102]. The microsomal protein concentrations used in Figure 8 were calculated to contain approximately the corresponding concentrations of oxidase indicated in Figure 8 for the purpose of comparison.

Reaction Rates

Initial reaction rates as functions of the substrate concentration were measured polarographically as described in Methods. Figure 9 shows the variation of initial activities for microsomes catalyzed reaction with change in β-NA concentration. The composition of the reaction mixture was as given in the legends to the figure. Two things are evident from this figure. First, the reaction velocity is inhibited at high substrate concentrations. This velocity slump at high substrate concentrations could be presumed to be due to substrate-inhibition. Secondly, the velocity curve as a function of substrate concentration does not obey the classical Michaelis-Menten kinetics. Right from the outset, it should be stressed here that the microsomal initial activity being referred to in the discussion above is the activity of amine oxidase which is specific to β-NA N-oxidation in the microsomal system. Of course, here, one might contend whether it is really possible to talk about a specific enzymic kinetics when, what is dealt with is not a pure enzyme, but whole microsomes. This would be breaking the traditional rules! However, this alternative approach

FIGURE 9. Microsomal N-oxidation initial activity as a function of substrate (β-NA) concentration. As described in Methods, the assay medium contained: 0.1M K-phosphate buffer, pH 7.4; 0.5mM $NADP^+$; 1mM G6P; 1.0 U/ml G6PD; 0.25mM $MgCl_2$; 29.0 U/ml catalase, 0.2mM O_2, 0.36 Mg/ml microsomes, and the indicated amounts of the substrate. The initial activities were measured at 38°C polarographically by a substrate-dependent increase in oxygen consumption. It is obvious from the figure that the rate does not follow the classical Michaelis-Menten kinetics.

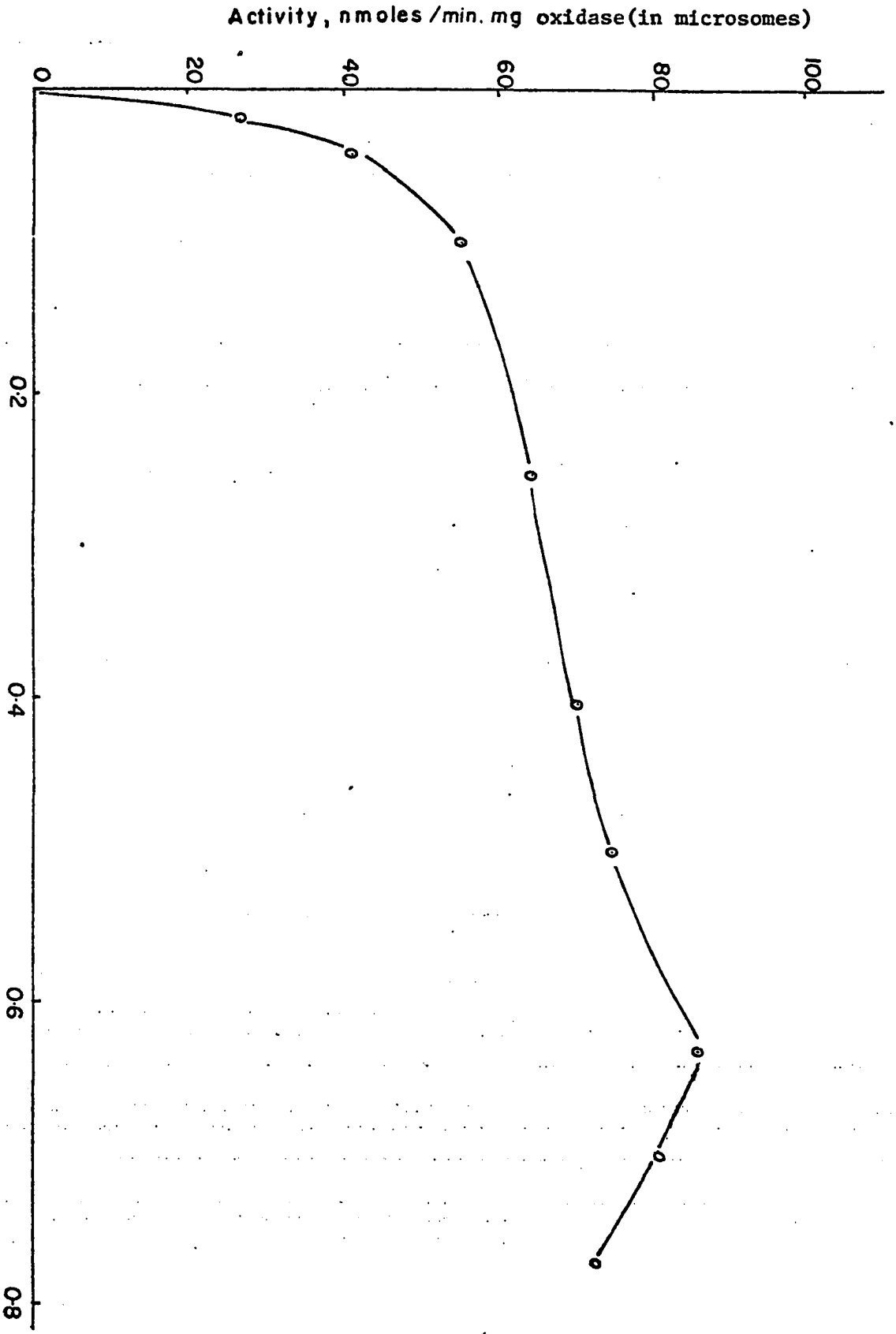
Activity, nmoles /min. mg oxidase(in microsomes)
0
20
40
60
80
100
0·2
0·4
0·6
0·8
[β-NA], mM

FIGURE 9

is a must in certain situations. If the interest is not in the application of an enzyme as a single isolated pure protein, but in the function of the enzyme as an integral component of a whole composite system, the kinetic behavior of the enzyme in question has to be investigated in its state of coexistence in the composite system. This is due to the fact that modification of the activity of the enzyme is possible in the integral system containing other enzymes, phospholipids and endogeneous substrates. Such may be the case with amine oxidase in microsomes. Since it is whole microsomes which is applied for metabolic activation in carcinogen screening attempts the activity of oxidase in microsomes in such a case of practical application is the point in discussion.

A similar experimental run was made with pure amine oxidase to determine initial activities as a function of β-NA concentrations. The result is shown in Figure 10. The amazing similarity between velocity curves of Figures 9 and 10 is one more indication that β-NA N-oxidation is oxidase-specific and that, even in whole microsomes, the enzyme catalytic behavior is not significantly altered. Both curves show the existence of strong allosteric effects of enzyme site interactions with binding of substrate molecules. Some distinguishing features however, are observed. The slope of the microsomal reaction rate curve of Figure 9 is lower than that of pure oxidase (Figure 10) at low substrate concentrations. Secondly, inhibition of activity (possibly,

FIGURE 10. MFMF amine oxidase N-oxidation initial activity vs. substrate (β-NA) concentration. The composition of the reaction mixture was as given in the legends to Figure 9, except that 0.036 Mg/ml pure amine oxidase was substituted for microsomes. The initial activities were measured polarographically at 38°C as described in Methods. Possible substrate-inhibition is apparent at high concentrations of the latter in both Figures 9 and 10.

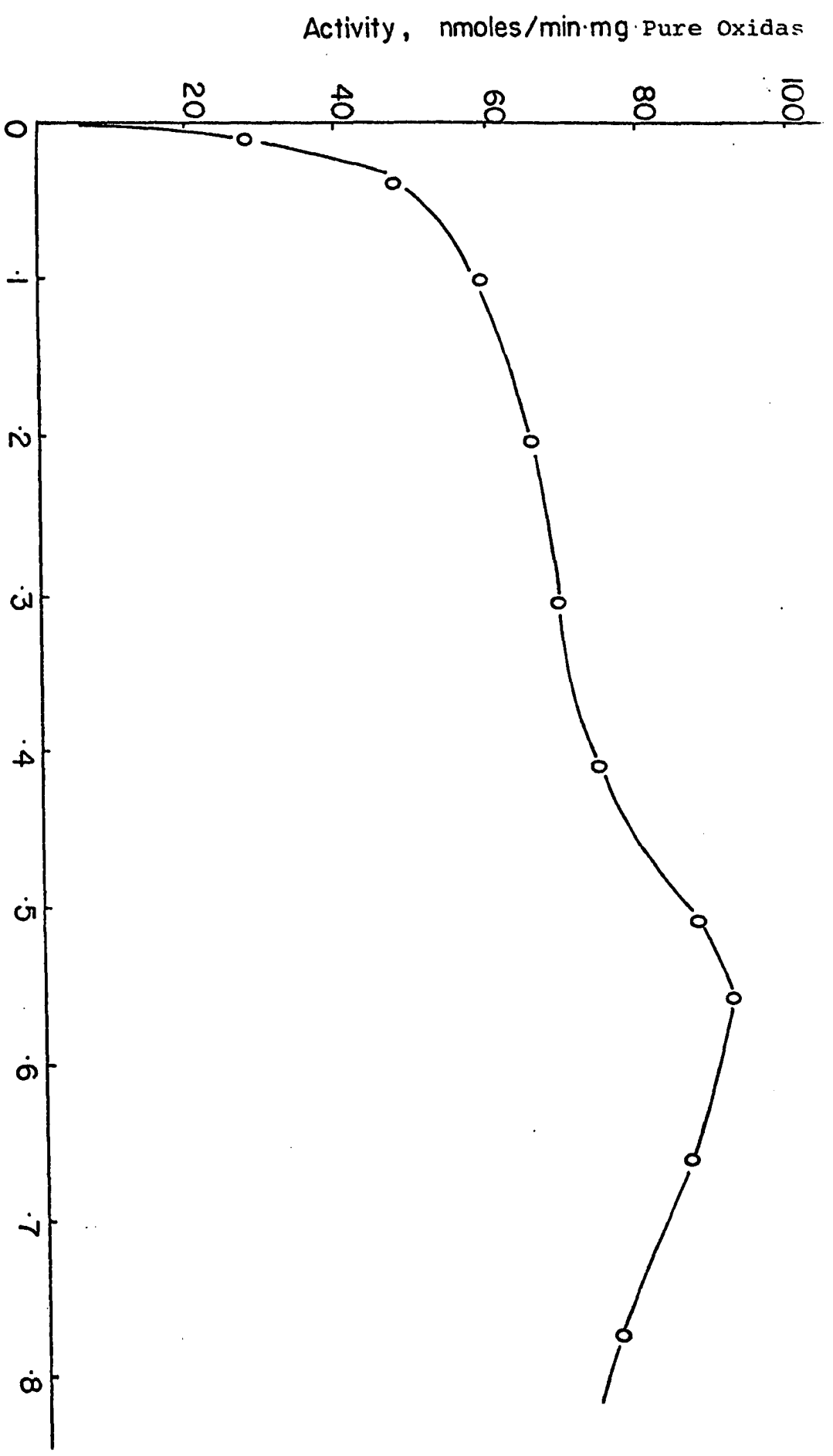
Activity, nmoles/min·mg Pure Oxidas
0
20
40
60
80
100
.1
.2
.3
.4
.5
.6
.7
.8
[B-NA], mM

FIGURE 10

substrate-inhibition) starts at a slightly lower substrate concentration in the case of pure amine oxidase-catalyzed reaction than that required for microsomes. Most likely, these differences are diffusion-related. In the case of pure amine oxidase-catalyzed reaction, substrate diffusion into the enzyme reaction sites can be expected to occur at a much faster rate than in the case of microsomes-catalyzed reaction, for the simple reason that the surface of the pure enzyme in its isolated form is totally exposed to substrate molecules and will not pose as much diffusion-restriction as it would when it is entrenched in the microsomal membrane.

The double reciprocal plot $\frac{1}{V}$ against $\frac{1}{[\beta\text{-NA}]}$ is shown in Figure 11 for both microsomes and oxidase catalyzed reactions of Figures 9 and 10. The maximum reaction rates (V_{max}), expressed in activity units, and the apparent Michaelis-Menten saturation constants (K_m), obtained by a reasonable extrapolation of the linear region, are given in Table 2-A.

TABLE 2-A

Kinetic Constants for Catalytic N-Oxidation of β-naphthylamine by Microsomes and Flavoprotein Amine Oxidase

	Microsomes	Oxidase
K_m, mM	0.10	0.07
V_{max}, $\frac{\text{nmoles}}{\text{min. mg. prot.}}$	94	86

FIGURE 11. Double-reciprocal Michaelis-Menten plots of β-naphthylamine N-oxidase activity for microsomes and for pure MFMF amine oxidase. The approximate (extrapolated) K_M values for the substrate are, 0.1 and 0.07 mM for microsomes and pure oxidase catalyzed reactions, respectively.

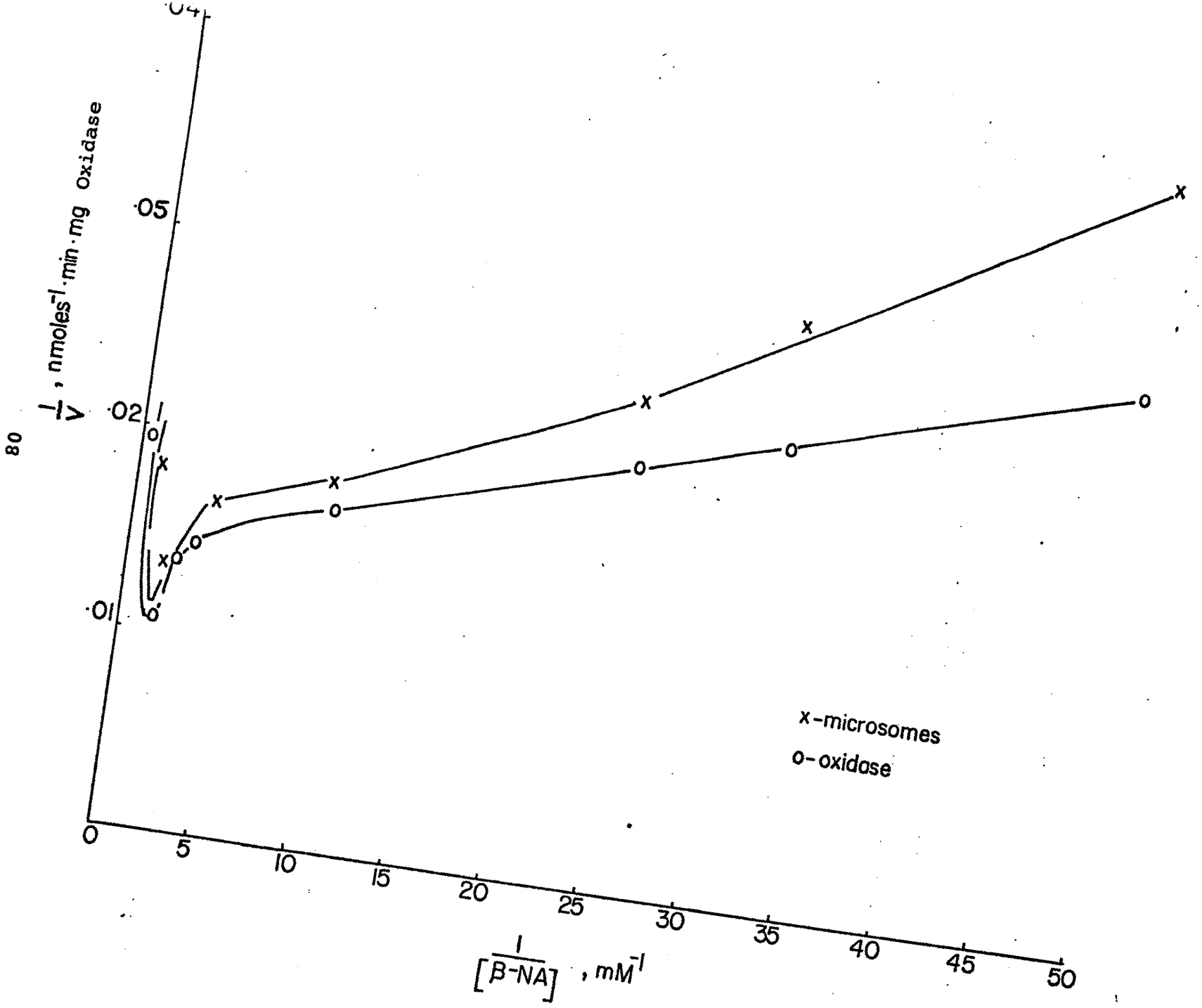
80
$\frac{1}{V}$, nmoles^{-1}·min·mg Oxidase
·04
·05
·02
·01
0
5
10
15
20
25
30
35
40
45
50
$\frac{1}{[B\text{-}NA]}$, mM^{-1}
x-microsomes
o-oxidase

FIGURE 11

As can be seen from the figures in the table above the concentration of β-NA required to give half-maximal velocity is approximately 43% higher than that required for pure oxidase at the same experimental conditions.

Figure 12 shows percent conversion of substrate as the concentration of the latter is increased. For each assay the reaction was run for 3 minutes. It is obvious from these data that conversion drastically increases at low substrate concentrations. Even though, such profiles of conversion vs. reactant concentration are not uncommon, the data of Figure 12 are of special significance for the design of the two-step sequential reaction which will be discussed in the later section of this chapter. Low β-NA concentrations assure high enzymic conversion to N-HO-β-NA and at the same time minimize accumulation of the substrate in the reaction mass, thus avoiding possible substrate-dependent side reactions.

Microsomal N-oxidation reaction rates were also measured as function of the concentrations of cosubstrates O_2 and NADPH while keeping the amounts of all the rest of the reagents constant. The Michaelis-Menten double reciprocal plots are given in Figure 13 for oxygen, and Figure 14 for NADPH. A summary of the apparent Michaelis-Menten kinetic constants is given in Table 2-B. The kinetic constants, which represent the concentration of the corresponding reagent required to half-saturate the enzyme, are very high for the substrate and NADPH as can be seen from Table 2-B.

FIGURE 12. Percent conversion vs. substrate (β-NA) concentration. Microsomes-catalyzed β-NA conversion to N-HO-βNA was measured in the indicated range of substrate concentrations. All the assays were run for 3 minutes at 38°C. The N-hydroxy β-naphthylamine product yields were calculated from amyl-acetate reducing equivalents determined by the method of Tsen [92]. N-HO-βNA product yield drastically falls at high substrate (β-NA) concentrations, possibly, due to the substrate-inhibition or side non-enzymic reaction.

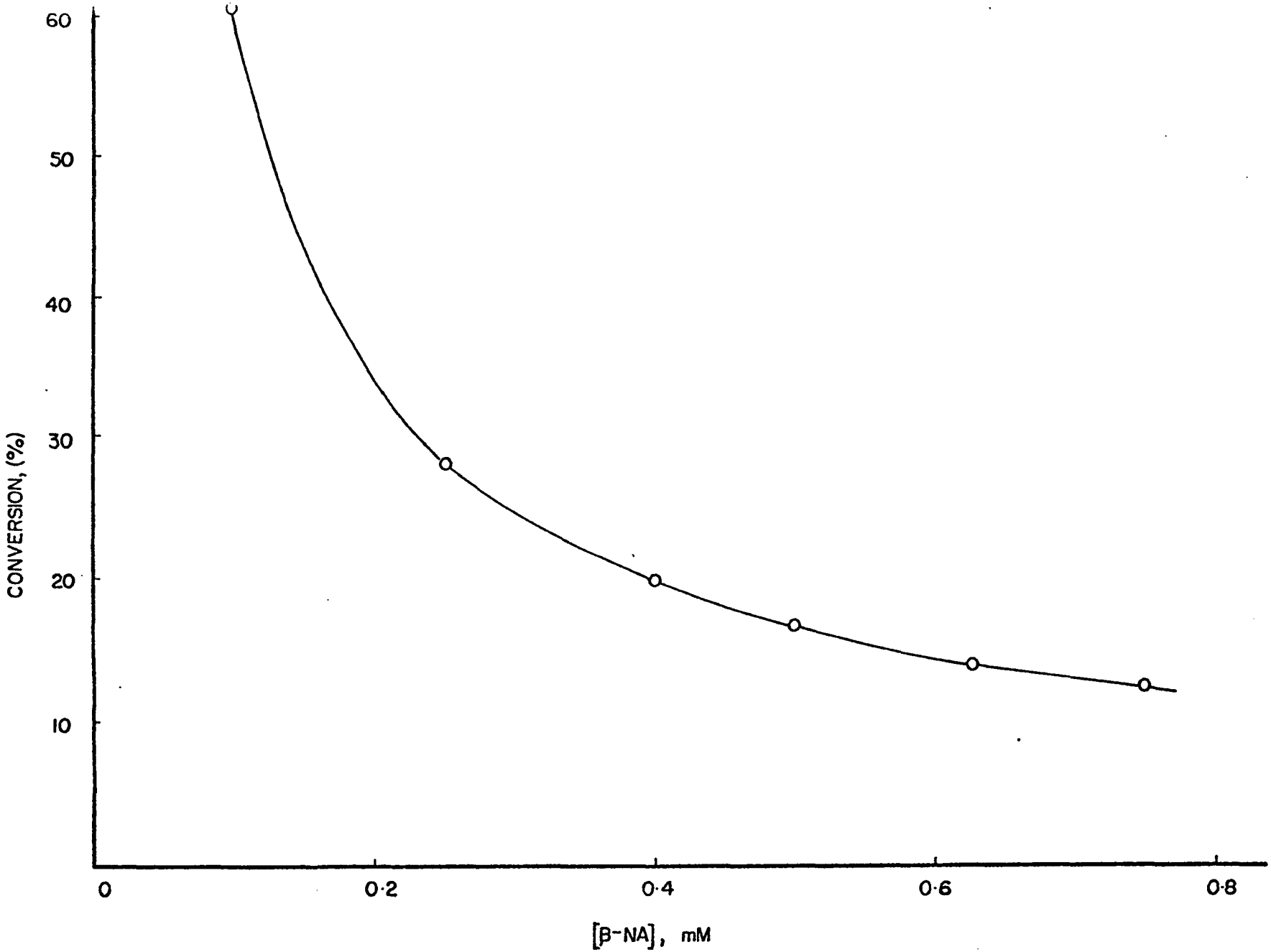

FIGURE 12

TABLE 2-B

Kinetic Constants for Catalytic N-Oxidation of β-naphthylamine by P.L. Microsomes

Constant	Value for β-NA(substrate) N-Oxidation
$K_{substrate}$, mM	0.10
K_{O_2}, μM	0.0155 (=1.55×10^{-5} mM)
K_{NADPH}, mM	1.110

This may be due to diffusion limitation through the microsomal membrane to the specific enzyme reaction sites. This effect would be especially significant in the case of a high molecular weight substance (cofactor) such as NADPH; and the value of the constant reflects the validity of this conclusion. Besides the diffusion limitation, there is a much more significant factor that tends to increase $K_{substrate}$. If we recollect the scheme in Figure 1, as discussed earlier, primarily the imine form (which is in equilibrium with the amine form) of the arylamine in the reaction mixture is N-oxidized due to its high necleophilicity.

Reaction Rate Model

As has been observed from the comparison of experimental reaction rate data for microsomes and pure oxidase, the catalytic N-oxidation of β-naphthylamine in microsomes can preliminarily be concluded as oxidase-specific. The next

FIGURE 13. Double-reciprocal plot of microsomal β-naphthylamine-N-oxidase activity vs. oxygen concentration. The assay was run at pH 7.4 and 38°C. Oxygen concentrations in the reaction medium were varied by diluting with an appropriate proportion of nitrogen. Initial activities were measured polarographically as described in Methods. From the plot, it appears that O_2 binding obeys the Michaelis-Menton kinetics. K_{O_2} is found to be 1.55×10^{-5}mM.

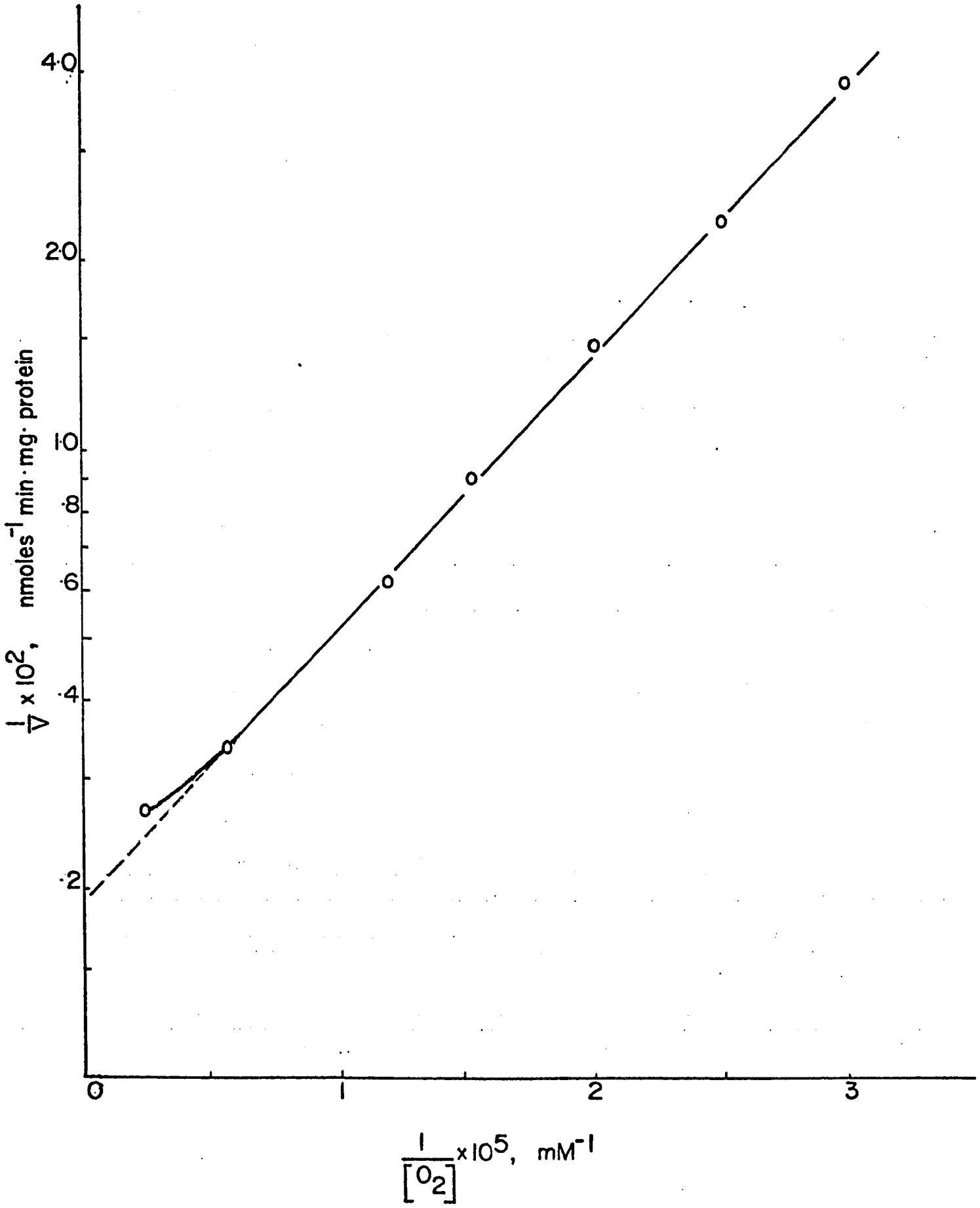
4·0
2·0
1·0
·8
·6
·4
·2
0
1
2
3
$\frac{1}{V} \times 10^2$, nmoles^{-1} min · mg · protein
$\frac{1}{[O_2]} \times 10^5$, mM^{-1}

FIGURE 13

FIGURE 14. Double-reciprocal plot of microsomal N-oxidation activity for β-NA vs. NADPH concentration. Initial activities were measured polarographically at 38°C, varying the concentration of the cofactor NADPH. The reaction mixture used was identical to that used for all kinetic measurements, and is given in Methods and in the legends to Figure 9. K_{NADPH} measured was equal to 1.11mM.

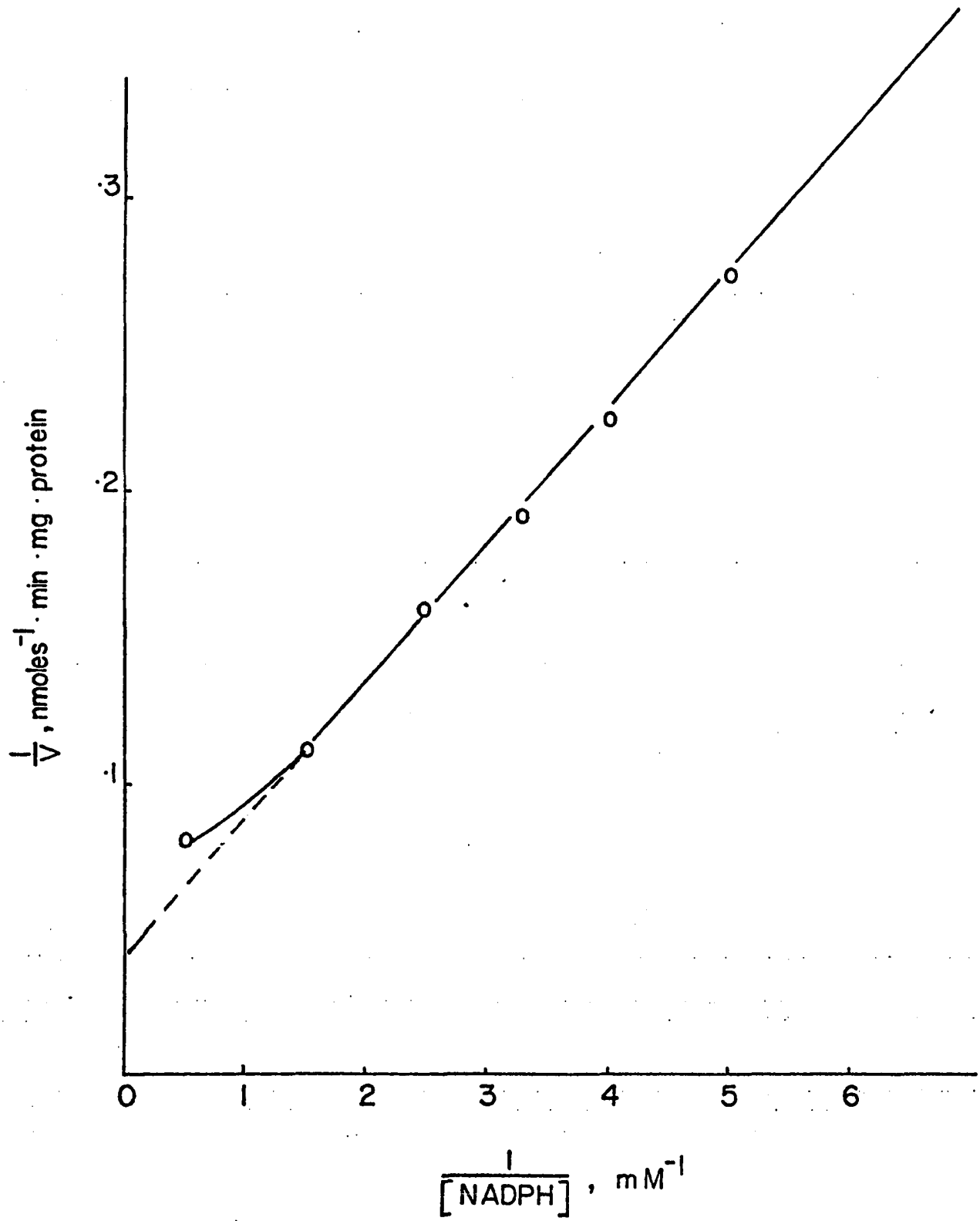

FIGURE 14

step was the determination of an approximate reaction rate model for β-naphthylamine catalytic N-oxidation by pure amine oxidase. When the oxidase experimental kinetic data were computer-fitted to the rate equation (1) which was proposed by Poulsen and Ziegler [102] for trimethylamine and methimazole oxidation by the same enzyme, a good agreement was obtained.

$$v = \frac{V_m}{\frac{K_a K_b}{AB} + \frac{K_a}{A} + \frac{K_b}{B} + \frac{K_c}{C} + 1} \qquad (1)$$

where, A, B, and C refer to NADPH, oxygen and substrate, respectively. The notations are that of Cleland [101]. K_a, K_b, and K_c are the values of the corresponding kinetic constants. This same rate model (equation (1)) also gave a satisfactory fit for microsomes-catalyzed β-NA N-oxidation experimental data.

The purpose of this treatise is not, however, to determine an accurate enzymic rate equation for microsomal oxidation which, to say the least, is quite complicated and has no practical significance. It is rather to define the significance of the wide variety of factors which affect the kinetics of product formation in the practical application of microsomes in large amounts for metabolic activation of carcinogens.

Effect of pH, Temperature and Microsomes Concentration on the Formation of N-HO-βNA

pH. Microsomal N-oxidation activities were measured at various reaction pH, ranging from pH 6.5 to 9.5. The plot of microsomal activity as a function of pH is shown in Figure 15. The composition of the reaction mixture is given in the legends to the figure. As can be seen from these data the pH maximum lies around 7.8. However, all routine kinetic assays were run at pH 7.4-7.5 in order to avoid rapid loss of enzymic activity at its optimal pH.

Temperature. Figure 16 shows the dependence of activity on temperature. N-oxidation activity maximum is indicated at 41°C, and then a sharp drop in activity is observed. For the same reason as for the pH maximum, the practical application of optimum temperature (41°C) for kinetic assays is offset by rapid enzyme denaturation. This is indicated clearly by Figure 17 which compares the stability of β-naphthylamine N-oxidation activity for microsomes at 37 and 41°C. For example, the activity that can be obtained after 6 minutes of incubation of microsomes at 41°C is about 17% of the original activity, while 65% is retained after incubating for the same period of time at 37°C. To give a vivid comparison, the activity obtained after 6 minutes at 37°C is by about 175% higher than that which is obtained after incubating at 41°C for the same period of time. Therefore, a physiological temperature, 37.5 ± .5°C, must be used for microsomal assays

FIGURE 15. β-naphthylamine N-oxidation activity as a function of pH. All initial activity runs with different pH's were carried out polarographically at 38°C. The pH of the reaction medium was monitored accurately by a pH Needle Electrode with an external micro-reference electrode (Microelectrodes, Inc., Londonderry, NH) coupled to a Perkin-Elmer digital pH meter. The assay mixtures were as given in Methods.

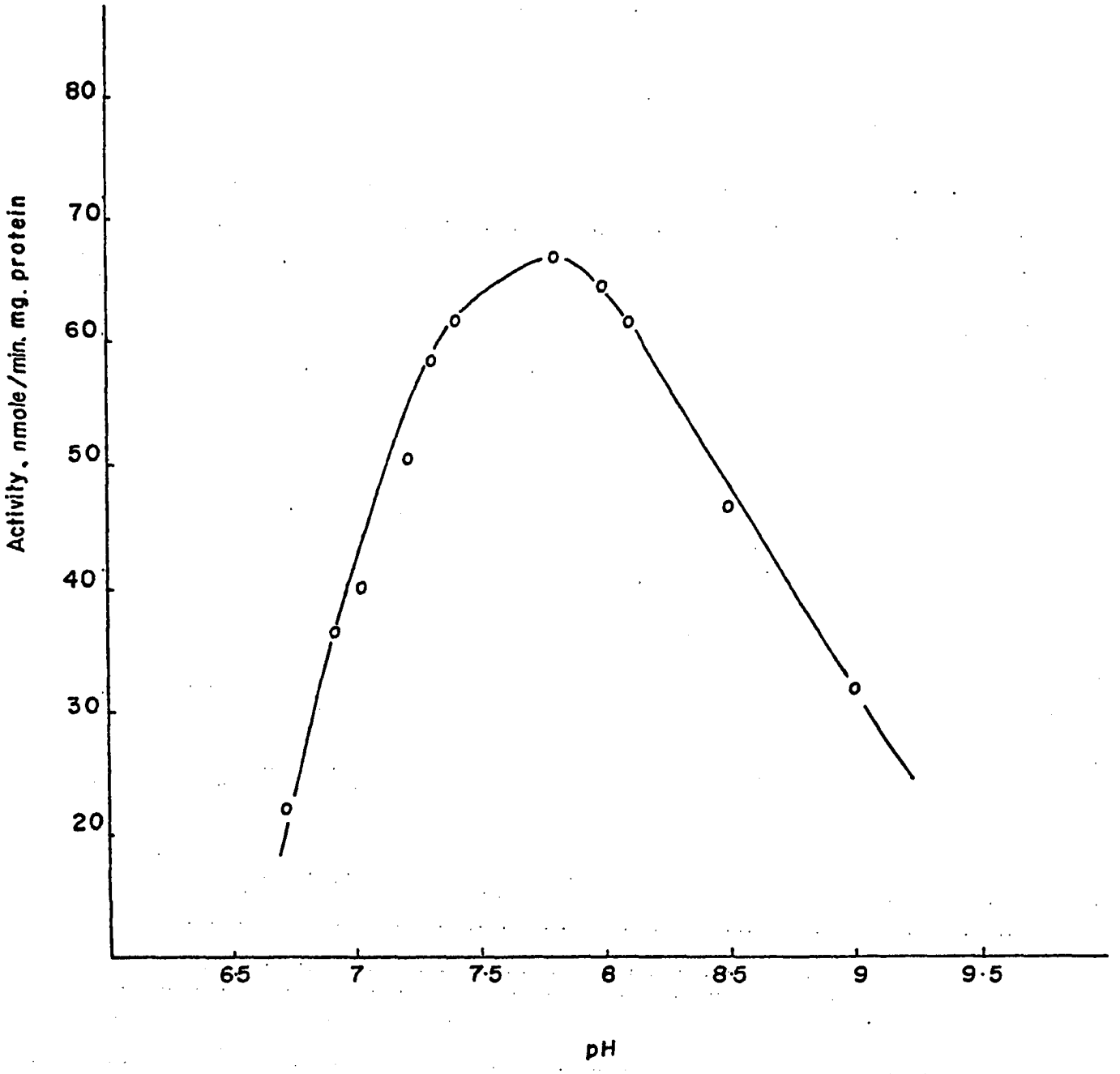
Activity, nmole/min. mg. protein
80
70
60
50
40
30
20
6·5
7
7·5
8
8·5
9
9·5
pH

FIGURE 15

FIGURE 16. β-naphthylamine N-hydroxylation activity as a function of temperature. The assay mixture was identical to that used for all kinetic measurements and is given in the legends to Figure 5, and in Methods.

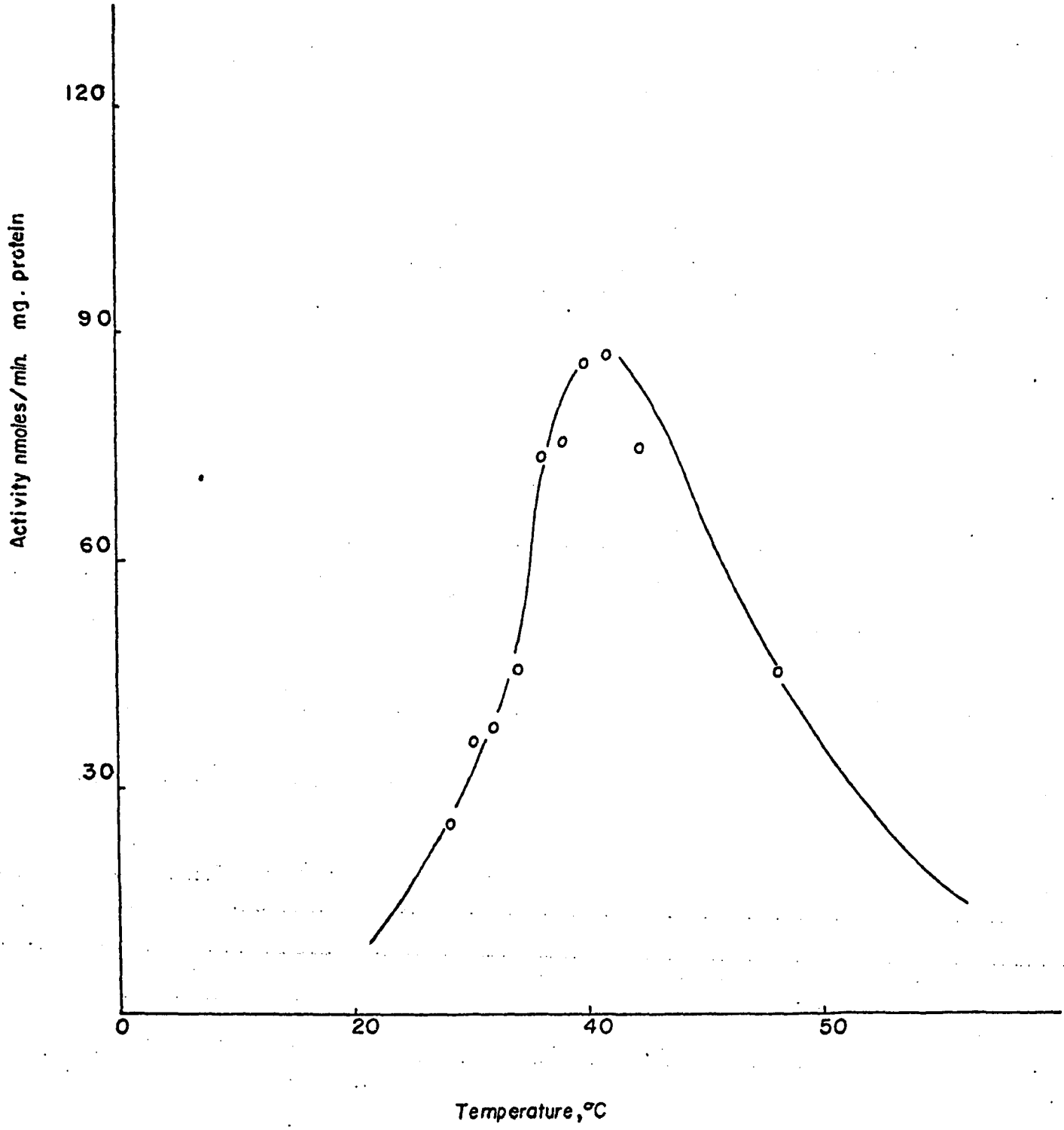
120
90
60
30
0
20
40
50
Activity nmoles/min. mg. protein
Temperature, °C

FIGURE 16

of any length of duration over 2 minutes. From this highly sensitive dependence of microsomal activity on temperature, as pointed out above, one can now realize the extent of damage of the activity of microsomal enzymes (and especially that of oxidase) if microsomes were subjected to, say, 45°C; even for a brief period. Such is the case, for instance, in carcinogen screening tests via metabolic activation. In the screening test procedure, microsomes are subjected to 45°C for a short period of time. It is most likely that this "brief" treatment of microsomes at such a high temperature level would cause a rapid irreversible deactivation of the enzymes, the half-life of some of which is as low as 2 minutes at 37°C [57]. Obviously, this may result in a significant loss of detection capability for carcinogenicity for a great many compounds of environmental concern.

Microsomes concentration. The effect of microsomal protein concentration on the rate of β-NA N-oxidation is shown in Figure 18. It is obvious that there is a limit to the amount of microsomes one can use with added benefit for metabolic activation assays. For instance there is no observable difference, in oxidation initial rates as well as product yield at any specified assay time, between 5.5 mg and 7.0 mg microsomal protein used in the assay. However, the rate of product formation increases almost linearly with microsomes concentration at lower ranges of the concentration of the latter.

FIGURE 17. Temperature-dependent inactivation of microsomal N-oxidation activity. Initial activities of N-HO-βNA formation as a function of microsomes incubation time were measured polarographically at two different temperatures (37°C and 41°C). The inactivation curves were obtained by incubating microsomes at a specified temperature (37°C or 41°C) for specified times as indicated in the figure and then subsequently measuring the initial activities of β-naphthylamine N-oxidation. The reaction mixture was as given in the legends to Figure 5 and in Methods.

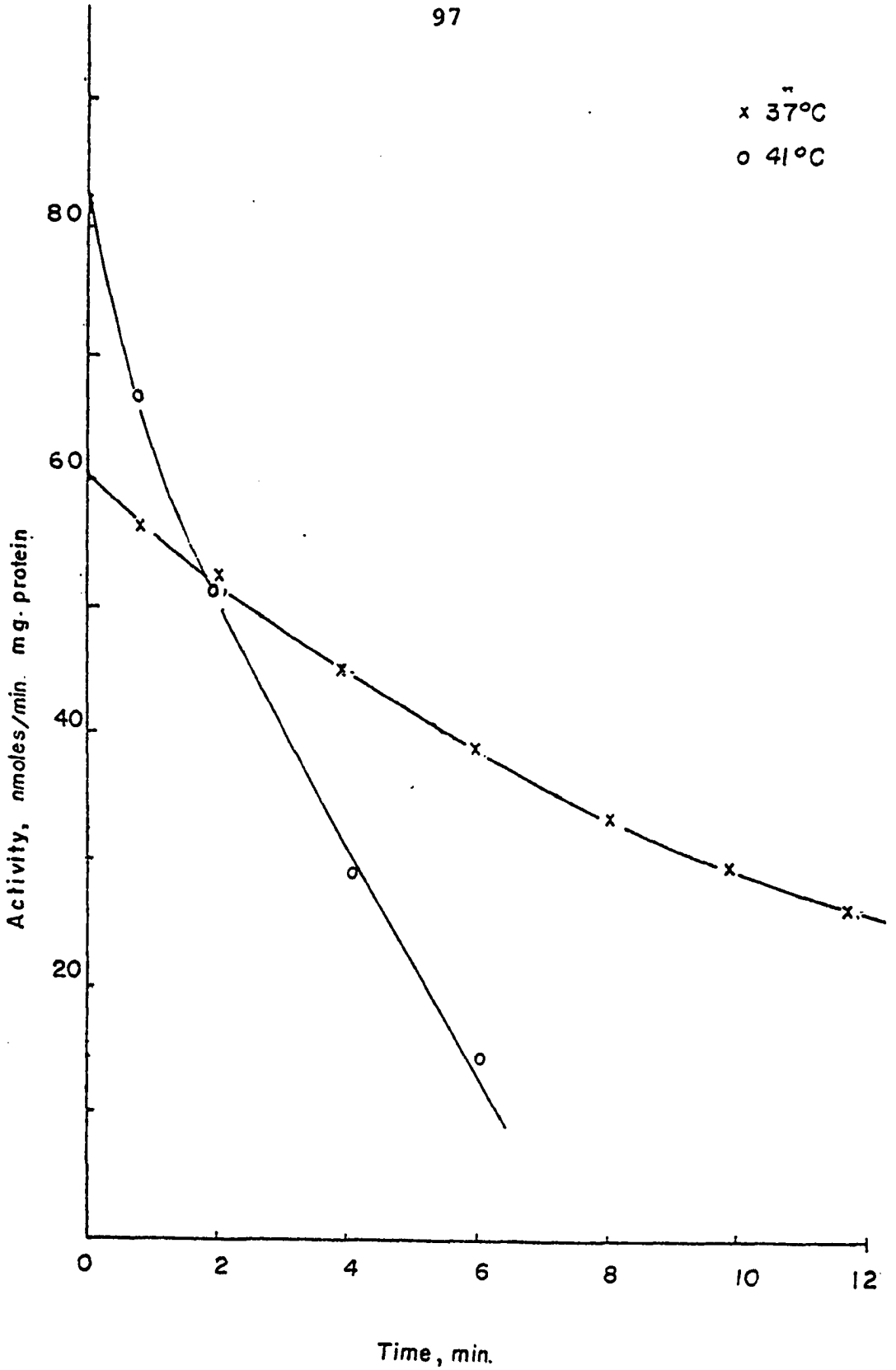
x 37°C
o 41°C
80
60
40
20
0
2
4
6
8
10
12
Activity, nmoles/min. mg. protein
Time, min.

FIGURE 17

FIGURE 18. Effect of the concentration of microsomal protein on the rate of β-NA N-oxidation. The N-oxidation initial rates were measured at 38°C polarographically by monitoring a substrate-dependent increase in oxygen consumption using a Clark-type oxygen-electrode with a strip-chart recorder as described in Methods. The reaction medium was the same as was used for all kinetic studies, and consisted of: 0.1M, K-phosphate buffer, pH 7.4, 0.5mM $NADP^+$, 1mM G6P and 1.0 U/ml G6PD, 0.25mM $MgCl_2$, 29.0 U/ml catalase, 0.2mM O_2, 0.5mM β-NA, and varying amounts of hog liver microsomes as indicated in the figure.

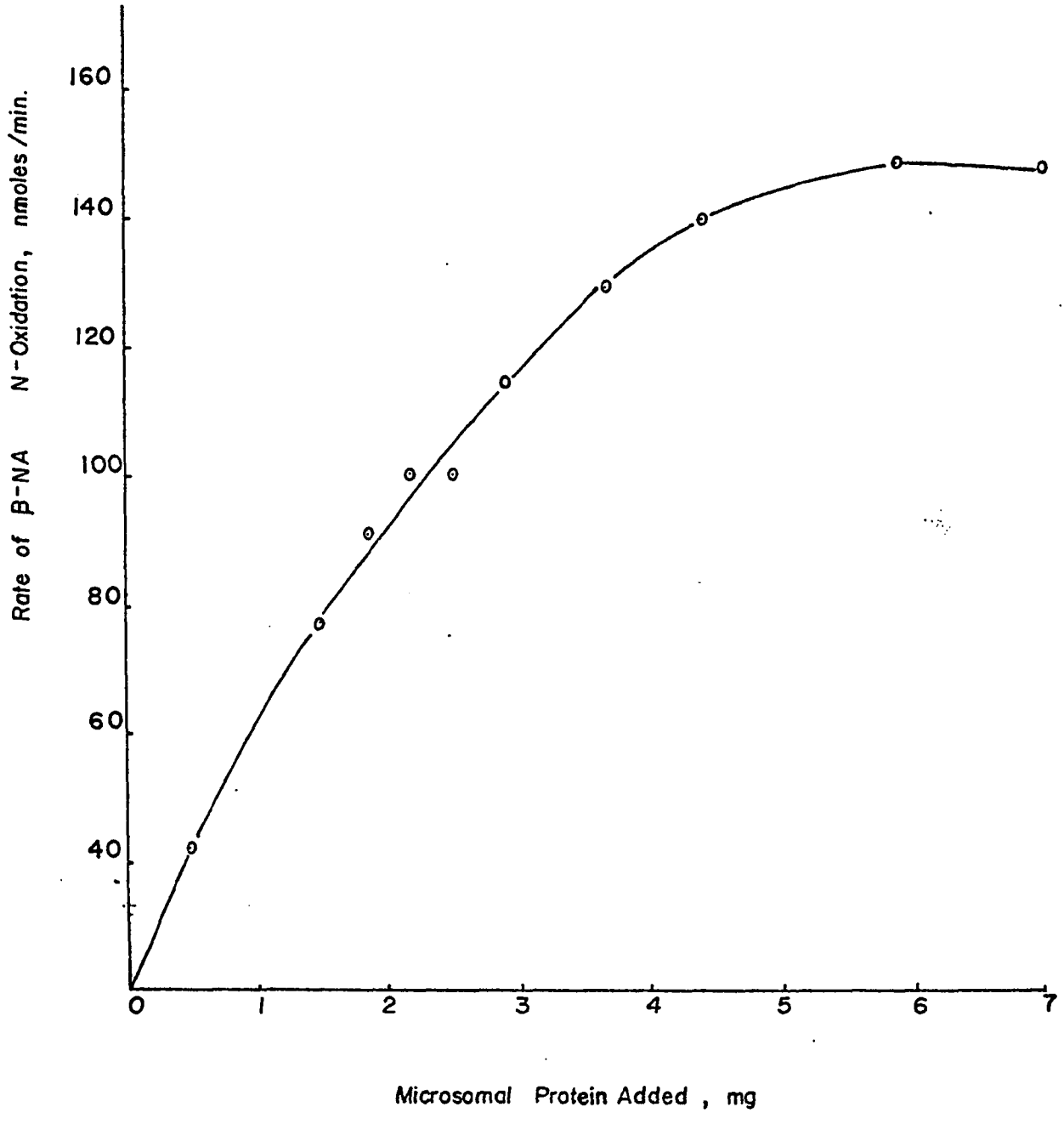
Rate of β-NA N-Oxidation, nmoles/min.
160
140
120
100
80
60
40
0
1
2
3
4
5
6
7
Microsomal Protein Added, mg

FIGURE 18

B. β-nitronaphthalene Reduction

In-vivo studies with rodents, by Kadlubar et al [62], had shown that β-nitronaphthalene (β-NN) can be metabolically converted to the N-hydroxy-β-naphthylamine N-glucuronide conjugate. Weisburger et al [98] attempted to show the reduction of β-NN in-vitro to β-naphthylhydroxylamine by rat and mouse liver microsomes. However, they reported a negative result. It has been well recognized that arylnitro compounds are reduced to the respective arylamines catalytically by a nitro-reductase in the post-mitochondrial supernatant, cytosols, or in microsomes. But in-vitro experimental efforts, to show that carcinogenic arylnitro compounds (such as β-nitro-naphthalene) are first converted to the carcinogenically active intermediate N-HO-βNA form by metabolic activation via nitro reductase in the microsomal fraction, have so far been unsuccessful. It was through the suggestion of Dr. Kadlubar of NCTR that the author of this work paid attention to β-NN metabolic activation problem.

To investigate β-NN reduction to β-naphthylhydroxylamine, a kinetic study technique analogous to the one used for β-NA oxidation was applied in this work, except that in the case of β-NN reduction, the reaction was carried out in oxygen-free atmosphere. Figure 19, shows the reaction time-history of the formation of N-hydroxy β-naphthylamine intermediate from β-nitronaphthalene. The experiment was performed

FIGURE 19. Reaction time-history of β-nitro-naphthaline-N-reductase activity in microsomes. The assay was conducted at 38°C, and the reaction medium contained: 0.1M K-phosphate buffer, pH 7.4, 0.5mM $NADP^+$, 1mM G6P, 1.0 U/ml G6PD, 0.25mM $MgCl_2$, 0.5mM β-NN, 0.36 Mg/ml pig liver microsomes, and 0.1 Mg/ml bovine serum albumin. Critical to the success of this experiment was the complete isolation of oxygen from the reaction mixture as described in the text. The time-optimum for maximum N-hydroxy product formation from β-NN is about 2 minutes as can be seen from the figure.

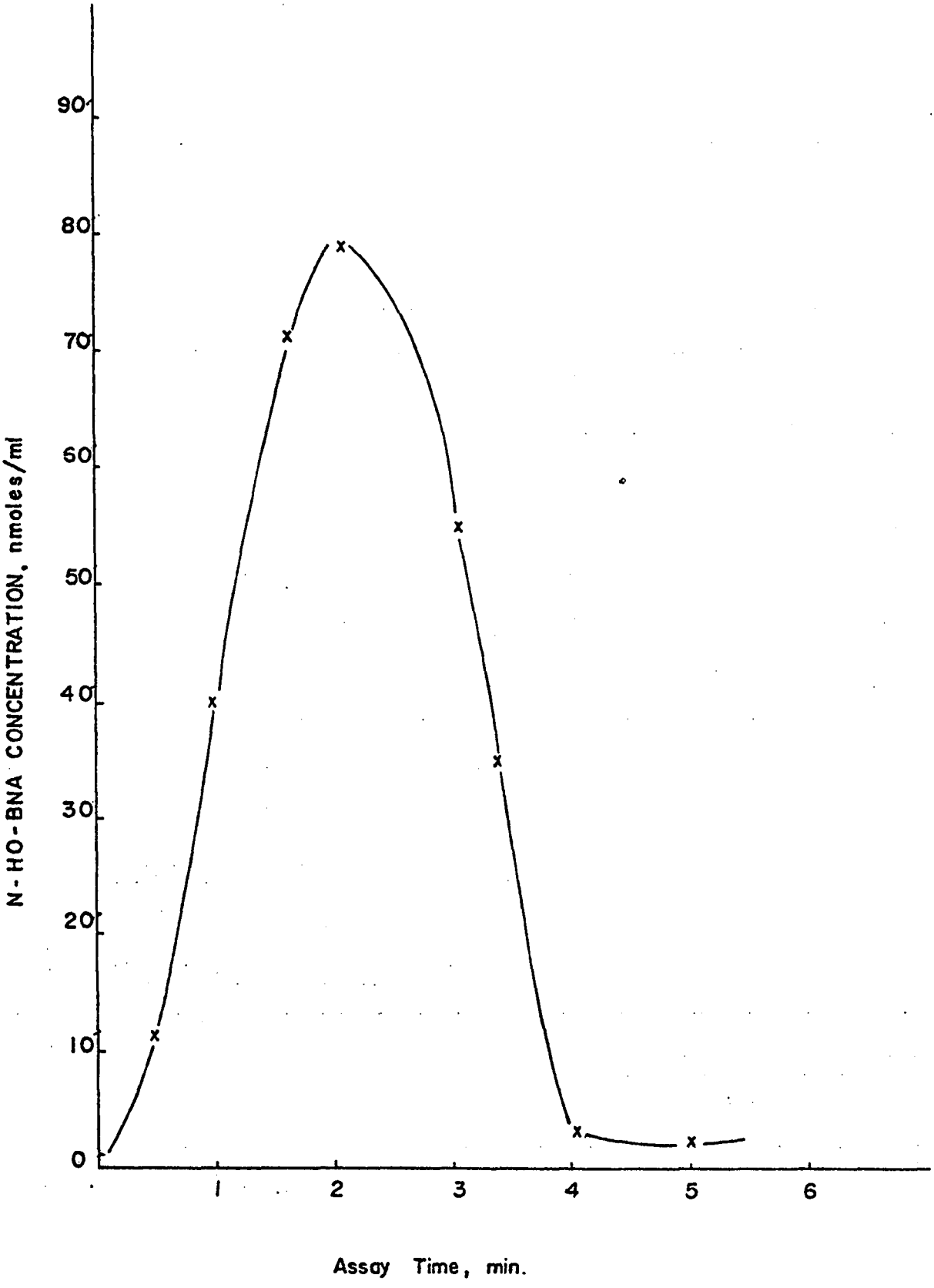
N-HO-BNA CONCENTRATION, nmoles/ml
0
10
20
30
40
50
60
70
80
90
1
2
3
4
5
6
Assay Time, min.

FIGURE 19

in the microreactor at 38°C, and the composition of the reaction mixture is given in the legends to the figure. As can be seen from these data the intermediate reduction product, N-HO-βNA, in this case is extremely unstable, possibly due to rapid total reduction to β-naphthylamine in the oxygen-free environment [98]. The product formation maximum lies distinctly around 2 minutes. This, in part, explains why the authors mentioned above (Weisburger et al), who run the assay for 5 minutes, could not detect the carcinogenic intermediate.

PART II.

Two-Step Sequential Reaction of Metabolic Activation and Deactivation of β-NA

1. The Reaction Kinetics

As has been discussed in Part I, β-naphthylamine is N-oxidized with the consumption of equimolar quantities of NADPH and molecular oxygen in the presence of microsomal flavoprotein oxidase to yield an active (carcinogenic) form N-HO-βNA. The latter, being an unstable and highly reactive compound, is stabilized and rendered inactive (non-carcinogenic) with the consumption of equimolar uridine 5'-diphosphoglucuronic acid (UDPGA) in the presence of a second liver microsomal enzyme, UDP-glucuronyltransferase (UDP-GT). The second step reaction yields a glucuronide conjugate which is carcinogenically inactive. Usually, an inert atmosphere is necessary

FIGURE 20. Experimental profiles of β-NA activation-deactivation sequential reaction products. The reaction was run in a 5 ml. water-jacketed (T=38°C), stirred-batch reactor. The assay mixture consisted of: 2.6 mls 0.1M K-phos. buffer, pH 7.5, 0.5mM $NADP^+$ and 0.2mM NADPH, 2.5mM G6P, 1 U/ml G6PD, 0.1mM EDTA, 0.1mM $MgCl_2$, 0.5mM UDPAG, 3.25 Mg/ml microsomes, 2.5mM UDPGA, 0.2mM O_2, and 30µℓ of 0.05M β-NA. Calculation of the concentration of the respective compounds was made from the analysis of 0.2ml serial aliquots. Analysis for the substrate was made by reading absorbance of the sample at 235nm; for N-HO-βNA- by amyl-acetate reducing equivalents; and for the glucuronide - by citric acid hydrolysis reverse reaction and subsequent analysis by the TPF method [98] as described in text in the Methods section.

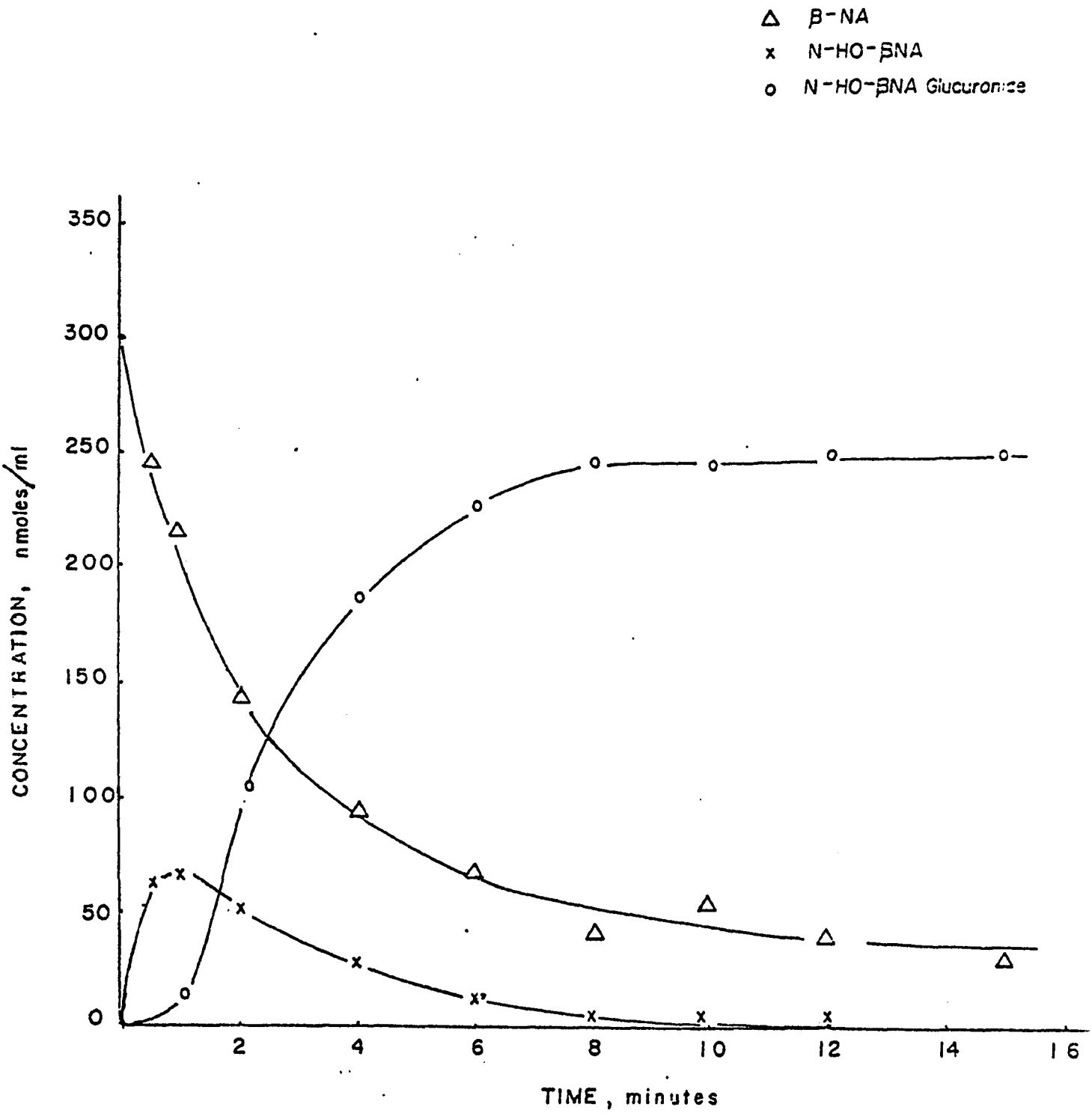
Δ β-NA
x N-HO-βNA
o N-HO-βNA Glucuronide
CONCENTRATION, nmoles/ml
350
300
250
200
150
100
50
0
2
4
6
8
10
12
14
16
TIME, minutes

FIGURE 20

when obtaining glucuronides from N-HO-βNA in a single second step enzyme reaction, in order to prevent ring-oxidation or oxidation to the Nitroso form. However, such an atmosphere is not conducive to the formation of the oxide from β-NA. It is therefore obvious that a reaction design was necessary to carry out the glucuronidation of β-naphthylhydroxylamine, (N-HO-βNA), in a two-step enzymic sequence from β-NA with minimal accumulation of the intermediate. As was described in the Methods Section, this was achieved by portional loading of the substrate in small amounts (15μℓ of .05M β-NA) every 4 minutes, the optimum conversion time determined from the kinetics of the first stage reaction. Figure 20 shows the experimental result of the time-concentration profiles of the substrate, the intermediate, and the N-glucuronide conjugate in the two-step sequential reaction for one single small amount(30μℓ) loading of the substrate. All the rest of the reaction components and cofactors as well as microsomes were used in excess. The reaction was run at 38°C in a 5 mℓ stirred-batch reactor. The composition of the reaction medium was as given in the Methods Section and is repeated in the legends to the figures. Due to excess concentrations of UDPGA and the microsomal UDP-glucuronyltransferase, the intermediate product (N-HO-βNA) of the first stage is rapidly consumed in the deactivation reaction. Thus, by pushing the equilibrium of the reaction far to the right, the accumulation of the intermediate is minimized. Surprisingly, the data of Figure 20 indicate that the dual enzymic sequential reaction

FIGURE 21. First order logarithmic plot of $\ell n\ C/C_o$ vs. t for β-NA N-oxidation. The first step, metabolic activation, reaction at low substrate concentration (150 nmoles/ml β-NA, as was applied in the two-step reaction at optimum time-intervals) satisfies first-order kinetics, with $k_1 = 1.6 \times 10^{-2}\ min^{-1}$.

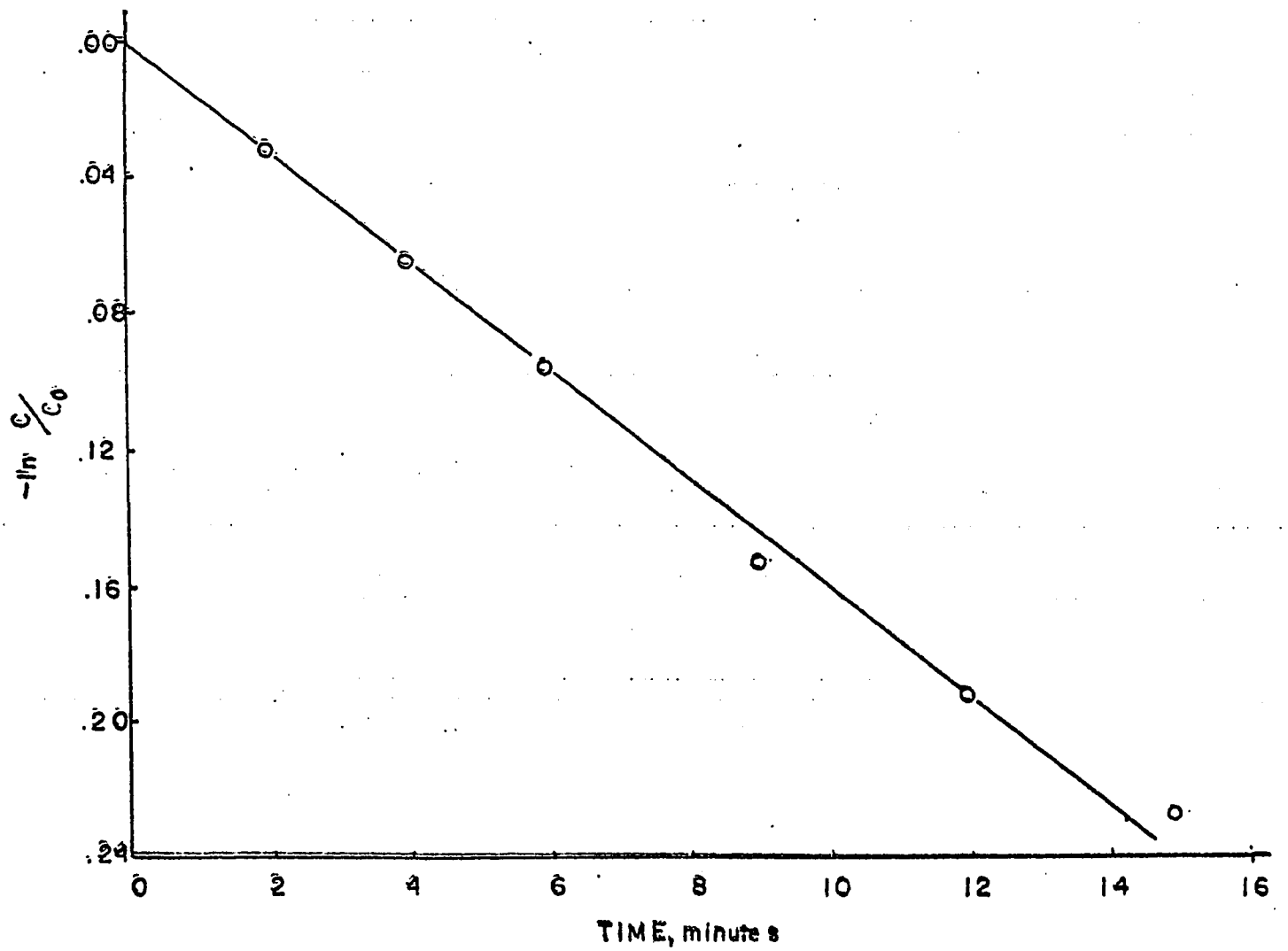

FIGURE 21

at the given and practical assay conditions can be modelled as two-step consecutive reactions of first order. The validity of such a model has been investigated. Figure 21 shows the plot of $\ell n\ C/C_o$ vs. time for β-naphthylamine N-oxidation reaction, i.e., for the 1st step reaction, where C_o is the initial concentration, and c is the concentration of β-NA at any given time during the reaction. The plot is fairly linear, indicating that first order approximation is possible. The kinetic rate constant for this first stage reaction (k_1), which is equal to the slope of the line, is 0.016 min^{-1}. The second step reaction, i.e., the conversion of N-HO-βNA to the N-glucuronide, was also run independently. As has been discussed earlier in Methods, UDP-N-acetylglucose-amine (UDPGA) was used in this step to inhibit the reverse reaction of the glucuronide back to the N-hydroxy. A similar plot (analoguous to Figure 21) of the experimental data for this second stage reaction is shown in Figure 22. This plot exhibits a linear behavior and thus the second stage reaction can also be satisfactorily approximated by first-order kinetics. The rate constant (k_2) obtained from the slope of the line is equal to 0.143 min^{-1}. Thus, it is clear that the activation/deactivation mechanism taking place in liver microsomes at low substrate concentrations and at excess concentrations of all the rest of the required reaction components can be modeled or approximated by two-step consecutive reactions of first order. Specifically for β-naphthylamine, under

FIGURE 22. First-order logarithmic plot of $\ell n\ C/C_o$ vs. t for N-HO-βNA N-glucuronidation. The second step, metabolic deactivation, reaction at low N-HO-βNA concentration (~100 nmoles/ml) approximately follows first-order kinetics, with $k_2 = 14.3 \times 10^{-2}\ min^{-1}$.

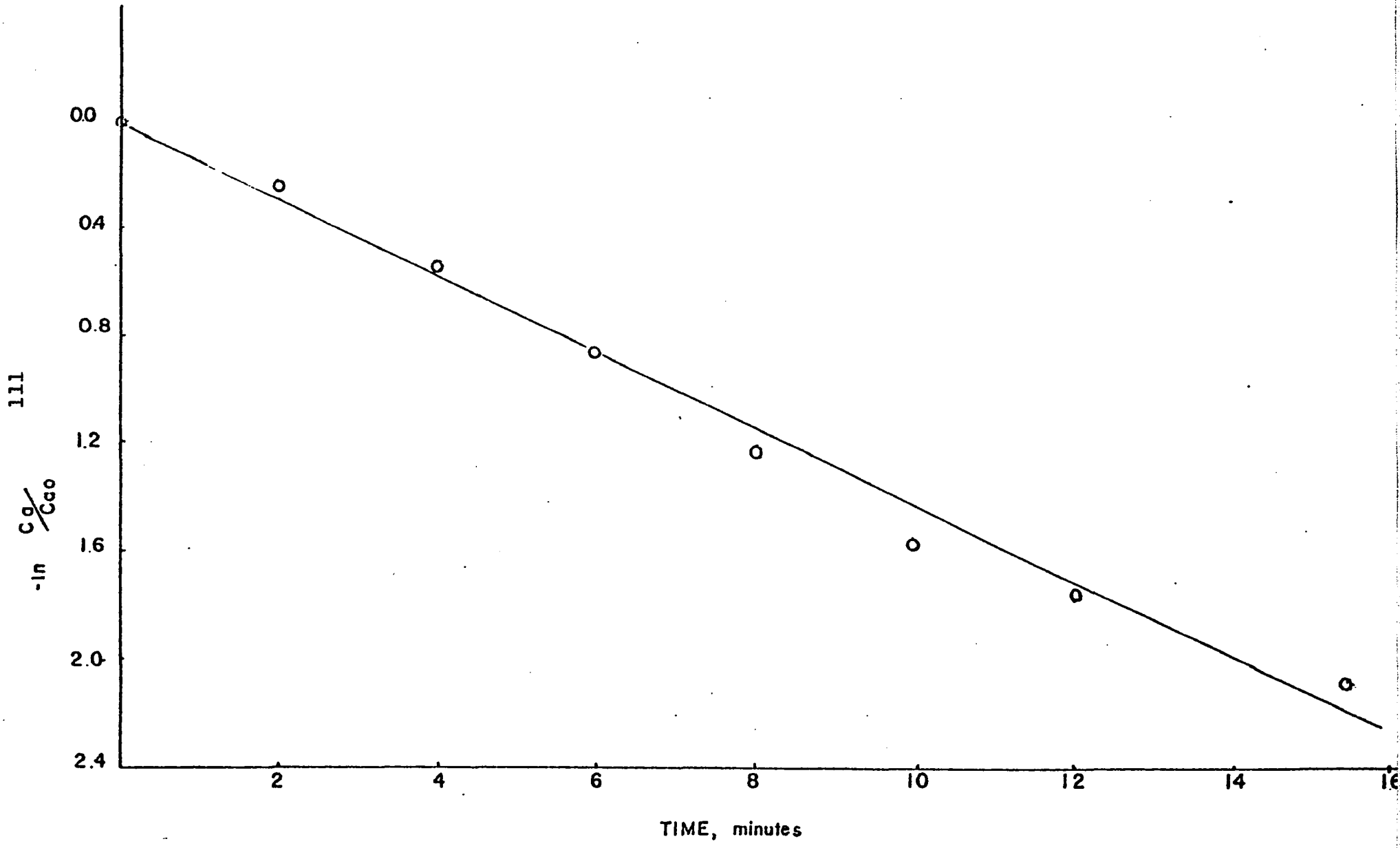

FIGURE 22

given assay conditions we can write the reaction scheme as:

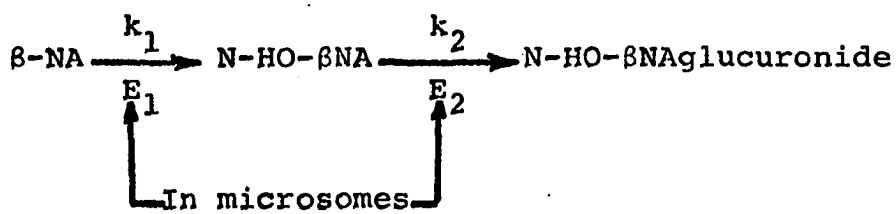

where, E_1 refers to microsomal flavoprotein mixed function oxidase (FMO), and E_2 symbolizes microsomal UDP-glucuronyl-transferase (UDP-GT).

Formulating the differential rate equations for the respective components in the reaction model, taking into consideration the decay of enzyme activity, we can write,

$$\frac{d[\beta\text{-NA}]}{dt} = - k_1 [\beta\text{-NA}][E_1/Eo_1] \quad (1)$$

$$\frac{d[\text{OH-}\beta\text{-NA}]}{dt} = k_1 [\beta\text{-NA}][E_1/Eo_1] - k_2[\text{OH-}\beta\text{NA}][E_2/Eo_2] \quad (2)$$

$$\frac{d[\beta\text{-NAG}]}{dt} = k_2 [\text{OH-}\beta\text{NA}][E_2/Eo_2] \quad (3)$$

where, in the above equations, OH-βNA stands for N-HO-βNA, and β-NAG symbolizes the glucuronide conjugate, and, Eo_1 and Eo_2 are the initial enzyme activities.

Assuming first order enzyme activity decay,

$$\frac{d[E_1]}{dt} = -k_1' [E_1] \quad (4)$$

and

$$\frac{d[E_2]}{dt} = -k_2' [E_2] \quad (5)$$

Equations 1-3 were solved on the computer in combination with equations 4 and 5 for the concentration profiles of the substrate the intermediate and the glucuronide conjugate as a function of reaction time, using the Continuous Systems Modelling Computer Program (CSMP). The decay constants k_1' and k_2' used in equations 4 and 5 for the respective enzymes, were determined from experimental measurement of the decline of activities as a function of incubation time at 37°C. They corresponded to 0.002 and 0.001 min^{-1} for oxidase and UDP-GT, respectively. The initial concentrations used in the solution of the model equations, i.e. the initial substrate concentration and the initial enzyme activities, were experimental initial values from the kinetic run of Figure 20. The CSMP program is given in Appendix A1. The print-plot solution output in concentration vs. time profiles is shown in Appendix A2 through A4 for the substrate, intermediate, and the glucuronide, respectively. In order to combine all the three profiles in one graph, the CSMP output data were taken and interphased with a DOT plotter. The resulting graphs are given in Figures 23 and 24. Due to minimal accumulation of the intermediate (N-HO-βNA) product with reaction time, the concentration-time profile of the latter was small in comparison to the concentration levels of the substrate and the glucuronide conjugate (Figure 23), and therefore the N-HO-βNA curve is shown separately in Figure 24 in an enlarged scale for clarity.

FIGURE 23. Computer-simulated profiles for β-NA and N-HO-βNAGluc. The profiles were obtained from computer (IBM-370) simulation of the proposed dynamic kinetic model for metabolic activation/deactivation consecutive reaction of β-naphthylamine. The data used for the simulation are given in Appendix A2 for β-NA, and Appendix A4 for N-HO-βNA Glucuronide. The DOT plot program is given in Appendix A5.

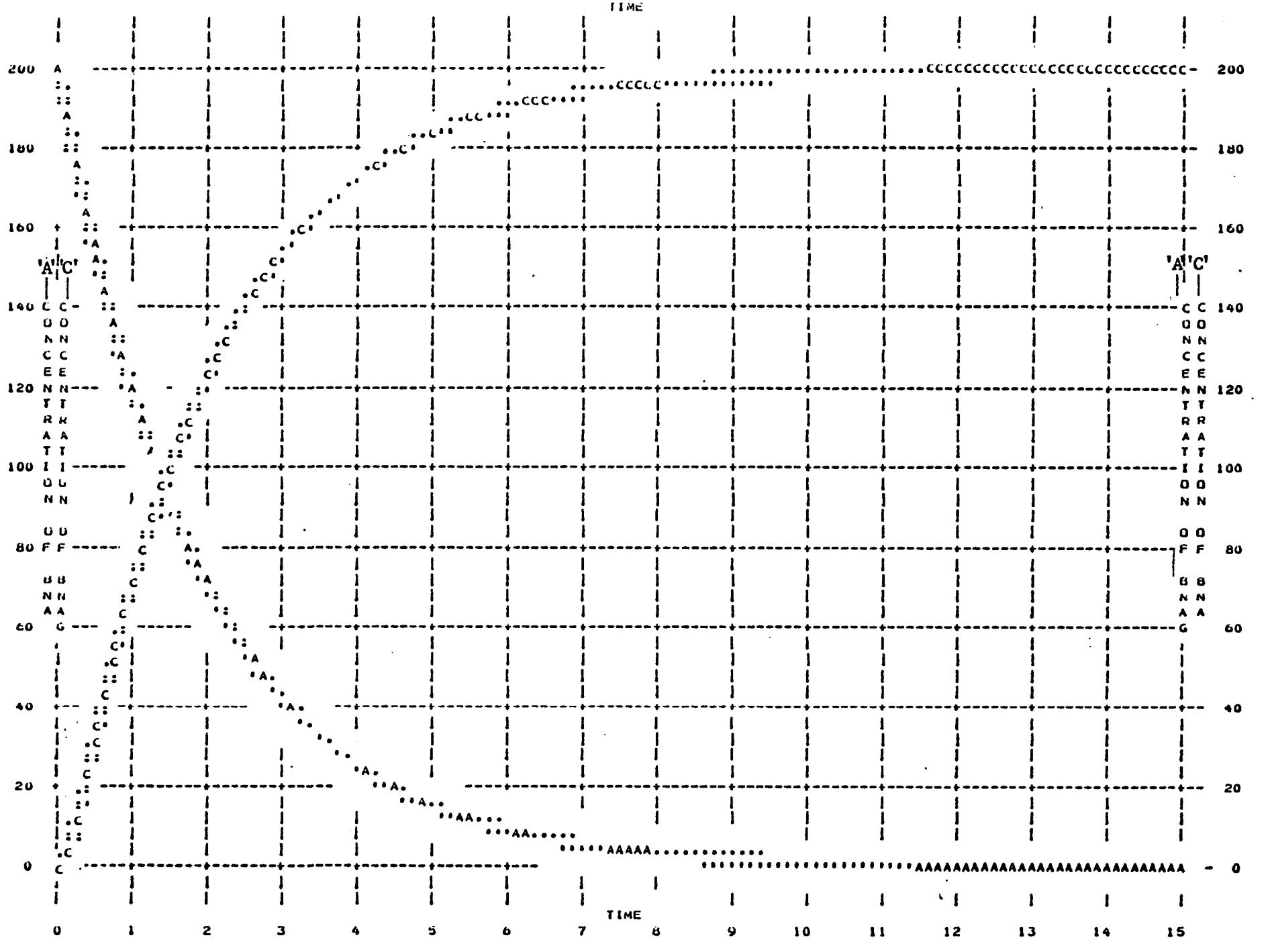
TIME
CONCENTRATION OF BACTERIA
200
180
160
140
120
100
80
60
40
20
0
A
C
0
1
2
3
4
5
6
7
8
9
10
11
12
13
14
15
TIME

FIGURE 23

FIGURE 24. Computer-simulated profile of N-hydroxy β-naphthylamine intermediate the profile was obtained from computer simulation of the proposed dynamic kinetic model for metabolic activation/ deactivation consecutive reaction. The data used for generation of this plot are given in Appendix A3. The DOT plot program is given in Appendix A5.

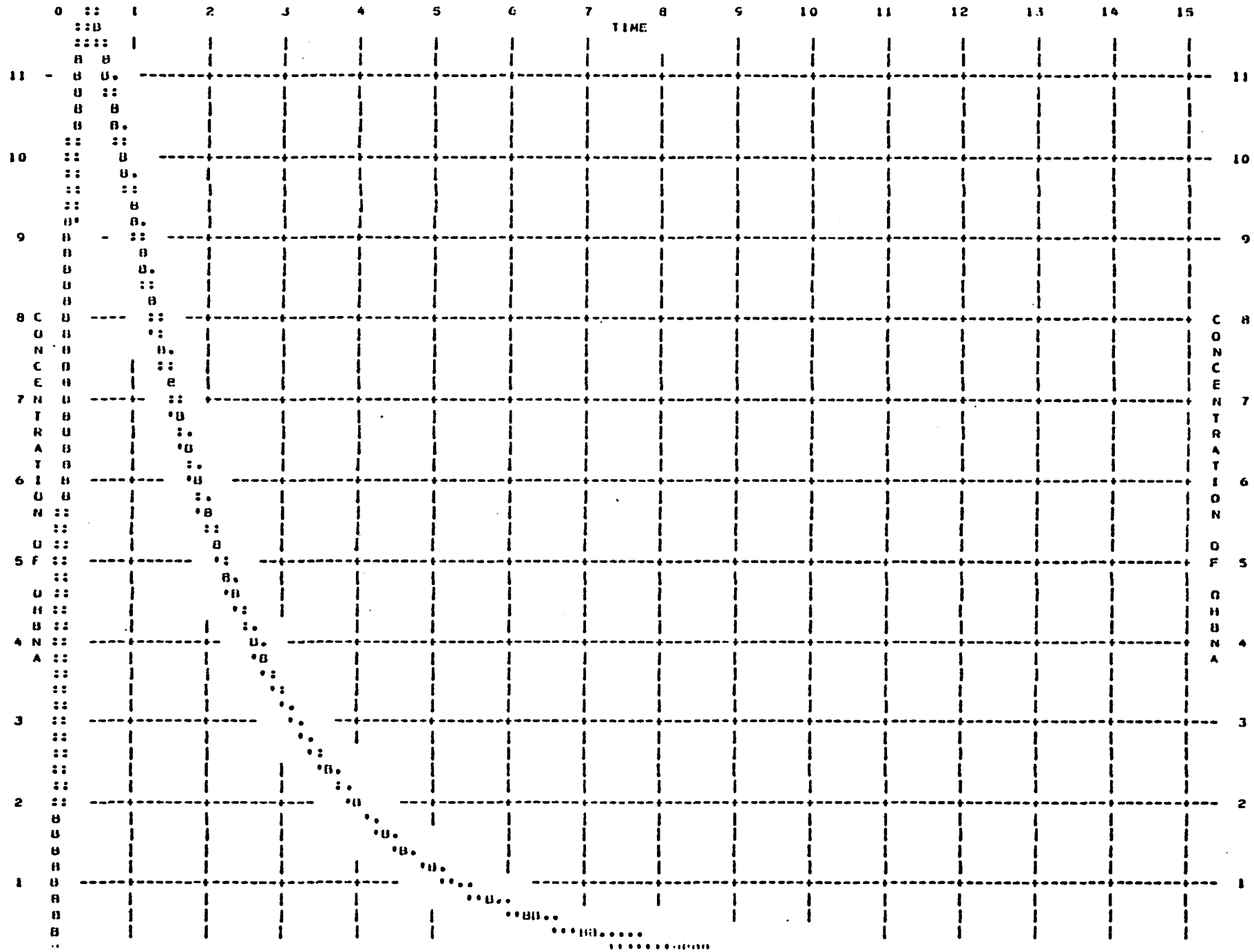

FIGURE 24

From the comparison of these data (Figures 23 and 24) and the experimental results of Figure 30 one can see then, that the simple theoretical two-step consecutive kinetic model explains the activation/deactivation phenomena satisfactorily well under given conditions. The appearance of significantly lower levels of the concentration profile of the N-hydroxy intermediate from the model solution in comparison to the experimentally observed profile may be due to possible over-estimation of the rate constant k_2 from the plot of Figure 22. In principle, with all the rest of the parameters in the model equations known, one can solve iteratively for the required k_2 that enables the model to satisfy the experimental data more accurately.

2. Product Analysis

Figure 25(a) shows the chromatographic elution peak from HPLC for the standard N-HO-βNA glucuronide which was synthesized starting from the N-hydroxy intermediate. In Figure 25(b), peaks for the two-step synthesis reaction sample are shown and Figure 25(c) depicts a single peak obtained from a combination of samples of Figures 25(a) and 25(b). The complete overlap of the product peak from the sequential bienzymic reaction with the standard glucuronide peak as shown in Figure 25(c), indicates that the activation/deactivation process prevails in carcinogen transformation in liver microsomes <u>in-vitro</u>.

FIGURE 25. Relative intensity of resolution vs. time. Resolution peaks obtained by HPLC for (a) standard N-glucuronide obtained by direct synthesis from N-HO-βNA, (b) N-glucuronide obtained by two-step synthesis from β-Na, (b) 1:1(v/v) combination of (a) and (b).

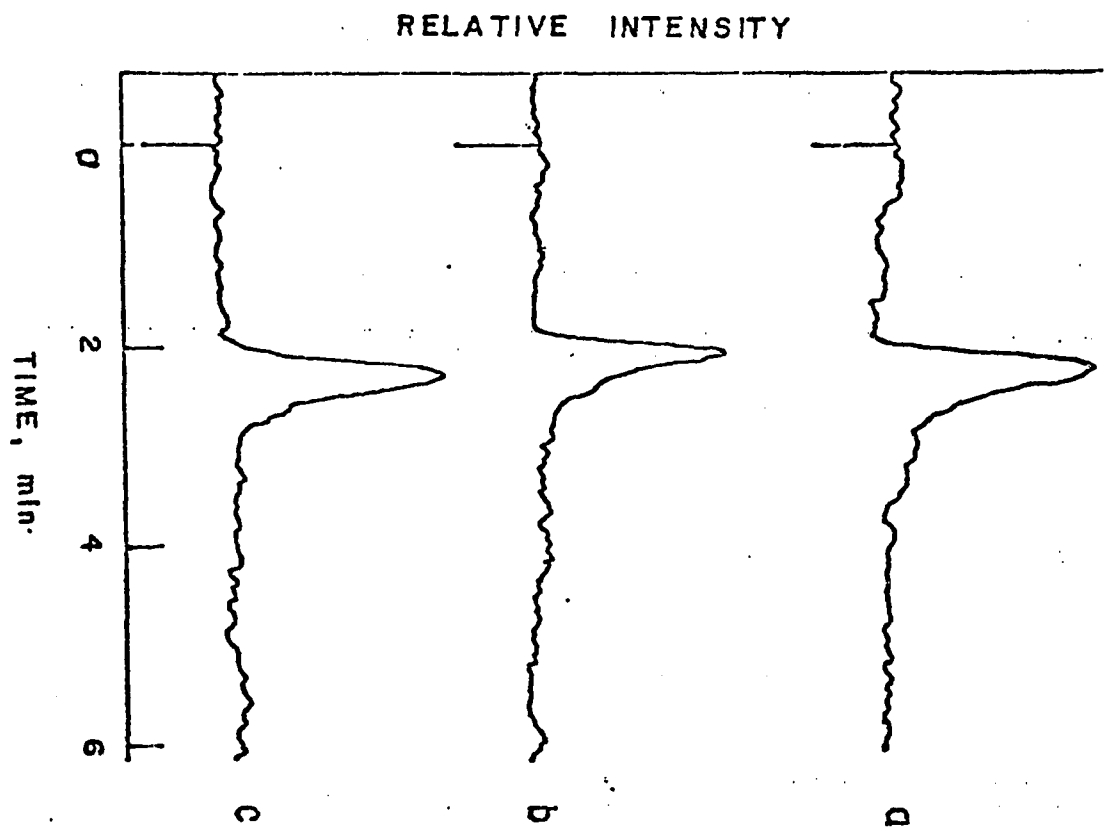

FIGURE 25

Figure 26 shows Sephadex gel-filtration chromatographic peaks of the glucuronide obtained from a single inactivation stage run, starting from the standard N-hydroxy intermediate. This elution peak coincides with the peak obtained by Kadlubar et al [62] for the same product using N-HO-βNA as the substrate. Figure 27 depicts the peaks obtained from the activation/deactivation model reaction. The indicated peak in Figure 27 exactly coincides with the peak in Figure 26 with respect to resolution time with all column operating conditions kept constant.

The product absorption peak was sought between 200-300 nm wavelength range. Earlier reports by Kadlubar, who studied the single activation stage, showed that the glucuronide in discussion has a UV-absorption maximum around 238 nm. Figure 28 shows the absorption maximum of the product from a wavelength scan between 200-300 nm on Beckman DB-GT grating spectrophotometer. It can be seen from this figure that the absorption peaks for both the standard glucuronide and the product obtained from the activation/deactivation model reaction coincide. Kadlubar and coworkers have conducted rigorous analysis of the molecular structure of the glucuronide conjugate by mass spectrometry.

The possibility of N-glucuronidation without intermediate oxidation also exists. The possibility of this reaction was investigated by attempting to synthesize the non-oxidized glucuronide under identical conditions, but

FIGURE 26. Relative absorbance vs. elution volume. The indicated absorbance peak was obtained from gel-filtration chromatography (Sephadex G-10-120) for the standard N-glucuronide. Column data: height -25.9 cm., I.D. - 2.54 cm., bed volume - 131.2 cm^3. Flow rate = 10 drops/minute. The pH of the elution fluid was 7.8, and consisted of 90% K-phos. buffer, 10% Methanol in 0.01M EDTA.

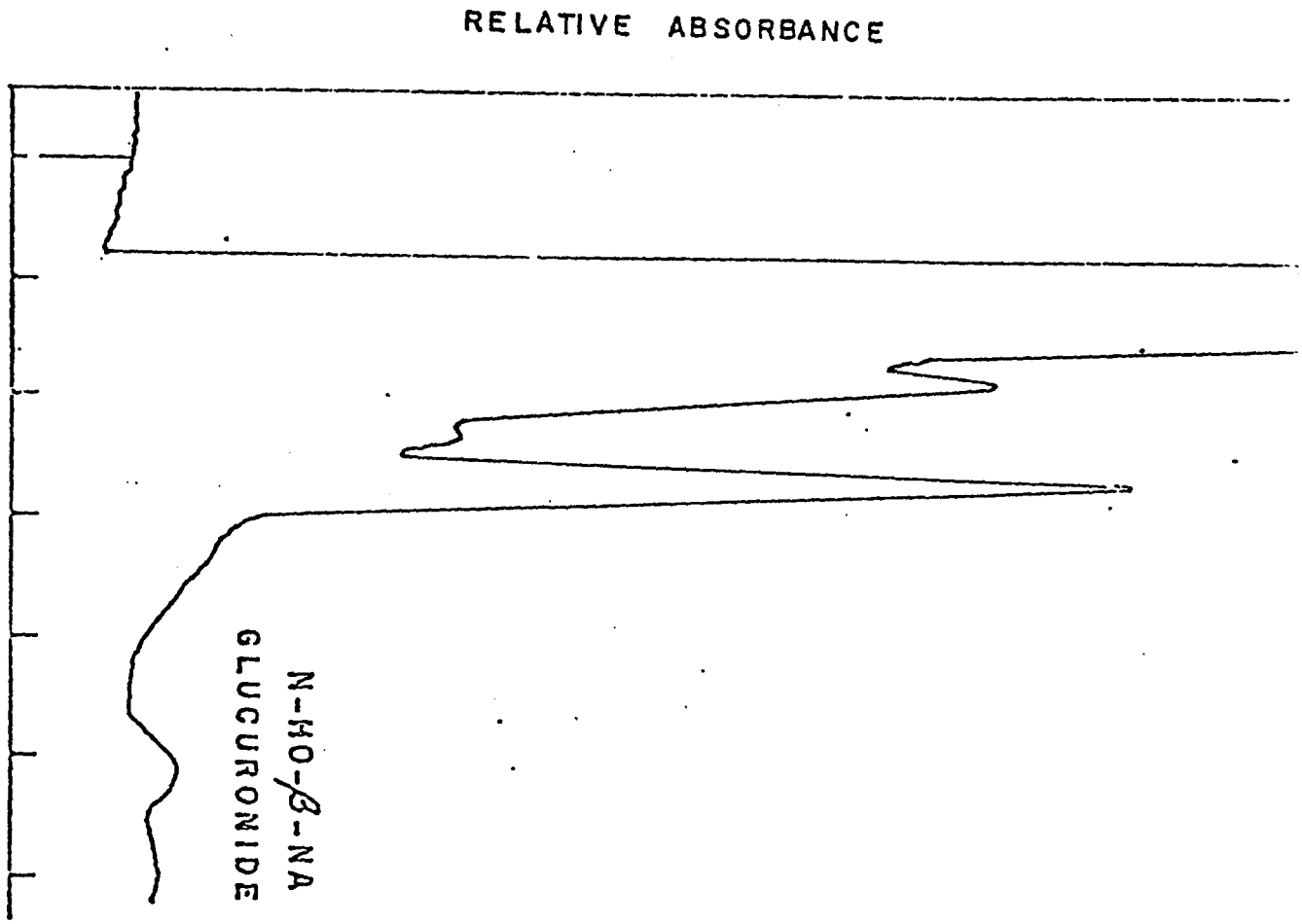
RELATIVE ABSORBANCE
0
200
400
600
ELUTION VOLUME, ml.
N-HO-β-NA
GLUCURONIDE

FIGURE 26

FIGURE 27. Relative absorbance vs. elution volume. The indicated absorbance peak, obtained by gel-filtration chromatography from the consecutive reaction of β-NA, corresponded to the N-glucuronide. This peak agrees with the standard N-glucuronide peak given in Figure 26. Column operation specifications are given in the legends to Figure 26.

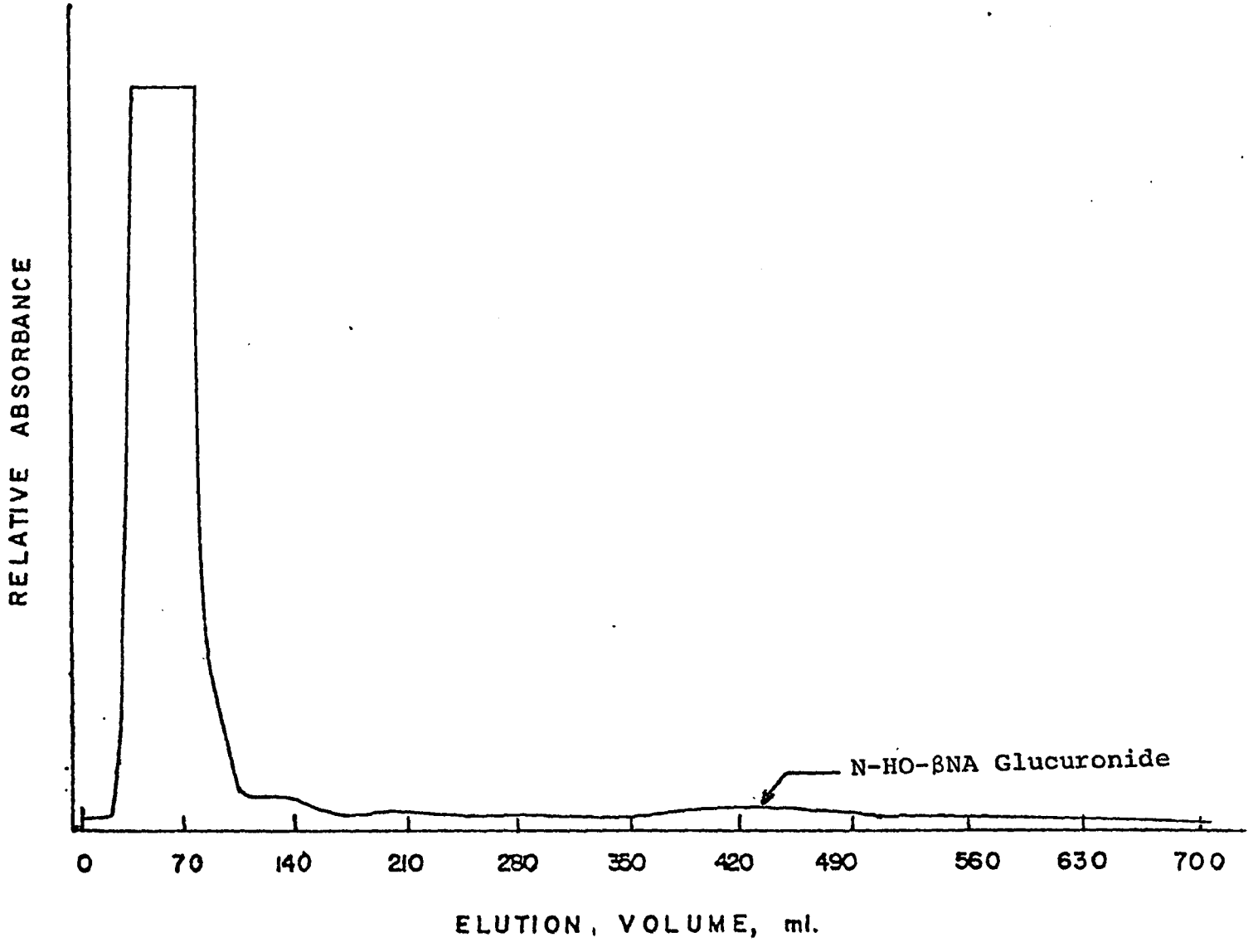
RELATIVE ABSORBANCE
N-HO-βNA Glucuronide
0
70
140
210
280
350
420
490
560
630
700
ELUTION, VOLUME, ml.

FIGURE 27

FIGURE 28. N-hydroxy β-naphthylamine glucuronide UV absorption curve. The glucuronide product fraction from the gel-permeation separation column was freeze-dried, and subsequently dissolved in water (1:10 v/v ratio). A sample of the solution was UV-scanned on a Beckman double-beam (DB-GT) spectrophotometer against H_2O. An absorption maximum was obtained at 238-240nm, which corresponded to the N-hydroxy β-naphthylamine glucuronide.

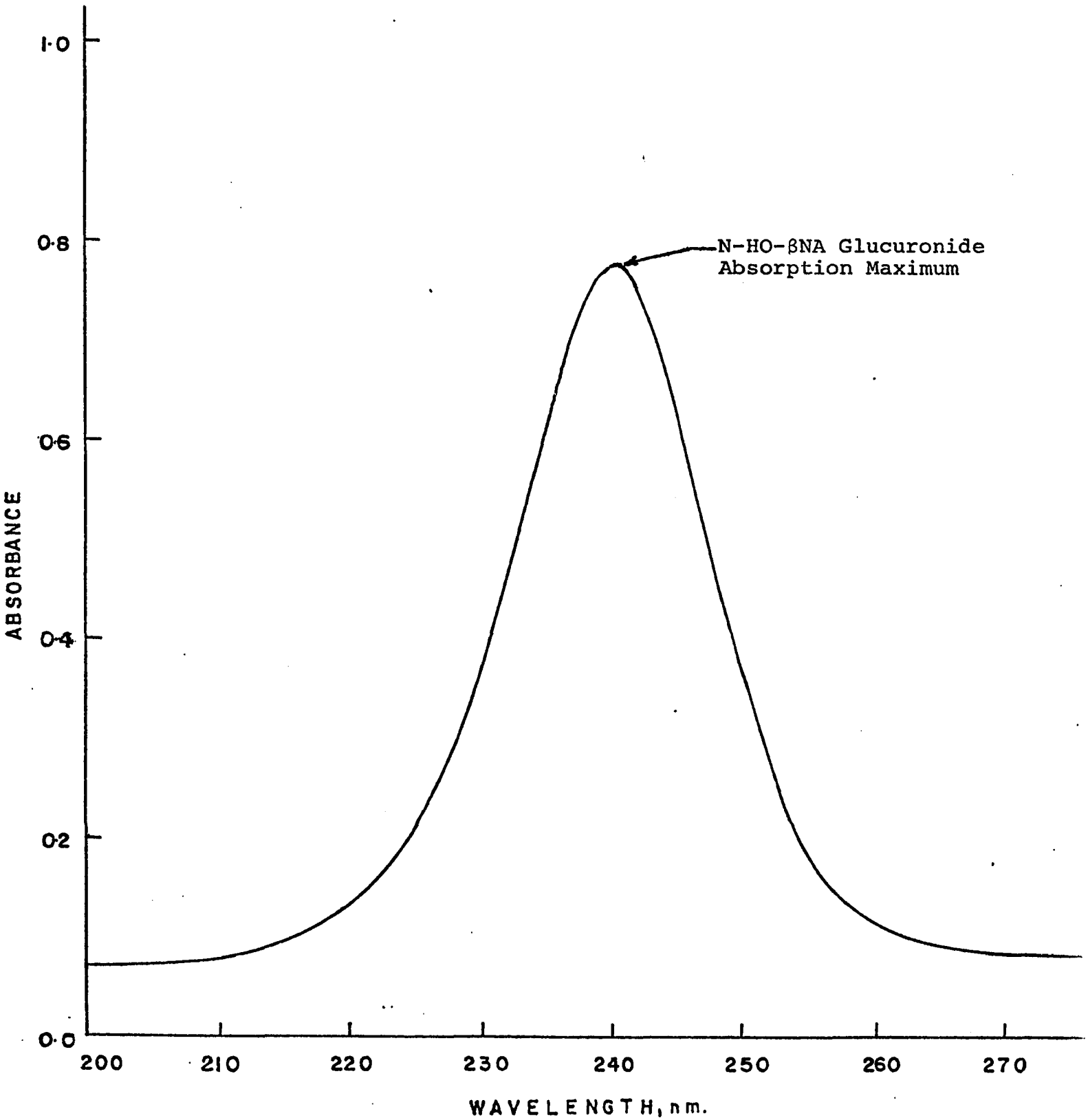
1·0
0·8
0·6
0·4
0·2
0·0
ABSORBANCE
N-HO-βNA Glucuronide
Absorption Maximum
200
210
220
230
240
250
260
270
WAVELENGTH, nm.

FIGURE 28

in the absence of NADPH - the required cofactor for oxidation. There was no identifiable peak in either the gel-filtration or the HPLC system indicating that the glucuronide conjugate obtained in this work was solely through the activation/deactivation sequential mechanism.

B. β-nitronaphthalene Sequential Reaction of Activation and Deactivation

β-NN in-vitro metabolic activation (partial reduction to N-HO-β-NA) has been discussed earlier in this chapter and the experimental result was presented in Figure 19. The experimental kinetic technique applied for the sequential activation/deactivation reaction run was described in the experimental section. The glucuronide conjugate product from the reaction mixture was separated and analyzed using the same technique, i.e., gel permeation chromatography (Sephadex G-10-120) and HPLC, analoguous to the procedure used for analysis of the N-glucuronide from β-NA. Figure 29 shows the elution peak of the product from the Sephadex separation column. As can be seen, the peak corresponding to the N-glucuronide conjugate, exactly analogous, to the one observed from β-NA sequential reaction (Figure 27), was obtained. The UV scan of a sample of the collected peak fractions showed an absorption maximum at 238 nm (identical to Figure 28), confirming that the deactivation product was N-hydroxy β-naphthylamine glucuronide. This conclusion was reaffirmed by mass spectrometry of the product with a kind collaboration of Kadlubar and coworkers of NCTR.

FIGURE 29. Relative absorbance vs. elution volume for N-HO-βNA Gluc from β-NN. The indicated absorbance peak was obtained from the gel-filtration chromatography for the N-hydroxy β-naphthylamine glucuronide upon separation of the reaction mass. As was described in Methods, in β-nitronaphthalene sequential reaction, 10µl of .05M substrate was added to the assay medium every 2 minutes for 12 minutes. The assay was run for 20 minutes. The product peak agrees with the corresponding N-glucuronide peak obtained from β-NA sequential reaction (Figure 27).

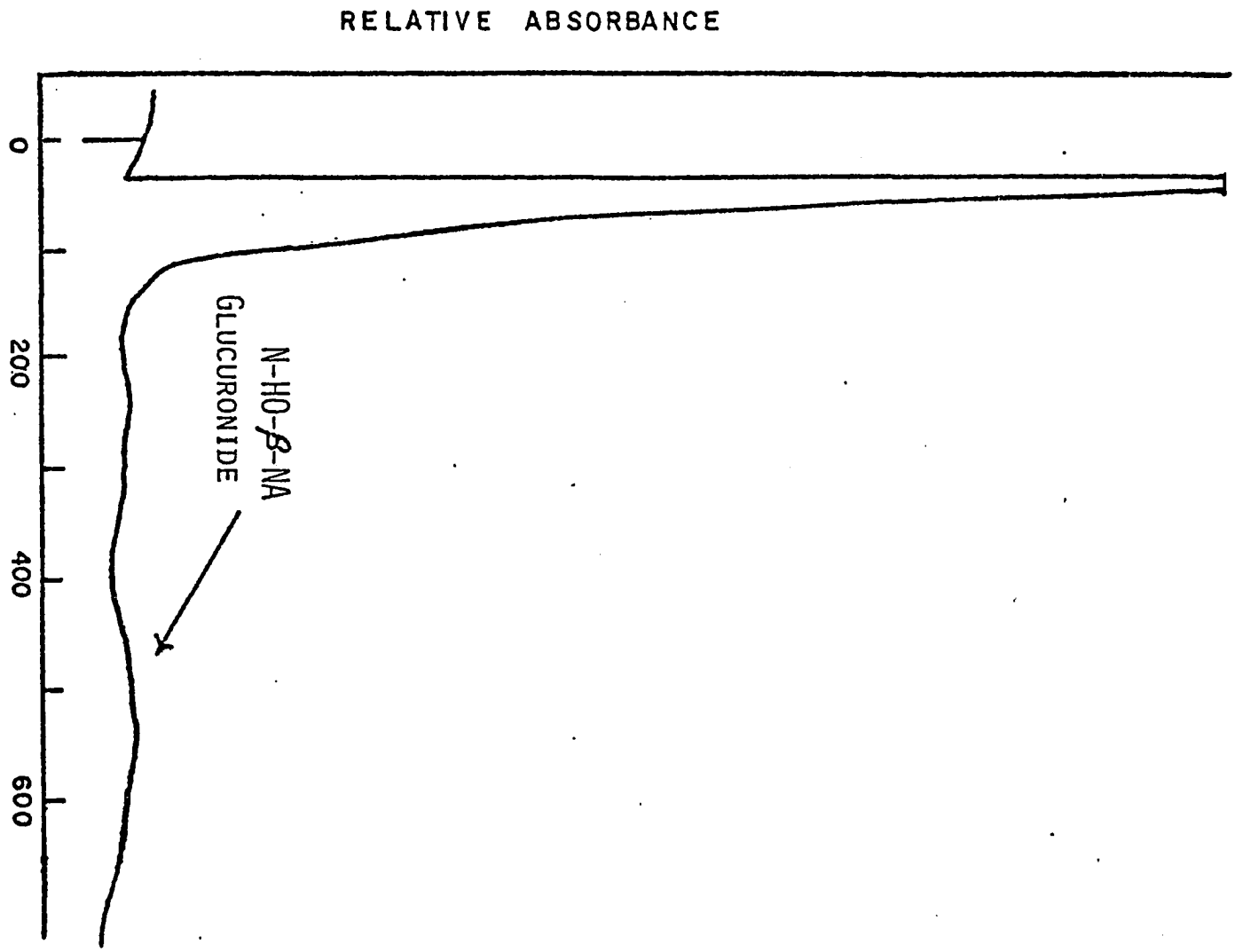
RELATIVE ABSORBANCE
0
200
400
600
N-HO-β-NA
GLUCURONIDE
ELUTION VOLUME, ml.

FIGURE 29

PART III.

Glass-Beads Immobilized Microsomes

Hog liver microsomes, with a total protein content of 70 mg/ml (Sigma Biuret Method) and an assayed β-NA N-oxidation activity of 55 nmoles/min. mg. prot. (with .5 mM β-NA F.C.) at 37°C, were immobilized on CPG porous glass beads using the immobilization technique described in Methods. The beads used were of nominal pore diameter of 1350Å, particle diameter range: 177-840 microns, and with a surface area of 34 m^2.

Figure 30 shows the N-oxidation activity of glass-beads immobilized microsomes as a function of the substrate (β-NA) concentration. The similarity between the activity curves for the native (liquid) microsomes (Figure 9) and immobilized microsomes (Figure 30) is obvious. It can be seen that, for instance, about 10 nmoles/min. mg. beads N-oxidation activity is obtained with 0.5 mM substrate concentration in the reaction medium. What this amounts to is that about 5-6 mg. of active glass-beads-microsomes conjugate solid phase, obtained through the given immobilization technique, would yield an equivalent activity as 1 mg. of native microsomal fraction. Such a high microsomal activity level exhibited after immobilization on a porous solid phase such as glass is truly marvelous if one has to consider the following two major "activity-limiting" factors associated with immobilized enzymes.

FIGURE 30. Glass beads-immobilized microsomes N-oxidation initial activity vs. substrate (βNA) concentration. The reaction was run at 38°C in the stirred-batch microreactor. The reaction medium contained, 0.1M K-phosphate buffer, pH 7.4, 0.5mM $NADP^+$, 1mM G6P, 1.0 U/ml G6PD, 0.15mM $MgCl_2$, 29.0 U/ml catalase, 0.2mM O_2, 20 mg. active glass-beads, and varying amounts of substrate as indicated in the figure.

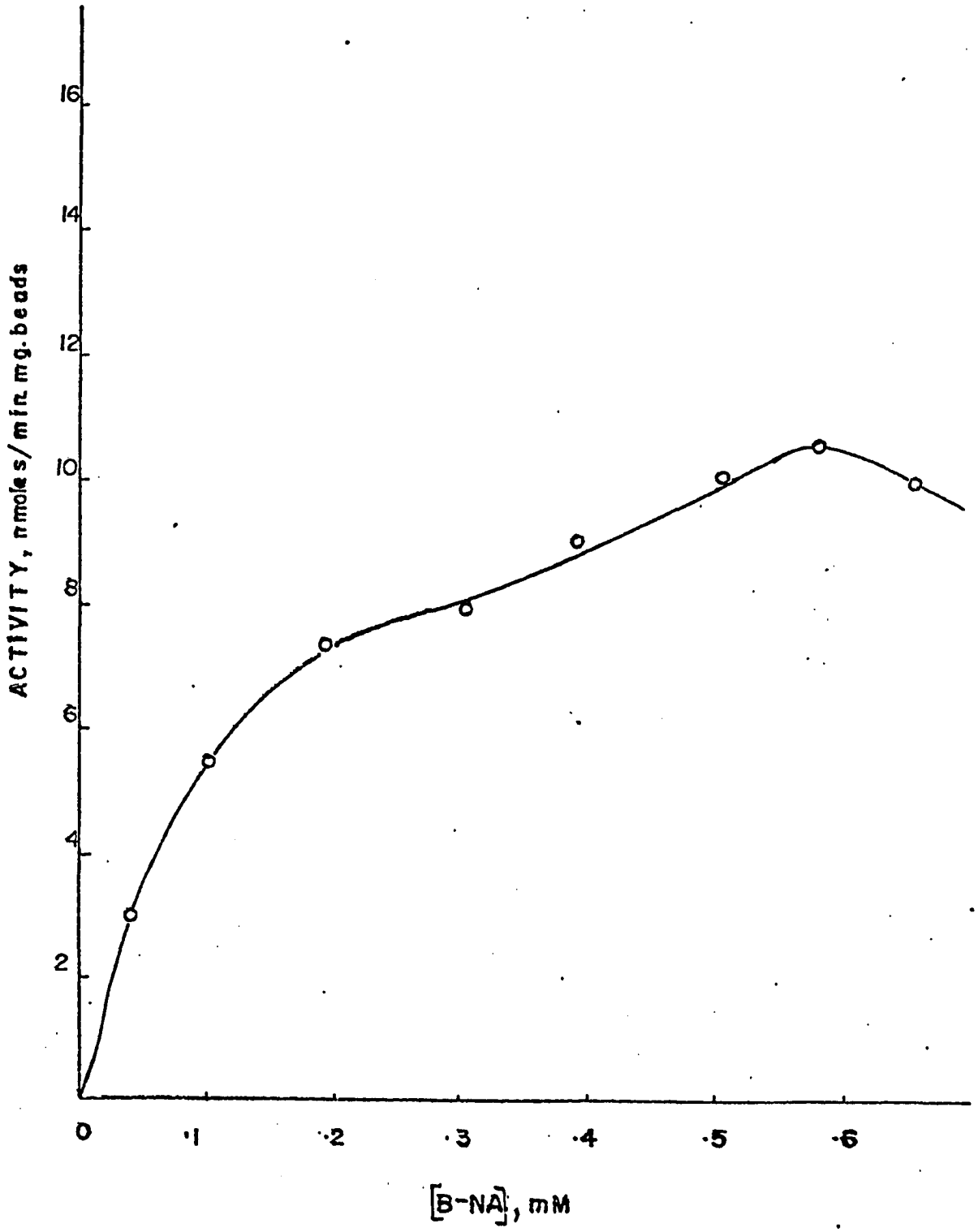

FIGURE 30

(1) Usually a very significant loss of enzyme activity, sometimes as high as 50% [71], is expected due to immobilization, i.e. due to participation of some of the active (catalytic) centers of the enzymes(s) in chemical bonding with the solid phase arm. (2) Even though the diffusion of the substrate molecules from the bulk reaction mass to the surface of the solid matrix in the batch reactor is enhanced by agitation, its diffusion into the pores of the solid phase (internal diffusion) to the enzyme catalytic sites is commonly a major limiting factor of the kinetics. Despite these limitations, immobilized microsomes have quite a high potential for the study of the kinetics of carcinogens.

One of the significant advantages of using glass beads-immobilized microsomes for in-vitro metabolic activation of carcinogens can be seen on Figure 31 which shows the reaction time-history of β-NA activation. As has been shown and discussed earlier in Part I of this chapter, one of the main kinetic problems encountered in metabolic activation of β-NA to its active intermediate form (N-HO-βNA) in liquid microsomal system was the unstability of the formation of the intermediate, i.e. its continuous decrease with time as the reaction progresses, after the first 4-5 min. (Figure 7). Surprisingly, this problem appears to be solved with the use of immobilized microsomes. As one can see from Figure 31, the formation of the N-hydroxy intermediate is stabilized and it doesn't seem to have been

FIGURE 31. Glass beads-immobilized microsomes reaction time-history for β-NA N-oxidation. The assay conditions and the reaction mixture used was as given in the legends to Figure 30, except that 0.5mM β-NA was used for the assay. β-naphthylhydroxylamine concentrations were calculated from 0.1ml serial aliquot samples using amyl-acetate reducing equivalents determined by the Method of Tsen [92]..

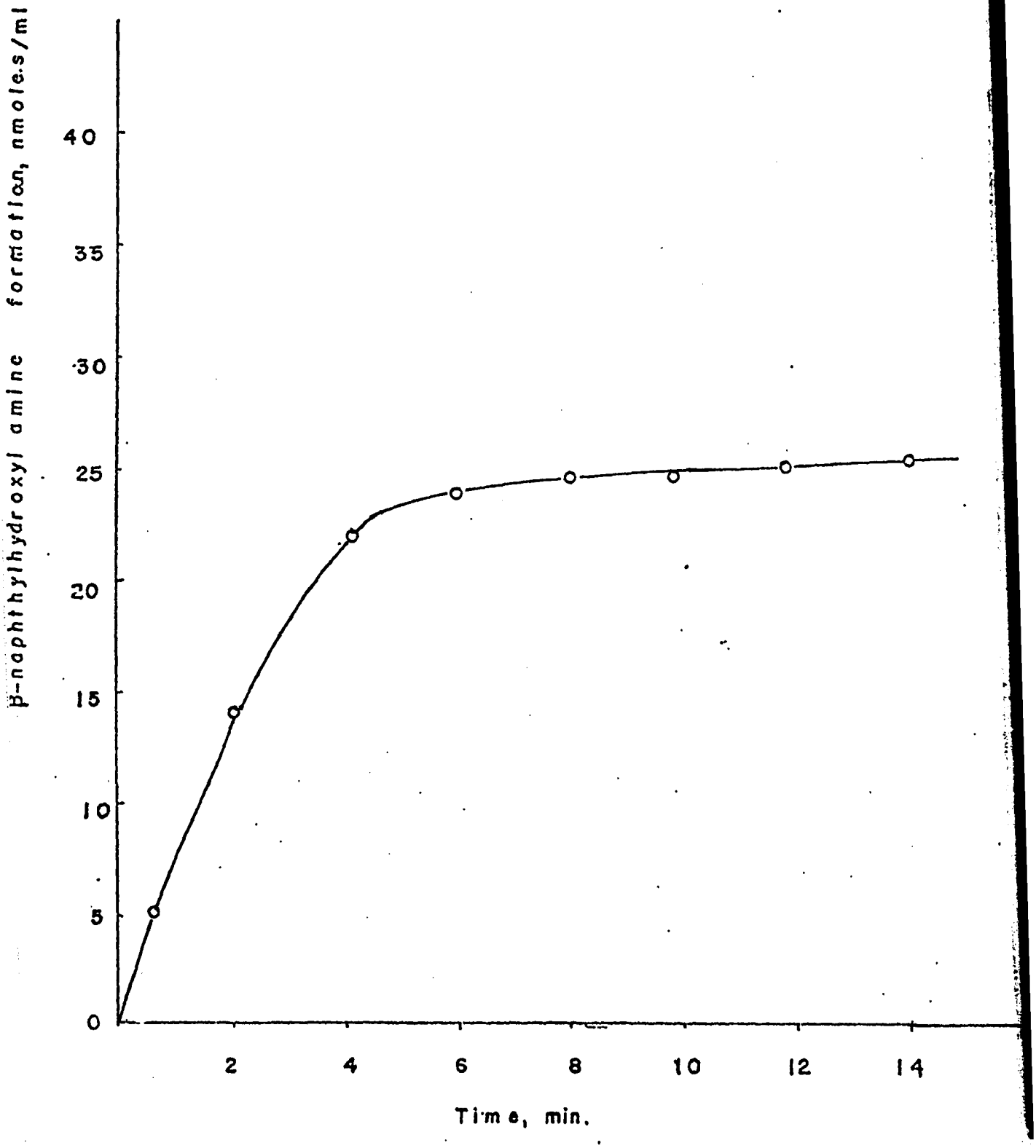
β-naphthylhydroxyl amine formation, nmoles/ml
0
5
10
15
20
25
30
35
40
2
4
6
8
10
12
14
Time, min.

FIGURE 31

attacked by another reaction pathway, which makes the detection of this active form much easier. This improvement in the stability of the formation, or rather the accumulation, of the intermediate in a reaction system using immobilized microsomes may be explained by the following. (1) In the solid phase, due to substrate diffusion constraint, reaction takes place at a relatively slow pace in comparison with the reaction velocity in a homogeneous system using liquid microsomes. Thus, a rapid accumulation of the reactive intermediate, which will subsequently cause a significant loss of the latter via side reactions, is possibly avoided by the use of glass-beads-immobilized microsomes. The most important advantages accruing from immobilization are the significant increase in the stability of activity and the reuseability of the active solid matrix. The half-life of the porous glass-beads-immobilized microsomes was about 5 days. The active matrix could be easily washed-off after a given assay, stored, and reused for another experimental run without a significant loss of the original activity.

The conjugative microsomal enzyme activity, especially that of UDP-GT, of the glass beads matrix was further investigated by running the glucuronidation reaction with N-hydroxy β-naphthylamine as a substrate. The reaction was run in a stirred 5 ml batch reactor at 37°C for 40 minutes under the atmosphere of nitrogen. Separation of the reaction product by the routine Sephadex gel-

FIGURE 32. N-hydroxy β-naphthylamine glucuronide hydrolysis curve. The N-glucuronide obtained by a one-step synthesis from N-HO-βNA using glass beads-immobilized microsomes was hydrolyzed back to the substrate (reverse reaction) by 2M citric acid, pH4 in the incubator at 38°C. The N-hydroxy was then analyzed from 0.1ml serial aliquots by using amyl-acetate reducing equivalents.

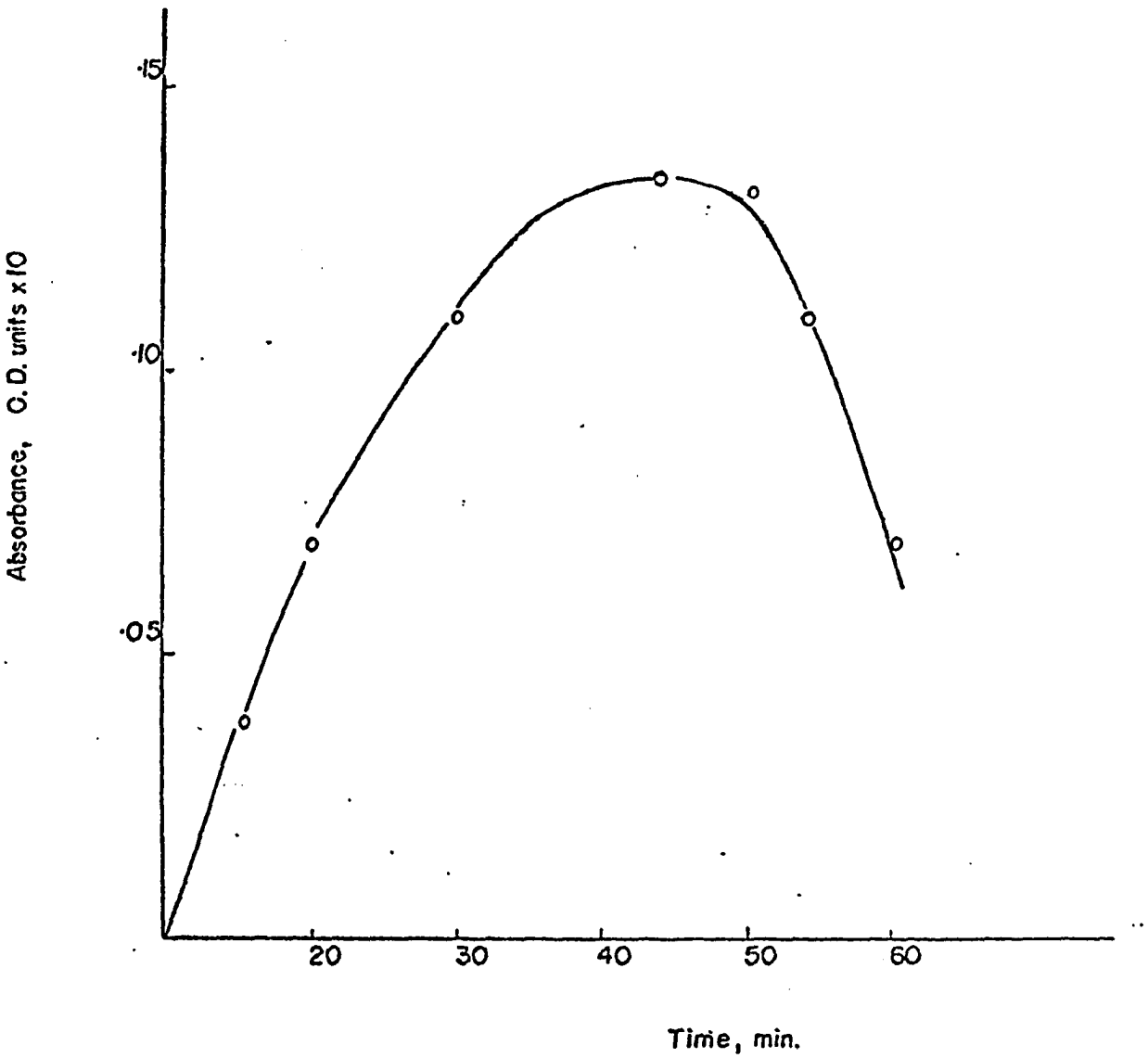

FIGURE 32

permeation chromatography and subsequent UV scan gave elution peak and absorption maximum exactly identical to the glucuronide peaks indicated in Figures 26 and 27, respectively. The N-hydroxy β-naphthylamine glucuronide conjugate is known to be susceptible to hydrolysis at an acidic pH to its parent compound N-hydroxy β-naphthylamine (reverse reaction). To further verify the validity the product obtained, this experiment was performed. Figure 32 shows the hydrolysis reaction profile of the freeze-dried and HPLC-purified sample of the glucuronide product to N-hydroxy β-naphthylamine with 2M citric acid at pH4. Thus, it is obvious that the application of glass-beads immobilized microsomes appears to be highly feasible for carcinogen screening tests via metabolic activation/deactivation procedure.

CHAPTER VI

CONCLUSION AND RECOMMENDATIONS

In order to assess the various factors affecting the fidelity of the present in-vitro short-term carcinogen-screening tests via metabolic activation, the kinetics of β-naphthylamine (β-NA) was studied using pig liver microsomes as an activation system of enzymes. The catalytic activation of β-NA to N-hydroxy β-naphthylamine (N-HO-βNA) in liver microsomes is specific to mixed-function microsomal flavoprotein oxidase (MFMFO) activity. The catalytic formation and accumulation of N-HO-βNA, a reactive carcinogenic intermediate form, in liver microsomal assay system is significantly affected by variables such as temperature, pH, reaction time, concentration levels of substrate and microsomes, and by diffusion limitation. The metabolic activation kinetics of β-nitronaphthalene (β-NN), an analog of aryl-nitro carcinogen compounds, to N-HO-βNA catalyzed by pig liver microsomal nitro-reductase was also shown successfully for the first time in-vitro.

Metabolic activation of carcinogens is usually accompanied by a deactivation reaction, involving a second (conjugative) enzyme. This bienzymic two-step consecutive

reaction has been successfully modeled in-vitro in a batch reactor for the substrates β-NA and β-NN. The pathway investigated here is the N-oxidation catalyzed by microsomal mixed-function amine oxidase (for β-NA), and partial N-reduction by nitro-reductase (for β-NN), and subsequent glucuronidation via microsomal UDP-glucuronyltransferase. Periodical addition of the substrates by small amounts to the reaction medium at optimum conversion time-intervals in a batch stirred microreactor seems to be the best kinetic strategy to study the sequential mechanism of metabolic activation/activation of chemical carcinogens. Moreover, this technique or procedure models the in-vivo metabolic reactions of chemical agents much closer, since foreign chemical agents usually enter the body in small amounts at a time from a given work environment. The consecutive bienzymic reaction kinetics can be adequately approximated by a dynamic model of two-step sequential reactions of first order. The rate constant of the second step (glucuronidation step) appears to be about a hundred times greater than that of the first step. A computer simulation of the proposed dynamic kinetic model satisfactorily agrees with the experimental data.

The stability of microsomal oxidative and conjugative enzyme activities can be greatly enhanced by immobilization of microsomes on CPG porous glass beads according to the procedure prescribed in this treatise. β-NA N-oxidation and glucuronidation activities of the glass-

beads-microsomes conjugate shown in this work positively indicate the potential of immobilized microsomes for use in carcinogen screening tests. The most significant advantage accruing from the application of immobilized microsomes is the observed improvement in the stability of formation and accumulation of the intermediate carcinogenic reactive form, N-hydroxy β-naphthylamine in this particular case.

However, the following recommendations have to be made at this point to further assess the potential of glass-beads immobilized microsomes activity for application in carcinogen screening tests in order to improve the quality of the outcome.

1. Glass-beads solid matrix with larger pore diameter than the 1350Å, if available commercially, would facilitate the immobilization of microsomes a considerable ease and thus might result in a much higher solid phase activity. Higher porosity is desirable due to the fact that, since microsomes are large membraneous sacs onto the surface-walls of which are embedded the required enzymes, it would be necessary to create a favorable pore size for a better loading of the microsomal entity for subsequent binding.

Possibly, this would result in a higher activity and stability of the solid-phase conjugate obtained. In fact, it was noticed during the experimental runs with current g.b. immobilized microsomes that in prolonged well-agitated reaction assays a slight amount of microsomal pellets were being knocked-off from the surface of the solid matrix, indicating that there is either some physical adsorption on the surface or relatively weak semi-loading and binding at the mouth of the pores due to the constraint in pore size.

2. The two-step metabolic activation and deactivation mechanism has to be successfully shown with sufficient activities for a typical carcinogen, preferably benzo[a]-pyrene in order to fully confirm their potential use with accrued advantages.
3. Since one of the benefits of immobilization of microsomes on the glass-beads solid matrix is the advantage of operation in reactors of various configurations to achieve desired con-

version of substrate the application of continuous plug-flow or fluidized-bed reactor configurations with recirculation are recommended for an in-vitro study of the metabolic kinetics of carcinogens and drugs. Such designs hopefully would give a better control of the main reaction products and minimize side reactions which could otherwise occur in batch reactor systems.

This work has been only a first step in applying chemical engineering principles to the area of carcinogen metabolism in test situations. Needless to say, there is a great deal of experimental and theoretical work to be done in order to better understand the complex kinetics in microsomes for an efficient utilization of the latter in carcinogen screening assays by metabolic activation.

BIBLIOGRAPHY

1. Commoner, B.; Carcinogens in the Environment, Chem. Tech., Feb. ed. 76 (1977).

2. Whelan, E.M.; Association of Food and Drug Officials Quarterly Bull. 41, 167 (1977).

3. Fox, J.L.; Chemical and Engineering News, Dec. 12, 34 (1977).

4. Frantz, C.N.; Malling, H.V.; Mutat. Res., 31, 365 (1975).

5. Hoover, R., et. al.; Environ. Res. 9, 196 (1975).

6. De Serres, et. al.; Mutat. Res. 33, 11 (1975).

7. Heidelberger, C.; Eur. J. Cancer Res. 6, 161 (1970).

8. Jerine, D.M., Daley, J.W.; Drug Metabolism, Taylor and Francis, London (1976).

9. Sims, P.; Grover, P.L.; Adv. Cancer Res. 20, 165 (1974).

10. Heidelberger, C.; Chemical Carcinogenesis, Ann. Rev. Biochem., 44, 79 (1975).

11. Nebert, et. al.; Cytochromes P-450 and b_5 D.Y. Cooper, et. al. eds., 127 (1975) Plenum, New York.

12. Nebert, et. al., Fed. Proc. Am. Soc. Exp. Biol. 35, 1133 (1976).

13. Thorgeirsson, S.S., Nebert, D.W.; Avd. Cancer Res. 25, 149 (1977).

14. Weisburger, H.J.; ChemTech, Dec. ed., 734 (1977).

15. Brady, D.R.; Crowder, R.D.; J. Biol. Chem., 253 (9), 3101 (1978).

16. Ebel, R.E., et. al.; Arch. Biochem. Biophys. 183, 317 (1977).

17. Culliton, B.J.; Science, 201, Sept. 29, 1199 (1978).

18. Maugh, T.H.; Science, Jan. 13, 162 (1978).

19. Maugh, T.H.; Science, 201, Sept. 29, 1200 (1978).

20. Whelan, E.M., Jour. Assoc. Food & Drug Adm. Officials, Quarterly Bulletin 35, 103, 1978.

21. Wei, J.; Technologists and the Environment; Chem. Tech., June 1978, pp. 340-351.

22. Maugh, T.H.; Science 201, Sept. 29, 1203 (1978).

23. Ames, B.N.; Chemical Mutagens: Principles and Methods for Their Detection, 1, Hollaender ed., Plenum, New York, 1971.

24. Ames, B.N., et. al.; Proc. Natl. Acad. Sci., U.S.A., 70, 782 (1973).

25. McCann, J.; Ames, B.N., et. al.; Proc. Natl. Acad. Sci., U.S.A. 72, 979 (1975).

26. Ames, B.N., McCann, J., Yamasaki, E.; Mutat. Res. 31, 347 (1975).

27. Ames, B.N.; Science, 191, 241 (1976).

28. Miller, E.C., Miller, J.A., Ann. Rev. Biochem. 28, 291 (1959).

29. Miller, E.C.; Cancer Res. 11, 100 (1951).

30. Mintz, B., Illmensee, K., Proc. Natl. Acad. Sci. U.S.A., 72, 3585 (1975).

31. Miller, J.A.; Cancer Res. 30, 559 (1970).

32. Miller, E.C., Miller, J.S.; Molecular Biol. Cancer, H. Busch ed., 377 (1974).

33. Miller, E.C., et. al.; Pharmacol. Rev. 28, 806 (1966).

34. Ames, B.N., et. al.; Proc. Natl. Acad. Sci., U.S.A., 70, 2281 (1973).

35. Kappas, A.; Alvares, A.P.; Scientific American, 25 June, 22 (1975).

36. Keevil, T., Mason, H.S.; Methods in Enzymol. Vol. LII, Biomembranes Part C, P.G. Fleischer & Parker, eds., 1978.

37. Mason, H.S.; Abstr. 130th. Meeting Am. Chem. Soc. 125, 51 (1956).

38. Ziegler, D.M., et. al.; Properties of a Purified Liver Mixed-Function Microsomal Amine Oxidase in Flavins and Flavoproteins, H.Kamine, ed., 1971.

39. Ziegler, D.M., et. al.; Biochemistry, 5, 2932 (1966).

40. Gold, M.S., Ziegler, D.M.; Xenobiotica, 3, 179 (1973).

41. Poulsen, L.L., et. al.; Biochem. Pharmacol. 23, 2431 (1974).

42. Boyland, E., Manson, D.; J. Chem. Soc., 606 (1962).

43. Boyland, E., Dukes, C.E., Grover, P.L.; Br. J. Cancer, 17, 79 (1963).

44. Booth, J., Boyland, E.; Biochem. J. 91, 362 (1964).

45. Arcos, J.C., Argus, M.F.; Adv. Cancer Res., 11, 305 (1968).

46. Cramer, Et. al.; J. Biol. Chem., 235, 885 (1960).

47. Bonser, G.M., Br. J. Cancer, 17, 127 (1963).

48. Bryan, G.T., et. al.; Cancer Res. 24, 596 (1964).

49. Radomski, J.L., Brill, E.; Science, 167, 992 (1970).

50. Boyland, E., Manson, D.; Biochem. J., 101, 84 (1966).

51. Troll, W., Nelson, N.; Fedn. Proc. 20, 41 (1961).

52. Lange, G., Arch. Pharmac. Exp. Path., 257, 230 (1967).

53. Uehleke, H.; Arch. Pharmac. Exp. Path., 259, 66 (1967).

54. Uehleke, H.; Xenobiotica, 1, 327 (1971).

55. Uehleke, H.; Drug Metab. Disp. 1, 299 (1973).

56. Ziegler, D.M.; Mitchell, C.H.; Arch. Biochem. Biophys. 150, 116 (1972).

57. Sofer, S.S.; Ph.D. Dissertation, University of Texas, Austin, 1974.

58. Sofer, S.S., Ziegler, D.M., Popovich, R.P.; Biochem. Biophys. Res. Comm., 57 (1), 183 (1974).

59. Poulsen, L.L., Masters, B.S.S., Ziegler, D.M.; Xenobiotica, 6 (8), 481 (1976).

60. Ziegler, D.M.; et. al.; Drug Metab. Disp., 1, 314 (1973).

61. Matthews, A., O'Brien, M.T., Sofer, S.S.; Oxidation and Glucuronidation of β-naphthylamine: Two-Step Reaction in One Model, AIChE 84th Natl. Conf., Enzyme Reaction Engineering Division, Atlanta, GA., February 1978.

62. Kadlubar, F.F., Flammang, T., Unruh, L.; "The Role of N-hydroxy Arylamine N-glucuronides in Arylamine-Induced Urinary Bladder Carcinogenesis," Conjugation Reactions in Drug Biotransformation; A. Aitio ed., 1978.

63. Hicks, R.M.; et. al.; Cancer Res., 37, 2943 (1977).

64. Clayson, D.B.; Cooper, E.H.; Adv. Cancer Res., 13, 271 (1970).

65. Vessey, D.A.; Goldenberg, J.; Zakim, D.; Biochimica et. Biophysica Acta, 309, 58 (1973).

66. Vessey, D.A., et. al.; J. Biol. Chem., 26 (10), 3023 (1972).

67. Zakim, D.; Goldenberg, J.; Vessey, D.A.; Biochem. & Biophys. Res. Comm., 52 (10), 453 (1973).

68. Zakim, D.; et. al.; The Enzymes of Biological Membranes, 2, 443 (1976).

69. Erickson, R.H.; Zakim, D.; Vessey, D.A.; Biochemistry, 17, 3706 (1978).

70. Kadlubar, F.F., et. al.; Cancer Res., 37, 805 (1977).

71. Zaborsky, O.R.; Immobilized Enzymes, C.R.C. Press, Cleveland, Ohio (1973).

72. Wingard, L.B., Jr.; Enzyme Engineering, Plenum Publishers, New York, 1972.

73. Kendall, E.P.; Weetall, H.H.; Enzyme Engineering, Vol. 3., Plenum Press, New York, 1978.

74. Epton, R.; Thomas, T.H.; Improving Nature's Catalysts, Aldrichimica Acta, 4, 61 (1971).

75. Barker, S.A.; et. al.; Carbohyd. Res. 20, 1 (1971).

76. Ohno, Y., Stahmann, M.A.; Macromolecules, 4, 350 (1971).

77. Robinson, P.J., et. al.; Biochim. Biophys. Acta 242, 659 (1971).

78. Bar-Eli, A.; Katchalski, E.; J. Biol. Chem. 246, 1213 (1971).

79. Maeda, H., Suzuki, H.; Nippon Nogei Kagaku Kaishi, 44, 547 (1970).

80. Goldstein, L., Lifshitz, A., Sokolovsky, M., Int. J. Biochem., 2, 446 (1971).

81. Goldstein, L., et. al.; Biochemistry 9, 2322 (1970).

82. Brown, E., Racois, A.; Bull. Soc. Chim. Fr. No. 12, 4351 (1971).

83. Lee, J.C.; Biochim. Biophys. Acta, 235, 435 (1971).

84. Barker, S.A., Somers, P.J., Epton, R.; Carbohyd. Res. 8, 491 (1968).

85. Sofer, S.S., Ziegler, D.M., Popovich, R.P.; Biochim. Biophys. Res. Comm., 57 (1) (1974).

86. Wolpert, M.K., et. al.; J. Pharm. Exp. Therap., 185, 202 (1973).

87. Ziegler, D.M., Mitchell, C.H., Arch. Biochem. Biophys. 150, 116 (1972).

88. Ziegler, D.M., Poulsen, L.L., Methods in Enzymol., Vol. L11, Biomembranes, Part C, 142 (1978).

89. Sofer, S.S., Ziegler, D.M., et. al.; Biotech. Bioeng., 107, 17 (1975).

90. Cho, Y.K., Bailey, J.E.; Biotech. Bioeng. 19, 769 (1977).

91. Buchholz, K., Godelmann, B.; Biotech. Bioeng., 20, 1201 (1978).

92. Tsen, C.C., Analyt. Chem. 33, 849 (1961).

93. Levenspiel, O., Chemical Reaction Engineering, John Wiley and Sons, Inc., 1974, pp. 174-200.

94. Carberry, J.J., Chemical and Catalytic Reaction Engineering, McGraw-Hill, 1976, pp. 42-50.

95. Segel, I.H.; Enzyme Kinetics, John Wiley and Sons, New York, 1975, p. 85.

96. Vessey, D.A., et. al; J. Biol. Chem. 24 (10), 3023 (1972).

97. Zakim, D., Vessey, D.A.; Biochem. Pharmacol. 26, 129 (1977).

98. Poirier, L.A.; Weisburger, J.H., Biochem. Pharmacol. 23, 661 (1974).

99. Ramachandran, K.B., Perlmuter, D.D.; Biotech. Bioeng. 18, 669 (1976).

100. Gurtoo, H.L., et. al.; J. Biol. Chem. 253 (11), 3952 (1978).

101. Cleland, W.W.; Biochim. Biophys. Acta, 67, 104 (1963).

102. Ziegler, D.M., Poulsen, L.L.; The Microsomal FAD-Containing Monooxygenase, in press (personal communication).

103. Gornall, A.G., Bardawill, C.J., David, M.M.; J. Biol. Chem., 177, 751 (1949).

APPENDIX A-1

KINETIC MODEL-CSMP COMPUTER PROGRAM

```
                ****CONTINUOUS SYSTEM MODELING PROGRAM****

                          *** VERSION 1.3 ***

      INCON O2 =1.00, BNA1 =200., CO2 = 50., UDPGA =1., OHBNA1 =0., BNAG1 =0.
      INCON E01 = 40., TPNH = 1.00, UDPAG = 1.00
      PARAMETER CK1 = 0. , CK2 = (.054,.016), CK3=0., CK4=0.143, CKM4=0.0
      PARAMETER CE1 = .002, CE2 = .001
      INITIAL
      DYNAMIC
               DE1=(-CE1)*E1
               E1= INTGRL(E01,DE1)
               DE2= (-CE2)*E2
               E2=INTGRL(E02,DE2)
            DBNA= -(CK2*BNA*TPNH*O2*E1+CK1*BNA)
               BNA=INTGRL(BNA1,DBNA)
            TEMP=CK2*BNA*TPNH*O2*E1+CKM4*BNAG*E2
            DOHBNA=TEMP-CK3*OHBNA-CK4*OHBNA*UDPGA*E2*UDPAG
               OHBNA=INTGRL(OHBNA1,DOHBNA)
            DBNAG=CK4*OHBNA*UDPGA*E2*UDPAG-CKM4*E2*BNAG
               BNAG=INTGRL (BNAG1,DBNAG)
      PRINT    BNA,OHBNA,BNAG
      PRTPLOT  BNA
      PRTPLOT  OHBNA
      PRTPLOT  BNAG
      LABEL    NMOLE/ML CONCENTRATION OF BNAPHTHYLAMINE VS. TIME
      LABEL    NMOLE/ML CONCENTRATION OF NOHBNA VS. TIME
      LABEL    NMOLE/ML CONCENTRATION OF NOHBNA GLUCURONIDE VS. TIME
      TIMER    FINTIM=15.
      TERMINAL
      END
      STOP

OUTPUT VARIABLE SEQUENCE
DE1     E1      DE2     E2      DBNA    BNA     TEMP    DOHBNA OHBNA   DBNAG
BNAG

 OUTPUTS     INPUTS    PARAMS  INTEGS + MEM BLKS  FORTRAN  DATA CDS
 15(500)   62(1400)  17(400)   5+  0=  5(300)    12(600)      13


      ENDJOB
```

APPENDIX A-2

CONCENTRATION-TIME PROFILE OF β-NA KINETIC MODEL COMPUTER SIMULATION

NMOLE/ML CONCENTRATION OF BNAPHTHYLAMINE VS. TIME PAGE 1

	MINIMUM	BNA	VERSUS TIME	MAXIMUM
	2.7494E-12	CK2	= 1.6000E-02	2.0000E+02
TIME	BNA	I		I
0.0	2.0000E+02	----------		+
1.5300E-01	1.8170E+02	----------		+
3.0600E-01	1.6507E+02	----------		+
4.5900E-01	1.4997E+02	----------		+
6.1200E-01	1.3626E+02	----------		+
7.6500E-01	1.2380E+02	----------		+
9.1800E-01	1.1249E+02	----------		+
1.0700E+00	1.0221E+02	----------		+
1.2230E+00	9.2874E+01	----------		+
1.3760E+00	8.4393E+01	----------		+
1.5300E+00	7.6689E+01	----------		+
1.6830E+00	6.9690E+01	----------		+
1.8360E+00	6.3332E+01	----------		+
1.9900E+00	5.7556E+01	----------		+
2.1430E+00	5.2308E+01	----------		+
2.2960E+00	4.7539E+01	----------		+
2.4500E+00	4.3207E+01	----------		+
2.6030E+00	3.9271E+01	----------		+
2.7560E+00	3.5694E+01	----------		+
2.9100E+00	3.2444E+01	----------		+
3.0630E+00	2.9491E+01	----------		+
3.2160E+00	2.6807E+01	----------		+
3.3700E+00	2.4366E+01	----------		+
3.5230E+00	2.2152E+01	----------		+
3.6760E+00	2.0138E+01	----------		+
3.8300E+00	1.8307E+01	----------		+
3.9830E+00	1.6644E+01	----------		+
4.1360E+00	1.5132E+01	----------		+
4.2900E+00	1.3758E+01	----------		+
4.4430E+00	1.2508E+01	----------		+
4.5960E+00	1.1373E+01	----------		+
4.7500E+00	1.0341E+01	----------		+
4.9030E+00	9.4030E+00	----------		+
5.0560E+00	8.5503E+00	----------		+
5.2100E+00	7.7751E+00	----------		+
5.3630E+00	7.0704E+00	----------		+
5.5160E+00	6.4294E+00	----------		+
5.6700E+00	5.8473E+00	----------		+
5.8230E+00	5.3178E+00	----------		+
5.9760E+00	4.8356E+00	----------		+
6.1300E+00	4.3966E+00	----------		+
6.2830E+00	3.9968E+00	----------		+
6.4360E+00	3.6338E+00	----------		+
6.5900E+00	3.3047E+00	----------		+
6.7430E+00	3.0055E+00	----------		+
6.8960E+00	2.7334E+00	----------		+
7.0500E+00	2.4851E+00	----------		+
7.2030E+00	2.2600E+00	----------		+
7.3560E+00	2.0614E+00	----------		+
7.5100E+00	1.8753E+00	----------		+
7.6630E+00	1.7061E+00	----------		+

NMOLE/ML CONCENTRATION OF BNAPHTHYLAMINE VS. TIME PAGE 2

	MINIMUM	BNA	VERSUS TIME	MAXIMUM
	2.7494E-12	CK2	= 1.6000E-02	2.0000E+02
TIME	BNA	I		I
7.8160E+00	1.5521E+00	----------		+
7.9700E+00	1.4121E+00	----------		+
8.1230E+00	1.2848E+00	----------		+
8.2760E+00	1.1690E+00	----------		+
8.4300E+00	1.0636E+00	----------		+
8.5830E+00	9.6721E-01	----------		+
8.7360E+00	8.8064E-01	----------		+
8.8900E+00	8.0134E-01	----------		+
9.0430E+00	7.2921E-01	----------		+
9.1960E+00	6.6359E-01	----------		+
9.3500E+00	6.0389E-01	----------		+
9.5030E+00	5.4956E-01	----------		+
9.6560E+00	5.0011E-01	----------		+
9.8100E+00	4.5521E-01	----------		+
9.9630E+00	4.1430E-01	----------		+
1.0120E+01	3.7708E-01	----------		+
1.0270E+01	3.4322E-01	----------		+
1.0430E+01	3.1240E-01	----------		+
1.0580E+01	2.8430E-01	----------		+
1.0730E+01	2.5868E-01	----------		+
1.0890E+01	2.3542E-01	----------		+
1.1040E+01	2.1429E-01	----------		+
1.1190E+01	1.9506E-01	----------		+

APPENDIX A-3

CONCENTRATION-TIME PROFILE OF N-HO-βNA KINETIC MODEL COMPUTER SIMULATION

MOLE/ML CONCENTRATION OF NCHBNA VS. TIME PAGE 1

MINIMUM CHBNA VERSUS TIME MAXIMUM
0.0 CK2 = 1.6000E-02 3.5974E+01
I I

TIME	CHBNA	I
0.0	0.0	+
1.6000E-01	1.1132E+01	----------+
3.0000E-01	1.3922E+01	----------+
4.3000E-01	1.3951E+01	----------+
6.0000E-01	1.3119E+01	----------+
7.5000E-01	1.2070E+01	----------+
9.0000E-01	1.1018E+01	----------+
1.0500E+00	1.0027E+01	----------+
1.2000E+00	9.1162E+00	---------+
1.3500E+00	8.2945E+00	---------+
1.5000E+00	7.5277E+00	---------+
1.6500E+00	6.8399E+00	---------+
1.8000E+00	6.2149E+00	---------+
1.9500E+00	5.6471E+00	--------+
2.1000E+00	5.1314E+00	--------+
2.2500E+00	4.6629E+00	-------+
2.4000E+00	4.2372E+00	-------+
2.5500E+00	3.8506E+00	-------+
2.7000E+00	3.4993E+00	------+
2.8500E+00	3.1801E+00	------+
3.0000E+00	2.8902E+00	------+
3.1500E+00	2.6267E+00	-----+
3.3000E+00	2.3874E+00	-----+
3.4500E+00	2.1699E+00	-----+
3.6000E+00	1.9723E+00	----+
3.7500E+00	1.7927E+00	----+
3.9000E+00	1.6295E+00	----+
4.0500E+00	1.4813E+00	----+
4.2000E+00	1.3465E+00	---+
4.3500E+00	1.2241E+00	---+
4.5000E+00	1.1126E+00	---+
4.6500E+00	1.0116E+00	---+
4.8000E+00	9.1971E-01	---+
4.9500E+00	8.3615E-01	---+
5.1000E+00	7.6023E-01	---+
5.2500E+00	6.9121E-01	+
5.4000E+00	6.2843E-01	+
5.5500E+00	5.7145E-01	+
5.7000E+00	5.1962E-01	+
5.8500E+00	4.7250E-01	+
6.0000E+00	4.2966E-01	+
6.1500E+00	3.9072E-01	+
6.3000E+00	3.5532E-01	+
6.4500E+00	3.2314E-01	+
6.6000E+00	2.9388E-01	+
6.7500E+00	2.6727E-01	+
6.9000E+00	2.4308E-01	+
7.0500E+00	2.2109E-01	+
7.2000E+00	2.0109E-01	+
7.3500E+00	1.8291E-01	+
7.5000E+00	1.6637E-01	+

MOLE/ML CONCENTRATION OF NCHBNA VS. TIME PAGE 2

MINIMUM CHBNA VERSUS TIME MAXIMUM
0.0 CK2 = 1.6000E-02 3.5974E+01
I I

TIME	CHBNA	I
7.6500E+00	1.5134E-01	+
7.8000E+00	1.3767E-01	+
7.9500E+00	1.2523E-01	+
8.1000E+00	1.1392E-01	+
8.2500E+00	1.0364E-01	+
8.4000E+00	9.4287E-02	+
8.5500E+00	8.5781E-02	+
8.7000E+00	7.8044E-02	+
8.8500E+00	7.1007E-02	+
9.0000E+00	6.4607E-02	+
9.1500E+00	5.8785E-02	+
9.3000E+00	5.3489E-02	+
9.4500E+00	4.8672E-02	+
9.6000E+00	4.4289E-02	+
9.7500E+00	4.0303E-02	+
9.9000E+00	3.6676E-02	+
1.0050E+01	3.3377E-02	+
1.0200E+01	3.0375E-02	+
1.0350E+01	2.7644E-02	+
1.0500E+01	2.5160E-02	+
1.0650E+01	2.2899E-02	+
1.0800E+01	2.0842E-02	+
1.0950E+01	1.8970E-02	+

APPENDIX A-4

CONCENTRATION-TIME PROFILE OF N-HO-βNA GLUCURONIDE KINETIC MODEL COMPUTER SIMULATION

NMOLE/ML CONCENTRATION OF NOMBNA GLUCURONIDE VS. TIME PAGE 1

MINIMUM 0.0 BNAG VERSUS TIME CK2 = 1.0000E-02 MAXIMUM 2.0000E+02

TIME	BNAG	I
0.0	0.0	+
1.5000E-01	7.1713E+00	-+
3.0000E-01	2.1007E+01	------+
4.5000E-01	3.6079E+01	----------+
6.0000E-01	5.0623E+01	-------------+
7.5000E-01	6.4129E+01	----------------+
9.0000E-01	7.6495E+01	-------------------+
1.0500E+00	8.7763E+01	----------------------+
1.2000E+00	9.8013E+01	------------------------+
1.3500E+00	1.0732E+02	--------------------------+
1.5000E+00	1.1579E+02	----------------------------+
1.6500E+00	1.2347E+02	------------------------------+
1.8000E+00	1.3045E+02	--------------------------------+
1.9500E+00	1.3680E+02	----------------------------------+
2.1000E+00	1.4256E+02	------------------------------------+
2.2500E+00	1.4780E+02	--------------------------------------+
2.4000E+00	1.5256E+02	--+
2.5500E+00	1.5688E+02	--+
2.7000E+00	1.6081E+02	--+
2.8500E+00	1.6438E+02	--+
3.0000E+00	1.6762E+02	--+
3.1500E+00	1.7057E+02	--+
3.3000E+00	1.7324E+02	--+
3.4500E+00	1.7568E+02	--+
3.6000E+00	1.7789E+02	--+
3.7500E+00	1.7990E+02	--+
3.9000E+00	1.8173E+02	--+
4.0500E+00	1.8339E+02	--+
4.2000E+00	1.8490E+02	--+
4.3500E+00	1.8627E+02	--+
4.5000E+00	1.8751E+02	--+
4.6500E+00	1.8865E+02	--+
4.8000E+00	1.8968E+02	--+
4.9500E+00	1.9061E+02	--+
5.1000E+00	1.9146E+02	--+
5.2500E+00	1.9224E+02	--+
5.4000E+00	1.9294E+02	--+
5.5500E+00	1.9358E+02	--+
5.7000E+00	1.9416E+02	--+
5.8500E+00	1.9469E+02	--+
6.0000E+00	1.9517E+02	--+
6.1500E+00	1.9561E+02	--+
6.3000E+00	1.9600E+02	--+
6.4500E+00	1.9637E+02	--+
6.6000E+00	1.9669E+02	--+
6.7500E+00	1.9699E+02	--+
6.9000E+00	1.9726E+02	--+
7.0500E+00	1.9751E+02	--+
7.2000E+00	1.9774E+02	--+
7.3500E+00	1.9794E+02	--+
7.5000E+00	1.9813E+02	--+

NMOLE/ML CONCENTRATION OF NOMBNA GLUCURONIDE VS. TIME PAGE 2

MINIMUM 0.0 BNAG VERSUS TIME CK2 = 1.0000E-02 MAXIMUM 2.0000E+02

TIME	BNAG	I
7.6500E+00	1.9830E+02	--+
7.8000E+00	1.9845E+02	--+
7.9500E+00	1.9859E+02	--+
8.1000E+00	1.9872E+02	--+
8.2500E+00	1.9883E+02	--+
8.4000E+00	1.9894E+02	--+
8.5500E+00	1.9903E+02	--+
8.7000E+00	1.9912E+02	--+
8.8500E+00	1.9920E+02	--+
9.0000E+00	1.9927E+02	--+
9.1500E+00	1.9934E+02	--+
9.3000E+00	1.9940E+02	--+
9.4500E+00	1.9945E+02	--+
9.6000E+00	1.9950E+02	--+
9.7500E+00	1.9954E+02	--+
9.9000E+00	1.9958E+02	--+
1.0050E+01	1.9962E+02	--+
1.0200E+01	1.9966E+02	--+
1.0350E+01	1.9969E+02	--+
1.0500E+01	1.9971E+02	--+
1.0650E+01	1.9974E+02	--+
1.0800E+01	1.9976E+02	--+
1.0950E+01	1.9978E+02	--+
1.1100E+01	1.9980E+02	--+

APPENDIX A-5

DOT PLOT

```
      CHARACTER*1 KE(3)
      CHARACTER*40 XLABEL, YLABEL
      REAL TIME(100), NUM1(100),NUM2(100),NUM3(100)
      DATA KE/'*','X','C'/
      XLABEL = 'TIME'
      YLABEL = 'CONCENTRATION'
      I=1
    5 READ(5,*,END=100) TIME(I),NUM1(I),NUM2(I),NUM3(I)
      I = I+1
      GOTO 5
  100 I = I-1
      CALL PLOT(0.,15.0,XLABEL,0.,200., YLABEL)
      DO 1000 J = 1,2
            CALL KEY(KE(J))
            IF ( J .EQ. 1) THEN DO
                  CALL DOT(TIME(1),NUM1(1),1)
            ELSE DO
                  CALL DOT(TIME(1),NUM3(1),1)
            END IF
            DO 500 K = 1,I
                  IF(J .EQ. 1) THEN DO
                        CALL DOT(TIME(K),NUM1(K),0)
                  ELSE DO
                        CALL DOT(TIME(K),NUM3(K),0)
                  END IF
  500       CONTINUE
 1000 CONTINUE
      CALL PAGE(1)
      STOP
      END

$EXEC
```